

Investigation of Exterior Girder Rotation and the Effect of Skew during Deck Placement

**Final Report
August 2019**



IOWA STATE UNIVERSITY
Institute for Transportation

Sponsored by
Iowa Highway Research Board
(IHRB Project TR-711)
Iowa Department of Transportation
(InTrans Project 16-580)

About BEC

The mission of the Bridge Engineering Center (BEC) is to conduct research on bridge technologies to help bridge designers/owners design, build, and maintain long-lasting bridges.

About InTrans

The mission of the Institute for Transportation (InTrans) at Iowa State University is to develop and implement innovative methods, materials, and technologies for improving transportation efficiency, safety, reliability, and sustainability while improving the learning environment of students, faculty, and staff in transportation-related fields.

ISU Nondiscrimination Statement

Iowa State University does not discriminate on the basis of race, color, age, ethnicity, religion, national origin, pregnancy, sexual orientation, gender identity, genetic information, sex, marital status, disability, or status as a U.S. veteran. Inquiries regarding non-discrimination policies may be directed to Office of Equal Opportunity, 3410 Beardshear Hall, 515 Morrill Road, Ames, Iowa 50011, Tel. 515-294-7612, Hotline: 515-294-1222, email eooffice@iastate.edu.

Disclaimer Notice

The contents of this report reflect the views of the authors, who are responsible for the facts and the accuracy of the information presented herein. The opinions, findings and conclusions expressed in this publication are those of the authors and not necessarily those of the sponsors.

The sponsors assume no liability for the contents or use of the information contained in this document. This report does not constitute a standard, specification, or regulation.

The sponsors do not endorse products or manufacturers. Trademarks or manufacturers' names appear in this report only because they are considered essential to the objective of the document.

Iowa DOT Statements

Federal and state laws prohibit employment and/or public accommodation discrimination on the basis of age, color, creed, disability, gender identity, national origin, pregnancy, race, religion, sex, sexual orientation or veteran's status. If you believe you have been discriminated against, please contact the Iowa Civil Rights Commission at 800-457-4416 or Iowa Department of Transportation's affirmative action officer. If you need accommodations because of a disability to access the Iowa Department of Transportation's services, contact the agency's affirmative action officer at 800-262-0003.

The preparation of this report was financed in part through funds provided by the Iowa Department of Transportation through its "Second Revised Agreement for the Management of Research Conducted by Iowa State University for the Iowa Department of Transportation" and its amendments.

The opinions, findings, and conclusions expressed in this publication are those of the authors and not necessarily those of the Iowa Department of Transportation.

Technical Report Documentation Page

1. Report No. IHRB Project TR-711	2. Government Accession No.	3. Recipient's Catalog No.	
4. Title and Subtitle Investigation of Exterior Girder Rotation and the Effect of Skew during Deck Placement		5. Report Date August 2019	
		6. Performing Organization Code	
7. Author(s) Katelyn Freeseaman (orcid.org/0000-0003-0546-3760), Brent Phares (orcid.org/0000-0001-5894-4774), Behrouz Shafei (orcid.org/0000-0001-5677-6324), and Abhijit Kulkarni (orcid.org/0000-0002-7657-5586)		8. Performing Organization Report No. InTrans Project 16-580	
9. Performing Organization Name and Address Bridge Engineering Center Iowa State University 2711 South Loop Drive, Suite 4700 Ames, IA 50010-8664		10. Work Unit No. (TRAIS)	
		11. Contract or Grant No.	
12. Sponsoring Organization Name and Address Iowa Highway Research Board Iowa Department of Transportation 800 Lincoln Way Ames, Iowa 50010		13. Type of Report and Period Covered Final Report	
		14. Sponsoring Agency Code IHRB Project TR-711	
15. Supplementary Notes Visit www.intrans.iastate.edu for color pdfs of this and other research reports.			
16. Abstract <p>Although bridge designers commonly use rules-of-thumb with regard to the geometry of the bridge deck overhang, these rules-of-thumb generally consider only the deck strength and deflection limits, and the effect due to construction loads during deck placement is often overlooked.</p> <p>This project investigated exterior girder rotation, girder and formwork deflection, and the effect of skew during bridge deck placement through a field review of construction practices and both a numerical, analytical study and a parametric, sensitivity study using calibrated finite element models.</p> <p>Three bridge construction projects were selected for field evaluation during deck placement. The projects were selected for their representation of variables of interest that included skew, relative girder depth, and span length.</p> <p>The parametric study involved six different parameters that were identified to investigate: brace strength, skew angle, diaphragm spacing, girder spacing, span ratio, and girder flange thickness. Three load cases were studied for each of the six parameters. Timber blocking and compression struts as temporary bracings were modeled using compression-only elements by providing the axial stiffness of the members.</p> <p>Key findings from the field review of construction practices and from the analytical and parametric studies, as well as overall findings, are included in this report, along with recommendations for future research.</p> <p>Of note, it appears that the cause of any possible deck thinning (or the greatest deflection and/or rotation of the girders) is a result of differential deflections, and not from the rotation of the exterior girders. While the bracing methods considered in this research were effective at restraining girder rotation for straight bridges or those with low skew, they were not as effective at reducing differential deflections caused by the concentrated screed load.</p> <p>While differential deflections during deck placement are not surprising due to this load location, the field data showed that, while the bridge does begin to return to its original location, there is permanent differential deflection of the bridge cross-section even after the screed load is off the bridge.</p>			
17. Key Words bridge deck reconstruction—bridge widening—exterior girder rotation—skewed bridges		18. Distribution Statement No restrictions.	
19. Security Classification (of this report) Unclassified.	20. Security Classification (of this page) Unclassified.	21. No. of Pages 124	22. Price NA

INVESTIGATION OF EXTERIOR GIRDER ROTATION AND THE EFFECT OF SKEW DURING DECK PLACEMENT

**Final Report
August 2019**

Principal Investigator

Brent Phares, Research Associate Professor
Bridge Engineering Center, Iowa State University

Co-Principal Investigator

Behrouz Shafei, Assistant Professor
Department of Civil, Construction, and Environmental Engineering, Iowa State University

Research Assistant

Abhijit Kulkarni

Authors

Katelyn Freeseaman, Brent Phares, Behrouz Shafei, and Abhijit Kulkarni

Sponsored by

Iowa Highway Research Board
and Iowa Department of Transportation
(IHRB Project TR-711)

Preparation of this report was financed in part
through funds provided by the Iowa Department of Transportation
through its Research Management Agreement with the
Institute for Transportation
(InTrans Project 16-580)

A report from

Bridge Engineering Center

Iowa State University

2711 South Loop Drive, Suite 4700

Ames, IA 50010-8664

Phone: 515-294-8103 / Fax: 515-294-0467

www.intrans.iastate.edu

TABLE OF CONTENTS

ACKNOWLEDGMENTS	xi
EXECUTIVE SUMMARY	xiii
CHAPTER 1. INTRODUCTION	1
Background	1
Goal	2
Report Layout	2
CHAPTER 2. LITERATURE REVIEW	3
Construction Loads	3
Failure Mechanisms	9
Bracing Techniques	11
Previous Research	12
CHAPTER 3. FIELD REVIEW OF CONSTRUCTION PRACTICES	16
Instrumentation	16
Cedar Fork Bridge Widening Project	18
Maple Bridge Construction Project	24
BNSF Railway Bridge Construction Project	39
CHAPTER 4. ANALYTICAL STUDY	48
Finite Element Modeling Techniques	48
Finite Element Analysis of Maple Bridge	50
Finite Element Analysis Results and Comparison with Field Investigations (Maple Bridge)	53
Finite Element Analysis of BNSF Railway Bridge	57
Finite Element Analysis Results and Comparison with Field Investigation (BNSF Railway Bridge)	59
Iowa DOT 160 ft Standard Bridge	63
CHAPTER 5. PARAMETRIC STUDY	73
Brace Strength	75
Skew Angle	79
Diaphragm Spacing	86
Girder Spacing	90
Span Ratio	95
Girder Flange Thickness	99
CHAPTER 6. FINDINGS AND CONCLUSIONS	104
REFERENCES	107

LIST OF FIGURES

Figure 1. Typical overhang formwork schematic (left) and in-field example (right).....	4
Figure 2. Finishing screed for deck construction.....	5
Figure 3. Skewed finishing screed.....	6
Figure 4. Screed rail placement on overhang formwork.....	6
Figure 5. Global superstructure distortion	9
Figure 6. Oil-canning	10
Figure 7. Girder warping (left) and torsional distortion (right)	10
Figure 8. Bracing examples: concrete diaphragms (top left), top bracing bars (top right), steel diaphragms (bottom left), and timber blocking (bottom right).....	11
Figure 9. Diagonal tie bar connected from exterior girder to first interior girder (left) and transverse tie bars connected from exterior girder to exterior girder (right).....	12
Figure 10. Girder rotation for experimental steel girder bridges	13
Figure 11. Sample instrumentation setup.....	17
Figure 12. Underside of Cedar Fork Bridge showing overhang	18
Figure 13. Cedar Fork Bridge screed orientation relative to deck skew	19
Figure 14. Screed traveling over an instrumented cross-sectional location of the Cedar Fork Bridge.....	20
Figure 15. Typical Cedar Fork Bridge gage layout	20
Figure 16. Cedar Fork Bridge instrumented cross-sectional locations	21
Figure 17. Cedar Fork Bridge tilt data for all locations	22
Figure 18. Cedar Fork Bridge maximum and residual rotations	23
Figure 19. Maple Bridge construction project	24
Figure 20. Screed orientation for the Maple Bridge	25
Figure 21. Updated bracing of the Maple Bridge	26
Figure 22. Typical unbraced dry run gage layout for the Maple Bridge	27
Figure 23. Maple Bridge instrumented unbraced dry run cross-sectional locations.....	27
Figure 24. Maple Bridge instrumented braced dry run cross-sectional locations.....	28
Figure 25. Maple Bridge instrumented braced deck pour cross-sectional locations	29
Figure 26. Maple Bridge instrumentation for the east (left) and west (right) spans during the braced deck pour	29
Figure 27. Maple Bridge rotation of the north exterior girder (center span) during all three runs	30
Figure 28. Maple Bridge rotation of the north exterior girder (east span) during all three runs.....	31
Figure 29. Maple Bridge deflection of the north formwork bracket (east span) during all three runs.....	32
Figure 30. Maple Bridge deflections of brackets and girders (east span) during deck placement	33
Figure 31. Maple Bridge deflections of brackets and girders (west span) during deck placement	34
Figure 32. Maple Bridge deflections of brackets and girders (east span) during all three runs	35
Figure 33. Maple Bridge deflection data for brackets and girders (east span) during deck placement	36

Figure 34. Maple Bridge deflection data for brackets and girders (west span) during deck placement	37
Figure 35. Maple Bridge dead load design deflections.....	38
Figure 36. BNSF Railway Bridge.....	39
Figure 37. Screed orientation for the 45° skew BNSF Railway Bridge	40
Figure 38. Temporary timber blocking locations in the exterior bays of the BNSF Railway Bridge.....	41
Figure 39. BNSF Railway Bridge instrumentation plan.....	42
Figure 40. BNSF Railway Bridge exterior girder field instrumentation	42
Figure 41. BNSF Railway Bridge deflection data for cross-section perpendicular to roadway orientation.....	43
Figure 42. BNSF Railway Bridge deflection data for cross-section along skew.....	44
Figure 43. Selected deflection data for cross-section perpendicular to roadway of BNSF Railway Bridge	45
Figure 44. Selected deflection data for cross-section along skew of BNSF Railway Bridge.....	45
Figure 45. BNSF Railway Bridge rotation data for south exterior girder	46
Figure 46. Selected rotation data for south exterior girder of BNSF Railway Bridge.....	47
Figure 47. Overhang details per construction documents (left) and FEA model (right)	50
Figure 48. Section properties of horizontal channel and vertical and diagonal legs	50
Figure 49. Maple Bridge model.....	51
Figure 50. Screed weight and dimensions	52
Figure 51. Bracing cases analyzed for the Maple Bridge	52
Figure 52. Maple Bridge north girder deflection.....	53
Figure 53. Maple Bridge south girder deflection.....	54
Figure 54. Maple Bridge north girder rotation.....	54
Figure 55. Maple Bridge south girder rotation	55
Figure 56. Maple Bridge north bracket deflection.....	55
Figure 57. Maple Bridge south bracket deflection.....	56
Figure 58. BNSF Railway Bridge model.....	57
Figure 59. Instrumentation plan of the BNSF Railway Bridge	58
Figure 60. BNSF Railway Bridge maximum cross-section deflection.....	59
Figure 61. BNSF Railway Bridge minimum cross-section deflection	60
Figure 62. BNSF Railway Bridge maximum diagonal deflection.....	60
Figure 63. BNSF Railway Bridge minimum diagonal deflection.....	61
Figure 64. BNSF Railway Bridge maximum diagonal rotation	61
Figure 65. BNSF Railway Bridge minimum diagonal deflection.....	62
Figure 66. BNSF Railway Bridge maximum south girder rotation.....	62
Figure 67. BNSF Railway Bridge minimum south girder rotation.....	63
Figure 68. Iowa DOT 160 ft Standard Bridge model	64
Figure 69. Cases investigated for 160 ft Standard Bridge	64
Figure 70. Span 1 vehicle and wet concrete load for 160 ft Standard Bridge	66
Figure 71. Span 2 vehicle and wet concrete load for 160 ft Standard Bridge	66
Figure 72. Span 3 vehicle and wet concrete load for 160 ft Standard Bridge	66
Figure 73. 160 ft Standard Bridge north girder deflection.....	67
Figure 74. 160 ft Standard Bridge south girder deflection	67
Figure 75. 160 ft Standard Bridge north girder rotation	68

Figure 76. 160 ft Standard Bridge south girder rotation	68
Figure 77. 160 ft Standard Bridge north bracket deflection	69
Figure 78. 160 ft Standard Bridge south bracket deflection	69
Figure 79. 160 ft Standard Bridge north girder deflection.....	70
Figure 80. 160 ft Standard Bridge south girder deflection	70
Figure 81. 160 ft Standard Bridge north girder rotation	71
Figure 82. 160 ft Standard Bridge south girder rotation.....	71
Figure 83. 160 ft Standard Bridge north bracket deflection	72
Figure 84. S160 ft Standard Bridge south bracket deflection.....	72
Figure 85. Iowa DOT 260 ft Standard Bridge model	73
Figure 86. Span 1 vehicle and wet concrete load for 260 ft Standard Bridge	74
Figure 87. Span 2 vehicle and wet concrete load for 260 ft Standard Bridge	74
Figure 88. Span 3 vehicle and wet concrete load for 260 ft Standard Bridge	75
Figure 89. 260 ft Standard Bridge north bracket deflection (brace strength)	76
Figure 90. 260 ft Standard Bridge south bracket deflection (brace strength).....	76
Figure 91. 260 ft Standard Bridge north girder deflection (brace strength)	77
Figure 92. 260 ft Standard Bridge south girder deflection (brace strength)	77
Figure 93. 260 ft Standard Bridge north girder rotation (brace strength).....	78
Figure 94. 260 ft Standard Bridge south girder rotation (brace strength).....	78
Figure 95. 260 ft Standard Bridge rotation difference for north girder (brace strength)	79
Figure 96. 260 ft Standard Bridge rotation difference for south girder (brace strength).....	79
Figure 97. 30° skew 260 ft Standard Bridge framing plan	80
Figure 98. 45° skew 260 ft Standard Bridge framing plan	80
Figure 99. 260 ft Standard Bridge Span 1 vehicle and wet concrete load for skewed bridges.....	81
Figure 100. 260 ft Standard Bridge Span 2 vehicle and wet concrete load for skewed bridges.....	81
Figure 101. 260 ft Standard Bridge Span 3 vehicle and wet concrete load for skewed bridges.....	81
Figure 102. 260 ft Standard Bridge north bracket deflection (skew angle).....	82
Figure 103. 260 ft Standard Bridge south bracket deflection (skew angle).....	82
Figure 104. 260 ft Standard Bridge north girder deflection (skew angle).....	83
Figure 105. 260 ft Standard Bridge south girder deflection (skew angle).....	83
Figure 106. 260 ft Standard Bridge north girder rotation (skew angle).....	84
Figure 107. 260 ft Standard Bridge south girder rotation (skew angle)	84
Figure 108. 260 ft Standard Bridge rotation difference for north girder (skew angle).....	85
Figure 109. 260 ft Standard Bridge rotation difference for south girder (skew angle)	85
Figure 110. 260 ft Standard Bridge north bracket deflection (diaphragm spacing)	86
Figure 111. 260 ft Standard Bridge south bracket deflection (diaphragm spacing)	87
Figure 112. 260 ft Standard Bridge north girder deflection (diaphragm spacing).....	87
Figure 113. 260 ft Standard Bridge south girder deflection (diaphragm spacing)	88
Figure 114. 260 ft Standard Bridge north girder rotation (diaphragm spacing)	88
Figure 115. 260 ft Standard Bridge south girder rotation (diaphragm spacing).....	89
Figure 116. 260 ft Standard Bridge rotation difference for north girder (diaphragm spacing)	89
Figure 117. 260 ft Standard Bridge rotation difference for south girder (diaphragm spacing)	90
Figure 118. 260 ft Standard Bridge north bracket deflection (girder spacing)	91

Figure 119. 260 ft Standard Bridge south bracket deflection (girder spacing).....	91
Figure 120. 260 ft Standard Bridge north girder deflection (girder spacing)	92
Figure 121. 260 ft Standard Bridge south girder deflection (girder spacing)	92
Figure 122. 260 ft Standard Bridge north girder rotation (girder spacing).....	93
Figure 123. 260 ft Standard Bridge south girder rotation (girder spacing)	93
Figure 124. 260 ft Standard Bridge rotation difference for north girder (girder spacing).....	94
Figure 125. 260 ft Standard Bridge rotation difference for south girder (girder spacing).....	94
Figure 126. 260 ft Standard Bridge north bracket deflection (span ratio).....	95
Figure 127. 260 ft Standard Bridge south bracket deflection (span ratio).....	96
Figure 128. 260 ft Standard Bridge north girder deflection (span ratio)	96
Figure 129. 260 ft Standard Bridge south girder deflection (span ratio)	97
Figure 130. 260 ft Standard Bridge north girder rotation (span ratio).....	97
Figure 131. 260 ft Standard Bridge south girder rotation (span ratio).....	98
Figure 132. 260 ft Standard Bridge rotation difference for north girder (span ratio)	98
Figure 133. 260 ft Standard Bridge rotation difference for south girder (span ratio).....	99
Figure 134. 260 ft Standard Bridge north bracket deflection (flange thickness).....	100
Figure 135. 260 ft Standard Bridge south bracket deflection (flange thickness).....	100
Figure 136. 260 ft Standard Bridge north girder deflection (flange thickness)	101
Figure 137. 260 ft Standard Bridge south girder deflection (flange thickness).....	101
Figure 138. 260 ft Standard Bridge north girder rotation (flange thickness).....	102
Figure 139. 260 ft Standard Bridge south girder rotation (flange thickness)	102
Figure 140. 260 ft Standard Bridge rotation difference for north girder (flange thickness).....	103
Figure 141. 260 ft Standard Bridge rotation difference for south girder (flange thickness)	103

LIST OF TABLES

Table 1. State overhang guidelines	8
Table 2. Bracing suggestions	14
Table 3. Characteristics of field-reviewed bridge construction projects	16
Table 4. Summary of object types used in FEA	49
Table 5. Section properties of objects used in Ida County Maple Bridge FEM	51
Table 6. Description of loads in the FEA model of the Maple Bridge	52
Table 7. Load cases for the BNSF Railway Bridge	58
Table 8. Load cases for the 160 ft Standard Bridge.....	65
Table 9. Loads considered for parametric study on the 260 ft Standard Bridge	74
Table 10. 260 ft Standard Bridge percentage of reduction in rotation with temporary bracing system during deck placement depending on skew angle.....	86

ACKNOWLEDGMENTS

This work was sponsored by the Iowa Highway Research Board and the Iowa Department of Transportation. The authors would like to thank the contractors and county engineers involved in the projects that were selected for field documentation. The contributions of the technical advisory committee members are also appreciated:

- Ahmad Abu-Hawash
- Dean Bierwagen
- Curtis Carter
- David Evans
- Mike Nop
- Gary Novey
- Wayne Sunday

EXECUTIVE SUMMARY

It is vitally important that, when new bridges are constructed (or when existing bridges are widened), the most current and best construction practices are followed so that the final product has a high likelihood of achieving the target design life.

Although bridge designers commonly use rules-of-thumb with regard to the geometry of the bridge deck overhang, these rules-of-thumb generally consider only the deck strength and deflection limits, and the effect due to construction loads during deck placement is often overlooked.

This project investigated exterior girder rotation, girder and formwork deflection, and the effect of skew during bridge deck placement through a field review of construction practices and both a numerical, analytical study and a parametric, sensitivity study using calibrated finite element models.

Three bridge construction projects were selected for field evaluation of bridge behavior during deck placement. Two of the projects were new construction and one was a widening project. The projects were selected for their representation of variables of interest that included skew, relative girder depth, and span length.

All three bridges were instrumented before deck placement using a combination of strain gages, tiltmeters, and deflection transducers. Strain, rotation, and deflection data were captured throughout the duration of each deck pour and also during two dry runs with the screed on the Maple Bridge. The researchers then analyzed and summarized the results.

To provide supplemental data while also validating the field observations, analytical models were created that incorporated a variety of variables thought to affect girder rotation. This analysis helped to provide an understanding of the effects caused by the loads when applied over the portion of overhang on the exterior girder in terms of deflection and rotation using finite element analysis (FEA) by correlating the results with the field data.

Upon calibration, a parametric study was conducted to expand upon the understanding of the structural behavior of bridges when different loads, such as concrete weight and screed load, are acting on them.

The three-dimensional (3D) FEA was performed using the structural analysis and design software for bridges, CSiBridge. The numerical study included the investigation of effects of different combinations of bracing, including cases of no timber blocking, only timber blocking, only temporary bracing, and temporary bracing with timber blocking—on three different bridges.

Finite element models (FEMs) for the Maple Bridge in Ida County and the BNSF Railway Bridge in Adams County were developed and used to compare with results from their field

investigations, while a 160 ft bridge with 0° skew from Iowa Department of Transportation (DOT) bridge standards was also modeled and studied for various configurations.

To investigate the parameters that affect the rotation and deflection of exterior girders, as well as the deflection of brackets, the researchers modeled and used the Iowa DOT 260 ft Standard Bridge. The goal of the parametric study was to identify the parameters for which the rotation and deflection of the exterior girders and brackets were most sensitive.

The parametric study involved six different parameters that were identified to investigate: brace strength, skew angle, diaphragm spacing, girder spacing, span ratio, and girder flange thickness. Three load cases were studied for each of the six parameters. The load cases were applied at the mid-span of the interior and each exterior span.

Temporary bracing by means of timber blocking and diagonal compression struts was modeled using compression-only elements by providing the axial stiffness of the members. This modeling technique is expected to simulate the actual situation of the bridge, as these members are expected to participate when subjected to a compression load.

Key Findings from Field Review of Construction Practices

- Concern for exterior girder rotation increased with an increase in skew. This is due to the unequal loading of the exterior girders when the screed is not oriented along the skew.
- The field review showed that the concrete is being placed right in front of the screed to keep up with placement, rather than placing the concrete unequally in front of the screed to combat the unequal loading of concrete caused by the skew during placement.
- While exterior girder rotation was evident for all instrumented deck placements, differential deflections were also present and seemed to have a greater effect on the deck thickness deficiencies that were observed at the Maple Bridge.
- The greatest exterior girder rotation observed for the three instrumented bridges was just over 1°, with a residual rotation of 0.75°. The greatest deflection observed during placement was approximately 2.5 in., with a residual deflection of just over 1 in.
- Temporary bracing of the exterior bays is not common practice based on conversations with contractors and field observations. Contractors mentioned that for other projects, if bracing was used by the contractor but was not called for in the plans, timber blocking was most often used. While this is an effective means for reducing girder rotation, it does not protect against differential deflection.
- Of the three deck placements that were monitored in the field, deck thinning was only noticed at one site, and it was not overly significant.

Key Findings from Analytical and Parametric Study

- The models confirmed that both differential deflection and exterior girder rotation can lead to deck deficiencies during deck placement, with the largest contribution coming from the differential deflection.
- Diagonal bracing in the exterior bays, combined with timber blocking in the adjacent bay, greatly reduced the exterior girder rotation for straight bridges. This bracing system also reduced the deflection performance, although to a limited extent.
- The skew angle influences the deflection and rotation of exterior girders. Deflection and rotation are not similar in the opposite two exterior girders. Unsymmetrical load distribution due to skewness increases the deflection and rotation of exterior girders, depending on the skew angle. The temporary bracing system was highly effective in reducing rotation of the 0° bridge. However, for a skew angle 30° and greater, the temporary bracing was not found to be effective in reducing rotation.

Key Findings Overall

Based on the modeling and field investigation efforts, it appears that the predominant cause of any possible deck thinning (or the greatest rotation and/or deflection of the girders) is a result of differential deflections, not from the rotation of exterior girders. While the bracing methods considered in this research were effective at restraining girder rotation for straight bridges or those with low skew, they were not as effective at reducing differential deflections caused by the concentrated screed load.

While differential deflections during deck placement are not surprising due to this load location, the field data showed that, while the bridge does begin to return to its original location, there is permanent differential deflection of the bridge cross-section even after the screed load is off the bridge.

Recommendations for Future Research

Further work is needed to address concerns regarding differential deflections and their impact on the long-term behavior and performance of bridges. In addition to differential deflection concerns, more work is also needed to address the effect of skew, as neither of these variables were the direct focus of this existing research. Of particular interest is determining what level of skew necessitates the positioning of the screed along the skew, rather than perpendicular to the roadway, as is often the current practice.

Implementation Readiness and Benefits

Implementation of this work will help the Iowa DOT Office of Bridges and Structures develop both design guidance and construction procedure recommendations that are aimed at reducing girder rotation (and especially for exterior girders) due to eccentric loads during deck placement. The goal is for the bridge designers to be able to provide guidance on the stiffness and/or bracing details for various configurations before the design is finalized.

The results of the proposed future work will also help the Office of Bridges and Structures to determine a skew threshold for which the finishing machine should be oriented parallel to the skew as opposed to the more common position perpendicular to the bridge centerline. When structural details cannot be provided that counteract the eccentric loads, the office can prescribe under which circumstances the deck placement equipment can be used in various orientations.

CHAPTER 1. INTRODUCTION

Background

With many of the nation's bridges approaching (or having already exceeded) their original design life, bridge replacement options, techniques, and technologies continue to need to advance to meet the challenges faced by the bridge engineering community. Recent statistics reveal there are about 600,000 bridges on the highway system and that approximately 25%, by deck area, are considered either structurally deficient or functionally obsolete. Although the situation has improved some in recent years, a significant problem still exists given the number of bridges needing regular replacement.

It is vitally important that, when constructed (or when only decks are replaced), the most current and best construction practices are followed so that the final product has a high likelihood of achieving the target design life. It has been observed that current construction practices associated with constructing bridge decks sometimes result in excessive out-of-plane and torsional loads on exterior girders. Structurally, this can result in decks that are too thin or girders with excessive (and unintended) internal stresses. Functionally, this can result in bridges that are difficult to maintain or have rideability issues.

During bridge deck concrete placement, contractors use a deck finishing machine to level the concrete at the correct elevation. Although there are various types of finishing machines, they all have the following characteristics: they ride on tracks or rails that are set on top or outside of the forms for the copings or barrier rails and they have adjustable screeds that may be adjusted to different elevations. Many finishing machines also have augers that may consolidate the concrete before the concrete is leveled by the screed, and they have guide tracks from which the screed and auger are suspended. Concrete is spread, compacted, and finished by attachments suspended from the carriage on each pass of the carriage back and forth across the bridge deck. On most projects, the carriage equipment is adjusted so concrete is worked in a direction transverse to the bridge centerline. These screeds have large loads that are concentrated on the exterior overhang supports, resulting in possible rotation and/or deflection of the exterior girders.

Field problems and difficulties during steel bridge construction have been reported in Iowa where the fascia girders experienced excessive rotation during construction. Many contractors prefer to place the screed rail on the formed exterior overhang since the finishing machine can finish the vast majority of the deck. When the screed rail is located outside the concrete placement, labor-intensive overhang placements are not necessary (Suprenant 1994). However, for steel girder bridges, the unbalanced overhang loading can lead to both local and global instability.

Locally, the overhang brackets often exert a large force on the web plate that can distort the web and increase the magnitude of any plate imperfection (Yang et al. 2010). Steel girder bridges require adequate lateral support of the compression flange to avoid being subjected to lateral torsional buckling during concrete deck placement (Roddis et al. 2008). Girder buckling capacity is a function of cross-frame diaphragm spacing, strength, and stiffness. For completed bridge

structures, the in-place concrete deck provides continuous structural lateral bracing for bridge girders. However, during construction, the deck is not present to provide the lateral bracing for the girders, which could result in lateral torsional buckling of the exterior girders. Therefore, alternate means of bracing might need to be provided.

Goal

This project aimed to address these concerns via the field documentation of deck placements, a parametric study using calibrated finite element (FE) models, and recommendations for future deck placements to avoid potential deck thinning or exterior girder movement/rotation.

Report Layout

The chapters in the remainder of this report follow the tasks that were undertaken for this project:

- Chapter 2: Literature Review
- Chapter 3: Field Review of Construction Practices
- Chapter 4: Analytical Study
- Chapter 5: Parametric Study
- Chapter 6: Findings and Recommendations

CHAPTER 2. LITERATURE REVIEW

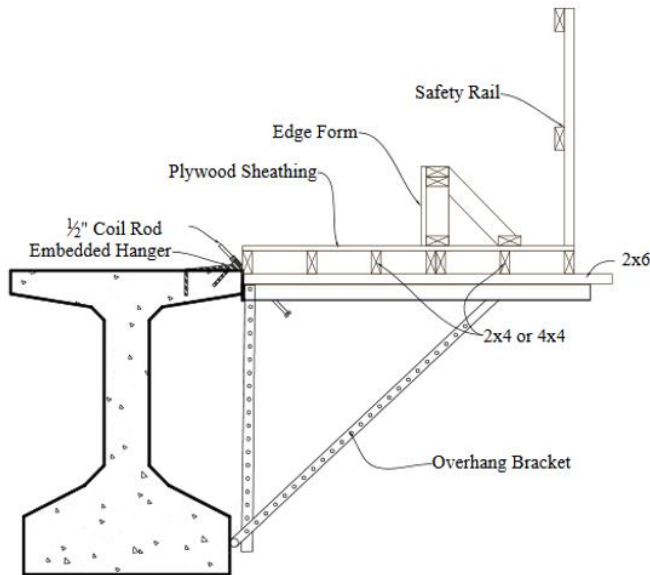
The issues commonly associated with deck construction can be exacerbated when economics result in designs with fewer and fewer girder lines. This situation can result in bridges with large overhangs and girder spacing. Furthermore, the practice of using common girder sizes for all girder lines limits the bridge designer's ability to economically design the fascia girder to withstand additional construction loads. Although designers commonly use rules-of-thumb with regard to the geometry of the overhang, these rules-of-thumb generally consider only the deck strength and deflection limits, and the effect due to construction loads is often overlooked (Yang et al. 2010).

In general, large eccentric construction loads come from two sources: large overhangs and deck finishing equipment typically positioned at the edge of the overhang. Combined, the resulting torsional loads have resulted in issues in both steel and concrete superstructures. In some cases, the most extreme situations have occurred during bridge widening projects. In the following sections, the loading on exterior girders, as well as the effects of the induced torsion, are outlined.

Construction Loads

Bridge deck construction and replacement methods place the following loads onto the exterior girder through overhang brackets: overhang formwork, fresh concrete weight, finishing screed, and construction personnel live loads. These loads all induce torsional moments on the fascia girders and must be taken into account when considering girder rotation.

Typical overhang formwork is shown in Figure 1.



Clifton and Bayrak 2008

Figure 1. Typical overhang formwork schematic (left) and in-field example (right)

The overhang formwork includes an overhang bracket, plywood sheathing, and edge formwork, as well as a safety rail along the edge of the overhang. Overhang brackets are typically attached to the bridge girders via coil rod and hangers embedded in the top flange, which are typically spaced 3 to 6 ft apart. All other loads for bridge deck construction are applied to the girder through this formwork via the overhang brackets.

Additional loads are applied to the girder through overhang formwork due to finishing efforts during construction. The largest loads of this type come from the finishing screed, as shown in Figure 2.



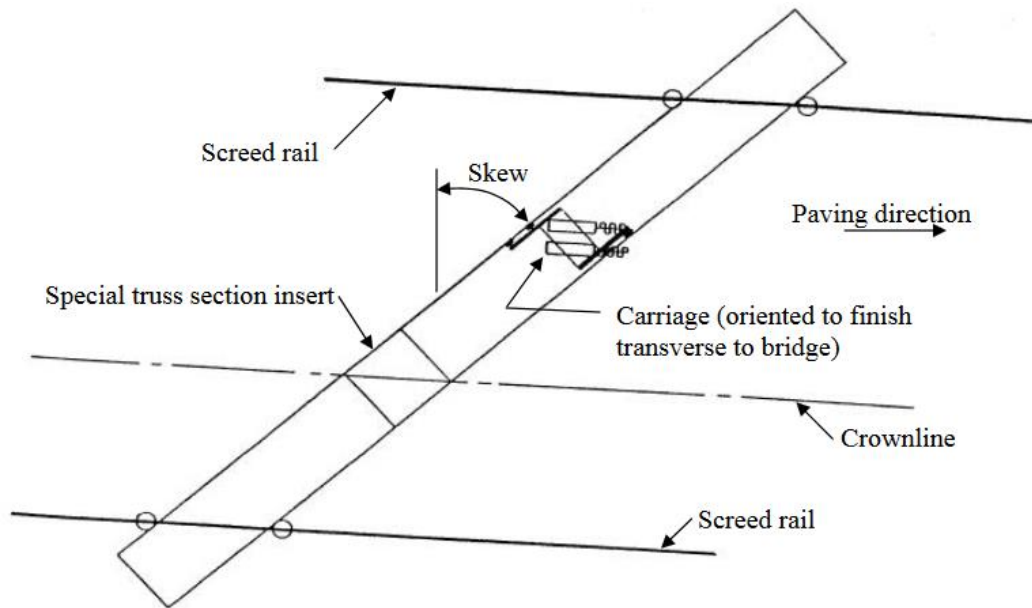
GOMACO 2016, © 1998–2019 GOMACO Corporation, used with permission

Figure 2. Finishing screed for deck construction

The deck finishing machine is used to level the concrete at the correct elevation. Although there are various types of finishing machines, they all have the following characteristics: they ride on tracks or rails that are set on top or outside of the forms for the copings or barrier rails and they have adjustable screeds that may be adjusted to different elevations. Many finishing machines also have augers that may consolidate the concrete before the concrete is leveled by the screed, and they have guide tracks from which the screed and auger are suspended. Concrete is spread, compacted, and finished by attachments suspended from the carriage on each pass of the carriage back and forth across the bridge deck. On most projects, the carriage equipment is adjusted so the concrete is worked in a direction transverse to the bridge centerline. This equipment consists of augers, finishing drums (sometimes called rollers or cylinders), and float pans (Halvorsen 1992).

Some finishing equipment features boom trusses with automatic machine move-up at the end of each carriage pass and automatic cushioned carriage travel reversal (TEREX Corporation 2019). A traveling carriage strikes off, paves, and textures the concrete with augers, paving rollers, a drag pan, and texturing. Some roller pavers have adjustable dual augers that strike off excess concrete forward on every pass, which provides higher production and reduced labor. Also enhancing productivity, the roller pavers move forward automatically to position the paving rollers for the next paving pass. Bridge pavers are equipped to pave a variety of surfaces, including flat, parabolic, crowned, skewed, super-elevated, and tapered surfaces (TEREX Corporation 2019).

Finishing screeds can also be placed such that the truss is skewed with respect to the screed rails, as shown in Figure 3.

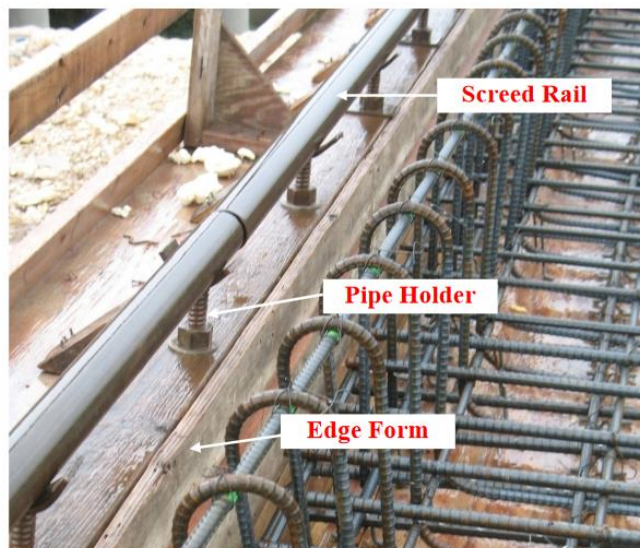


Ohio DOT 2007

Figure 3. Skewed finishing screed

This allows for concrete placement parallel to the skew of the substructure. The carriage can also be skewed with respect to the truss and should always be oriented transverse to the bridge for concrete finishing (Ohio DOT 2007). Skew is an important variable to consider when discussing exterior girder rotation and is further discussed later in this report.

The weight of the screed is supported by a screed rail on the edge of the overhang formwork, as shown in Figure 4.



Clifton and Bayrak 2008

Figure 4. Screed rail placement on overhang formwork

To eliminate or minimize the amount of hand finishing required, contractors often prefer that the screed rail be placed on the outer edge of the overhang formwork, thus creating a large moment arm for the heavy weight of the screed (Suprenant 1994). Field problems and construction difficulties in Iowa have been attributed to this screed placement during steel bridge construction.

State Guidelines

Many transportation departments provide guidelines on overhang geometry, but guidelines are generally based on rules of thumb (Yang et al. 2010). Typical bridge overhangs range from 3.5 to 6 ft and vary based on state specifications and design guidelines. A summary of some state specifications is shown in Table 1.

Table 1. State overhang guidelines

State	Specifications		
California	For composite box girders, 60 percent of the average distance center-to-center of flanges of adjacent boxes, but shall in no case exceed 6 ft (2004).		
Colorado	For precast concrete and steel I-girders, use maximum of center-to-center spacing $\div 3$ or flange \div web distance + 12 in. For steel box girders, use center-to-center spacing $\div 3$. Overhang criteria may be exceeded with approval from Staff Bridge Engineer (1991).		
Connecticut	Minimum of 4 ft or depth of the member (2003).		
Delaware	Normal overhang is 2 ft 6 in. Maximum overhang is half the beam spacing or 4 ft, whichever is less (2005).		
Florida	Use empirical design method for overhangs less than 6 ft and traditional design method for total deck overhang if less than 6 ft (2008).		
Kansas	Use Torsional Analysis of Exterior Girders (TAEG) software to determine torsional loads (2006).		
Maine	<i>Type of Beam</i>	<i>Beam Spacing</i>	<i>Maximum Deck Overhang</i>
	Structural Steel	Less than 9 ft	3 ft or depth of the beam
		9 ft to 10 ft 6 in.	1/3 of the beam spacing or depth of the beam
		Greater than 10 ft 6 in.	3 ft 6 in. or depth of beam
	Concrete	All	2 ft
Michigan	Follow typical details; maximum overhang = 2 ft 6 in.		
Montana	For steel girders, the overhang width restrictions (more strict of): 1. Not more than 0.30 to 0.35 times the beam spacing to balance moments in interior and exterior beams 2. Not more than the depth of the beam, or 3. Not more than 1,200 mm. For prestressed concrete beams, the overhang dimension are standardized (2002).		
Nebraska	Max overhang = 4 ft 6 in. For up to five-girder bridges, minimize overhang, and, if the exterior girder controls, use exterior girder design for all girders. For more than five-girder bridges, minimize the overhang and use the interior girder design for the entire bridge (2006).		
Nevada	Deck overhangs shall be considered as falsework and designed as such (2001).		
New York	The recommended maximum overhang of a concrete deck slab beyond the centerline of the steel fascia I-girder is 4 ft. In addition, the maximum overhang for steel fascia I-girders less than 5 ft in depth should be limited to 3 ft. The use of an overhang greater than 3 ft with steel fascia I-girders less than 5 ft in depth requires a detailed analysis (2008).		
Ohio	In order to facilitate formwork 1. deck slab overhangs should not exceed 4 ft (2004).		
Oregon	Deck overhangs should be no more than one-half the span length (2004).		
South Carolina	Deck overhangs shall be designed in accordance with Section 13 of the LRFD Specifications.		
Texas	Maximum overhang is lesser of 3 ft 11 in. or 1.3 times the depth of the girder from the centerline of the beam (2001).		
West Virginia	For bridges with structurally continuous concrete barriers, the minimum total overhang width shall be 3.0 times the depth of the deck, measured from the center of the exterior girder (AASHTO 9.7.2.4). The maximum total overhang width shall be the smaller of 0.625 times the girder spacing and 6 ft (2004).		

Source: Fasl 2008

The Iowa DOT prefers that deck overhangs be a maximum of 4 ft, and they are typically 37 in. or 42 in., depending on bridge type (Iowa DOT 2016). Iowa DOT design guidelines also call for the following loads to be considered for girder designs with respect to constructability:

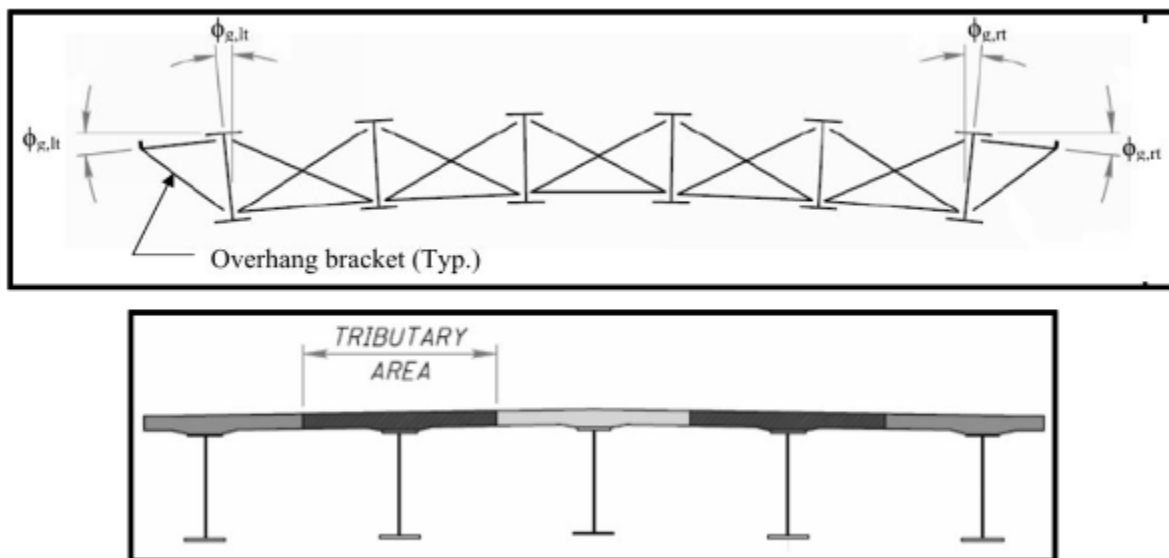
- Dead load of forms (0.010 ksf)

- Dead load of edge rail and walkway applied at edge of deck form (0.075 klf)
- Construction live load (0.050 ksf)
- Live load of finishing machine located along edge of the deck form (6 kips)
- Wind loads

The design manual also calls for the designer to consider the deck pouring sequence.

Failure Mechanisms

When failures do occur as a result of loads on the exterior girder, they are typically one of three failure types: global superstructure distortion, oil-canning, or girder warping. Global superstructure distortion is the distortion of the transverse section of the bridge caused by differential deflections between adjacent girders (see Figure 5).

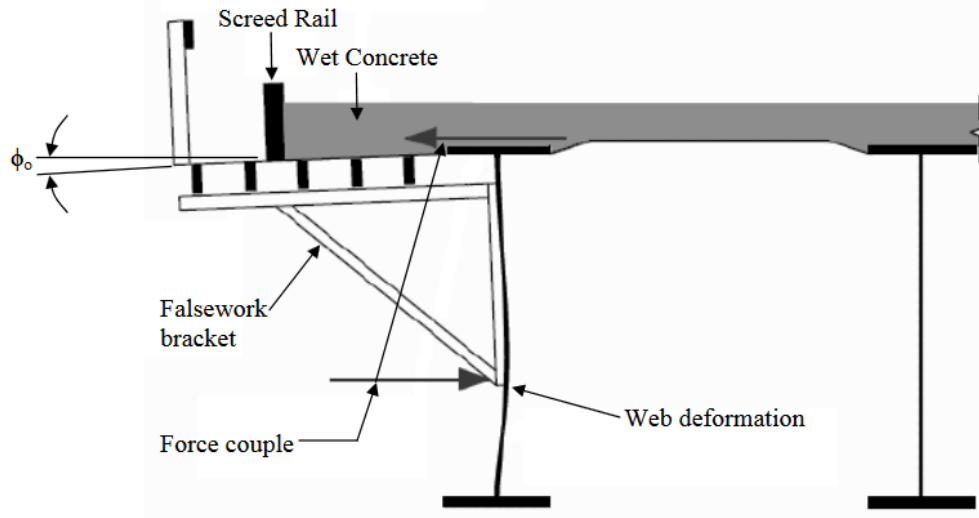


Shergalis and Law 2016

Figure 5. Global superstructure distortion

Global superstructure distortion most commonly occurs between the exterior girders and adjacent interior girders due to differing tributary load areas.

Oil-canning occurs when large lateral loads initiated from the cantilevered deck slab overhang bracket deform the girder web (see Figure 6).

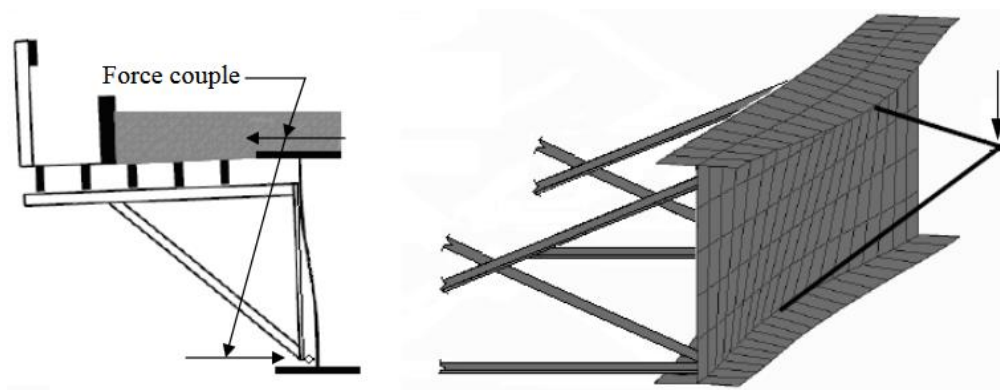


Ohio DOT 2007

Figure 6. Oil-canning

This type of failure has led to requirements for the point of contact of the bracket to be near the bottom flange of the exterior girder to reduce the deformation. For steel girder bridges, the unbalanced overhang loading can lead to both local and global instability. Locally, the overhang brackets often exert a significant force on the web plate that can distort the web and increase the magnitude of any plate imperfection (Yang et al. 2010).

Girder warping occurs due to loading on the exterior girder between points of lateral bracing due to the deck slab overhang formwork (see Figure 7).



Ohio DOT 2007

Figure 7. Girder warping (left) and torsional distortion (right)

The twist is produced due to girder warping and pure torsional distortion. This phenomenon is not an issue for pre-stressed I-beams.

Bracing Techniques

Steel girder bridges require adequate lateral support of the compression flange to avoid being subjected to lateral torsional buckling during concrete deck placement (Roddis et al. 2008). Girder buckling capacity is a function of cross-frame diaphragm spacing, strength, and stiffness. For completed bridge structures, the in-place concrete deck provides continuous structural lateral bracing for bridge girders. Whereas, during construction, the deck is not present to provide the lateral bracing for the girders and can result in lateral torsional buckling of the exterior girders. Therefore, alternative means of bracing may need to be provided.

Bracing elements have historically included transverse ties, diagonal ties, intermediate cross-frames, timber blocks, horizontal and diagonal steel pipes, and additional diaphragms. Some of these bracing types are shown in Figure 8.



Yang et al. 2010

Figure 8. Bracing examples: concrete diaphragms (top left), top bracing bars (top right), steel diaphragms (bottom left), and timber blocking (bottom right)

Cast-in-place diaphragms (Figure 8 top left) are expensive due to time-intensive form and casting efforts, so steel diaphragms (Figure 8 bottom left) are more common. In recent years, diaphragms are rarely used on concrete bridges, so temporary bracing such as top bracing bars (Figure 8 top right) and timber blocking (Figure 8 bottom right) have been used instead. Dislodging of diagonal timber blocking has been seen frequently in the field and renders the

system ineffective in handling twist. As such, horizontal timber blocking combined with top bracing bars has been used in place of diagonal blocking and has been more effective (Yang et al. 2010). Transverse and diagonal tie bars are shown in Figure 9.



Ashiquzzaman et al. 2016a

Figure 9. Diagonal tie bar connected from exterior girder to first interior girder (left) and transverse tie bars connected from exterior girder to exterior girder (right)

Tie bars can have corresponding constructability issues due to the presence of other bridge deck reinforcement.

In-plane bracing, sometimes referred to as wind bracing, can be used to provide lateral bracing for steel bridges. The elimination of in-plane steel bracing, which is a common practice in bridge superstructure design, places an increased significance on the bracing role of cross-frame diaphragms during deck placement (Roddis et al. 2008). To act as effective braces, the cross-frame diaphragms must be both strong and stiff enough to provide lateral stability to the compression flange of the exterior girders.

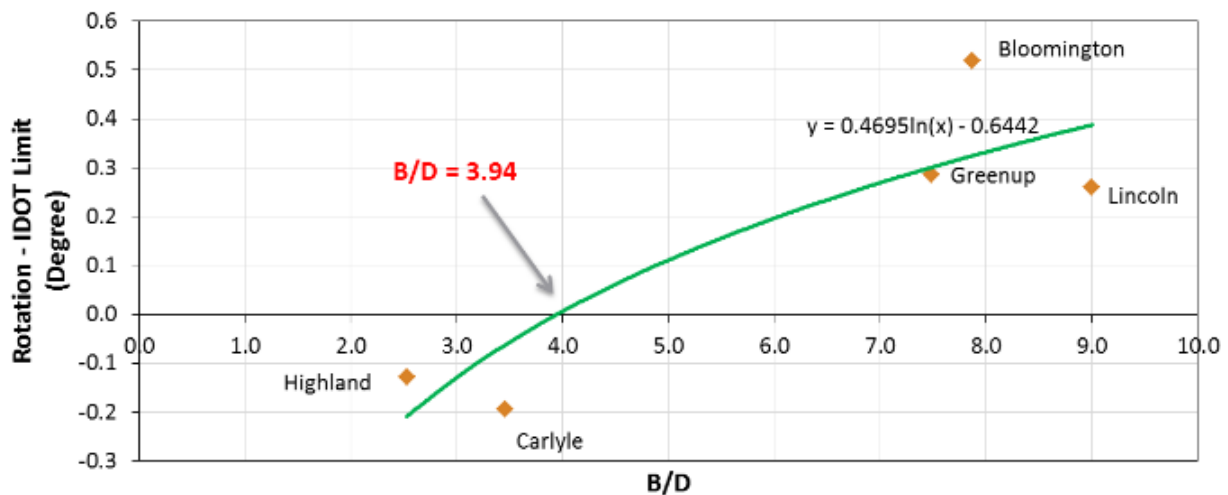
Previous Research

Previous research efforts have focused on the effect of bridge deck overhangs on exterior girders and the effectiveness of bracing elements to resist girder twist. A study performed for the Kansas DOT (KDOT) developed a torsional analysis program, called the Torsional Analysis of Exterior Girders (TAEG). This program uses the stiffness method to calculate the stresses and deflections of the flanges due to torsional loads, resulting in the forces on brackets and diaphragms. TAEG can be used as a design tool to evaluate the response of exterior girders when eccentric loading is applied, with specific handling of the effect of temporary supports (Roddis et al. 1999).

Work has also been done to determine the performance of concrete flanges in withstanding the construction loads during bridge deck overhang placement (Clifton and Bayrak 2008). Other work has focused on the performance of bracing elements.

A comprehensive study on the effectiveness of girder rotation prevention systems was completed for the Illinois DOT (IDOT) in 2016 (Ashiquzzaman et al. 2016a). This study looked at six steel-girder bridges and one concrete-girder bridge, all of which were instrumented during deck construction with tilt sensors and strain gages. The researchers found that construction loads had a significant effect on exterior girder rotation, and that skewed bridges had more rotation compared to zero-skew bridges as a result of the increased torsional moments due to bridge geometry. The concrete girder bridge experienced minimal rotation, most likely due to its torsional stiffness and girder rigidity. For all bridges, it was generally seen that the rotation of the first interior girder was negligible compared to exterior girder rotation.

The researchers also used a scaled bridge prototype to consider bracing elements including transverse ties, diagonal ties, intermediate cross-frames, timber blocks, and horizontal and diagonal steel pipes. The results showed that the most effective bracing system was intermediate cross-frames with top and bottom angles in addition to straight and diagonal transverse ties that were currently used by IDOT. An alternative was to place transverse ties and diagonal pipes in the exterior panels while maintaining a maximum spacing-to-girder depth ratio of 3.94 (see Figure 10).

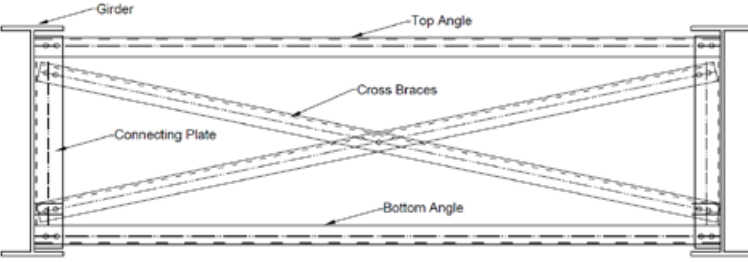
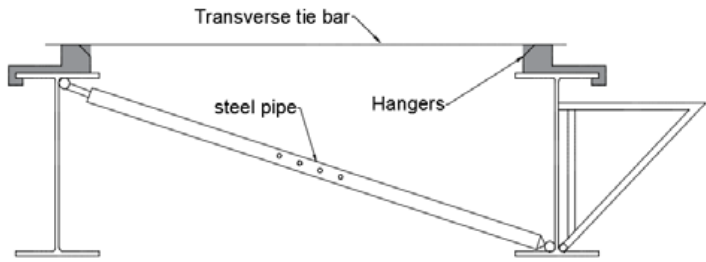
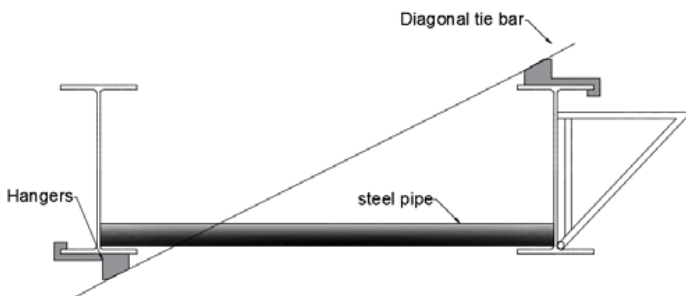


B = diaphragm spacing and D = girder depth
Ashiquzzaman et al. 2016a

Figure 10. Girder rotation for experimental steel girder bridges

The summarized suggestions for reduced girder rotation from Ashiquzzaman et al. (2016a) are shown in Table 2.

Table 2. Bracing suggestions

Recommended Options for Field Implementation	Bracing System Detail	Remarks
1. Intermediate cross frames with top- and bottom-angle section		<ul style="list-style-type: none"> • Avoids the need for ties, tie bars, and quality control • No close observation required in the field to maintain quality control • Economically efficient
2. Transverse ties (exterior girder to first interior girder) + diagonal pipe		<ul style="list-style-type: none"> • Diagonal pipes are reusable but heavy and difficult to install • Does not eliminate need for quality control for ties and pipes • Not as economically efficient
3. Adjusted diagonal ties + horizontal pipe		<ul style="list-style-type: none"> • Diagonal ties require modification of the hangers to proper angle • Does not eliminate the need for quality control of ties and steel pipes • Steel pipes are reusable • Not as economically efficient

Source: Ashiquzzaman et al. 2016a

The recommended systems include intermediate cross-frames with angle sections on the top and bottom, transverse ties and diagonal pipes, and diagonal ties and horizontal pipes.

The general findings of this study were that the rotation of the girder increased when the ratio of diaphragm or cross-frame spacing to bridge girder depth increased. The skew angle of the bridge was also seen to increase the rotation on the side of the bridge (which was farther from the piers) (Ashiquzzaman et al. 2016a).

Field studies have seen improper or inadequate tightening of transverse tie bars, as well as bending of diagonal tie bars due to unadjusted angles of the bars. Additional field observations have shown that proper installation of tie bars is difficult due to the presence of other deck reinforcement, and that timber blocking was often improperly shimmed (Ashiquzzaman et al. 2016b). In general, a lack of quality control for rotation prevention systems has been seen by a number of researchers.

CHAPTER 3. FIELD REVIEW OF CONSTRUCTION PRACTICES

Three bridge construction projects were selected for field evaluation of bridge behavior during deck placement. The projects represented variables of interest that included skew, relative girder depth, and span length. A summary of the bridge characteristics is included in Table 3.

Table 3. Characteristics of field-reviewed bridge construction projects

Bridge	FHWA No.	Project Type	Span Lengths	Deck Overhang	Skew	Girder Sizes
Cedar Fork	143850	Widening	45 ft 9 in., 58 ft 6 in., and 45 ft 9 in.	34 in.	15°	W24×84, W27×102
Maple	700805/29102	New Construction	102 ft, 136 ft, and 102 ft	37 in.	0°	W44×230, W44×290
BNSF Railway	59340	New Construction	78 ft, 104 ft, and 78 ft	37 in.	45°	W40×199, W40×167

Instrumentation

All three bridges were instrumented before and during deck placement using a combination of strain gages, tiltmeters, and deflection transducers. Strain, rotation, and deflection data were captured throughout the duration of each deck pour. Figure 11 shows a typical field instrumentation setup in which the tiltmeter is mounted to the web of the girder, strain gages are placed on the girder flange and formwork support bracket, and deflection chains are mounted to the girder flange and deck formwork. Note that while critical locations such as mid-span were often the intended gage location, if there was a diaphragm nearby, the gages were placed midway between the nearest diaphragms.

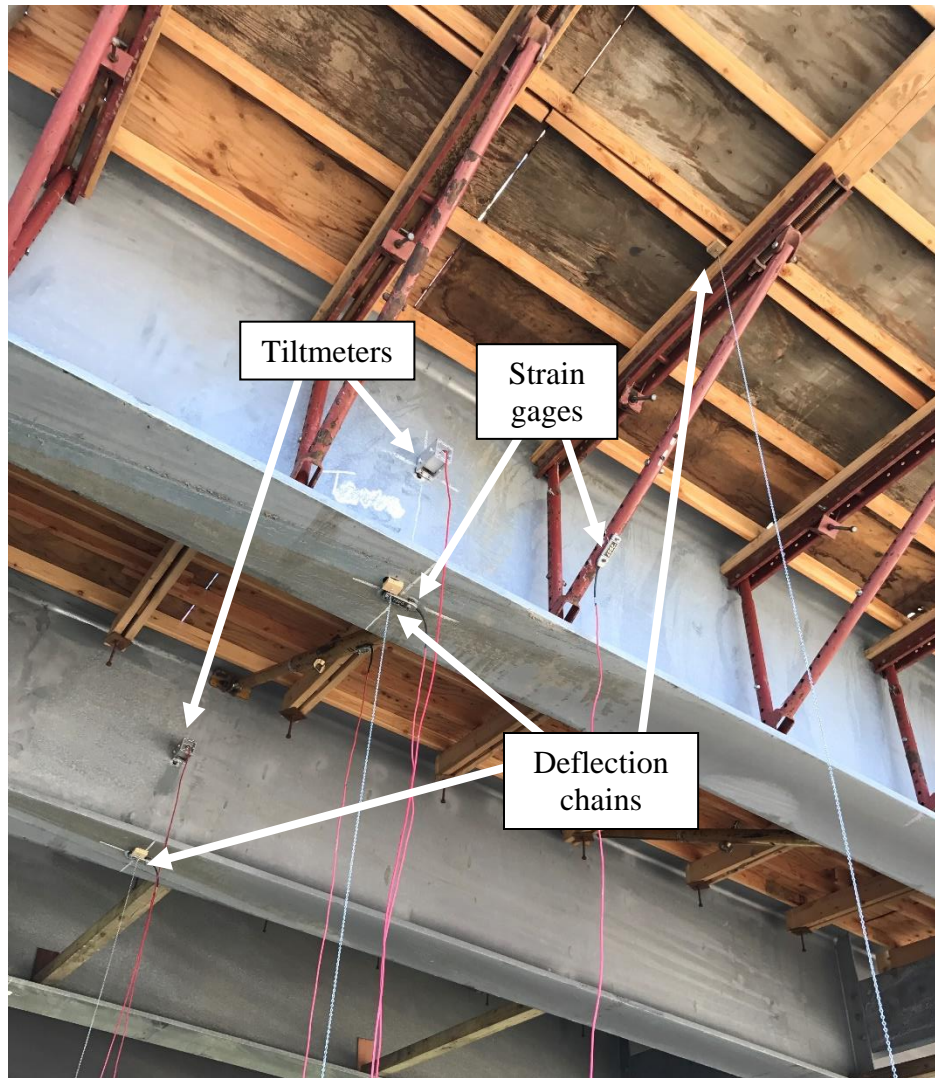


Figure 11. Sample instrumentation setup

Each deflection chain shown in Figure 11 is attached to a transducer stabilized on the ground beneath it. Deflections were not always able to be measured depending on the ground surface beneath the locations of interest (i.e., if water or unstable ground was present, deflection measurements were not possible).

Cedar Fork Bridge Widening Project

The Cedar Fork Bridge was a bridge widening project over the Cedar Fork Creek in southeast Iowa. This four-girder bridge project, shown in Figure 12, involved widening a 28 ft bridge to 30 ft.



Figure 12. Underside of Cedar Fork Bridge showing overhang

No bracing was used for this bridge. The bridge was instrumented prior to deck placement using strain gages and tiltmeters to measure strain and rotation throughout the duration of the deck pour. Due to the depth of the creek under the bridge and the lack of equipment available on site, the center span was not instrumented. The instrumentation plan is discussed in the next section.

The bridge had a skew of 15° , and the screed traveled perpendicular to the roadway for deck placement, as shown in Figure 13.



Figure 13. Cedar Fork Bridge screed orientation relative to deck skew

As can be seen, the orientation of the screed combined with the skew of the deck allowed for the screed load to be partially on the bridge on one side, but off the bridge on the other. Given that data were acquired throughout the deck pour, key screed milestones were marked in the data, such as the screed being directly over a gage, pier, or other location of interest (as shown in Figure 14).



Figure 14. Screed traveling over an instrumented cross-sectional location of the Cedar Fork Bridge

Cedar Fork Bridge Instrumentation Plan

A total of 7 tiltmeters and 41 strain gages were included in the instrumentation of the Cedar Fork Bridge. The typical gage layout at each instrumented cross-sectional location is shown in Figure 15.

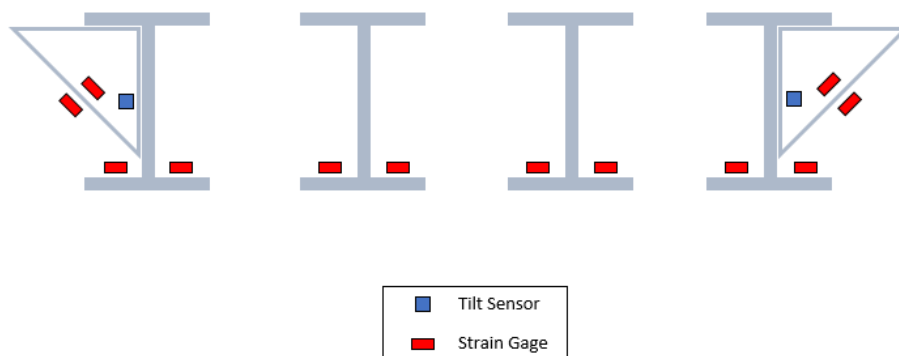
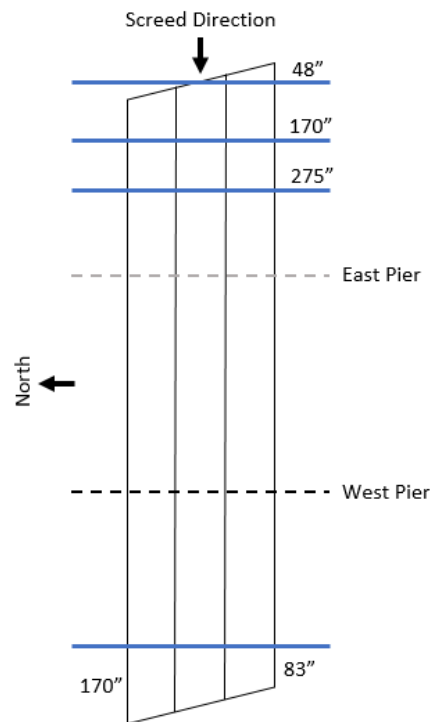


Figure 15. Typical Cedar Fork Bridge gage layout

The cross-sectional locations that were instrumented along the length of the bridge are shown in Figure 16.



Measurements correspond to distance from the abutment

Figure 16. Cedar Fork Bridge instrumented cross-sectional locations

The location that was instrumented on the west end span was a distance of 83 in. from the south end of the west abutment and 170 in. from the north end of the west abutment due to the skew of the bridge. This same location was also instrumented on the east end span, in addition to the mid-span of the east span. The final instrumented location was 48 in. from the east abutment; this was chosen as the screed would be partially on and off the bridge at this location.

Cedar Fork Bridge Deck Construction Results

A multitude of strain and rotation data was collected from the instrumentation during deck placement. The rotation data proved most valuable and are shown in Figure 17.

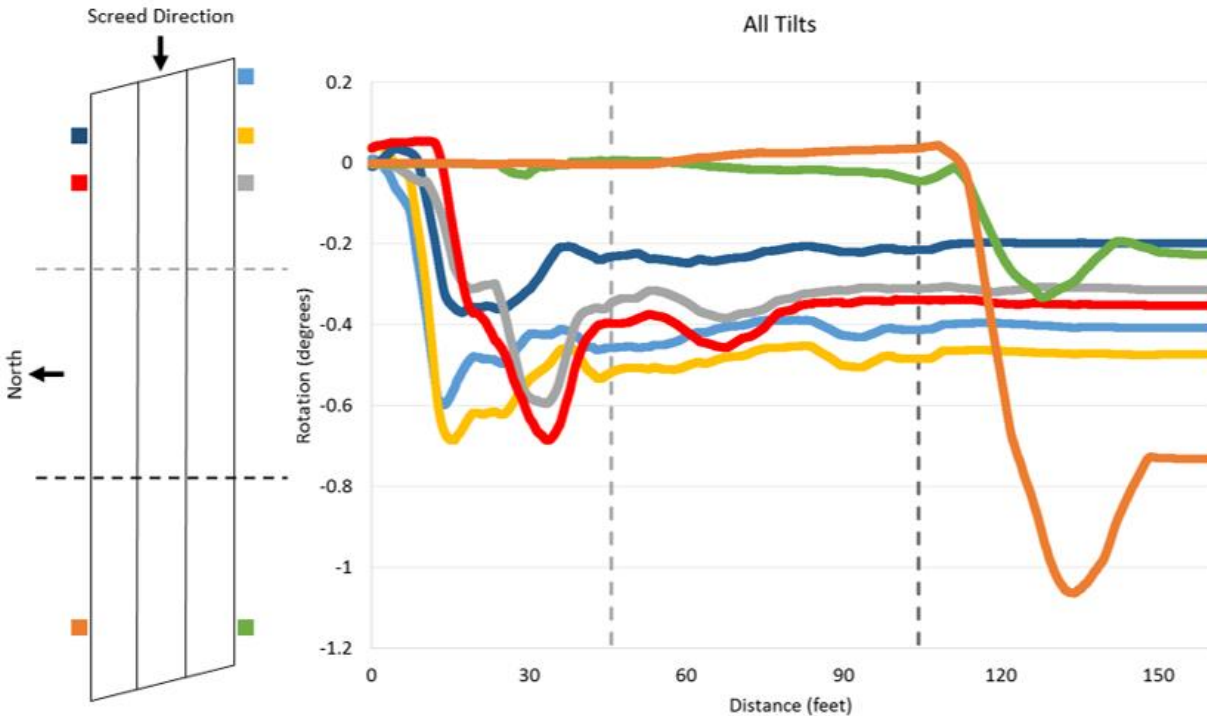


Figure 17. Cedar Fork Bridge tilt data for all locations

The rotation is plotted with respect to screed location, with the east and west piers marked via dotted lines. Note that data were collected after the screed had moved off from the bridge, and is the reason for data after 150 ft. As one would expect, the greatest rotations measured at each individual location were seen when the screed was directly over that gage. The greatest overall rotation was seen when the screed was directly over the instrumented cross-sectional location in the west end span. The maximum rotation of the north exterior girder at this location was 1.06° , while the rotation at the south exterior girder at this same point was 0.33° . This shows the strong effect of skew on the rotation of the exterior girders.

Another key takeaway from the results shown in Figure 17 is regarding the effect of the already placed concrete. Due to symmetry, the green and navy data lines and the orange and yellow data lines should be relatively equivalent in maximum magnitudes if the effect of concrete is excluded. In reality, the green and navy lines are very similar, but the orange line experienced significantly greater maximum rotation than the yellow (1.06° compared to 0.68°). This indicates that the increased dead load of the concrete on the bridge toward the end of the pour (i.e., over the orange and green gage locations) significantly increased the rotation felt by the exterior girders.

The rotation data also provided insight as to long-term rotational behavior of the beams. Figure 18 shows the residual and maximum rotations at each tiltmeter location.

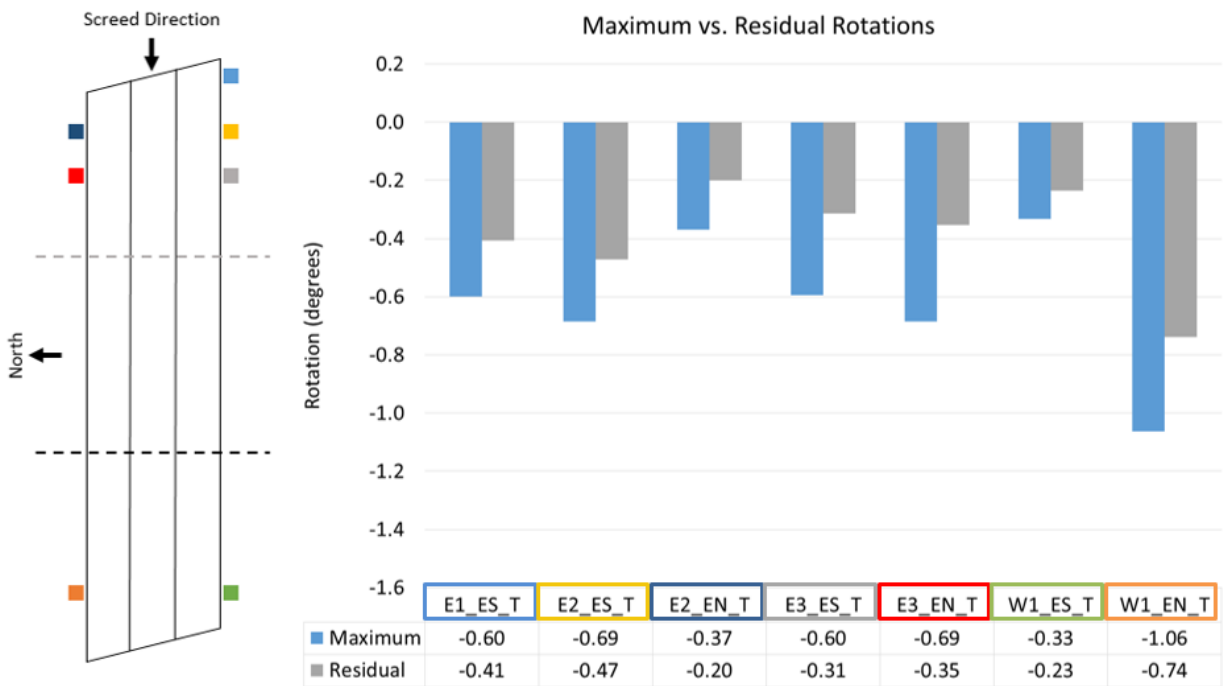


Figure 18. Cedar Fork Bridge maximum and residual rotations

The residual rotation is defined as the rotation measured at the end of data acquisition, or the permanent rotation experienced by the beam after the deck pour is complete. This residual rotation can be seen in the previous graph as the data points that fall after a distance of 150 ft. The average residual rotation was 62% of the maximum rotation experienced at any given location, with a standard deviation of 9%. This means that the girders were able to only partially return to their original orientation and that the bridge experienced permanent rotation as a result of the deck placement.

Maple Bridge Construction Project

The Maple Bridge was a twin bridge construction project over the Maple River in western Iowa. Each six-girder bridge, shown in Figure 19, has a width of 40 ft and an overall length of 340 ft.



Figure 19. Maple Bridge construction project

The first bridge was constructed prior to the research team's involvement and deck deficiencies were seen. As a result of this, it was requested that instrumentation be performed on the second bridge prior to deck placement to identify the cause of the previous bridge's deck deficiencies.

The bridge was instrumented prior to dry runs and deck placement using strain gages, tiltmeters, and deflection transducers to measure strain, rotation, and deflection throughout the duration of the deck pour. Due to the presence and depth of the river mid-span under the center span, deflections were not able to be captured for this span. The bridge had zero skew, and the screed traveled perpendicular to the roadway for deck placement, as shown in Figure 20.



Figure 20. Screed orientation for the Maple Bridge

Maple Bridge Instrumentation Plan

Because of a unique instrumentation opportunity, three rounds of data sets were obtained for the Maple Bridge project. The pair of identical bridges were to be constructed simultaneously, with no temporary bracing called for in the plans. However, the pouring of the deck on the first of the two bridges resulted in thickness deficiencies, with girder rotation suspected as the cause.

The second bridge was then instrumented several times, both without and with temporary bracing, to monitor the effectiveness of bracing during dry runs of the screed. The updated bracing plans of the exterior bays called for timber blocking at the diaphragm locations and diagonal pipes between diaphragms, as shown in Figure 21.

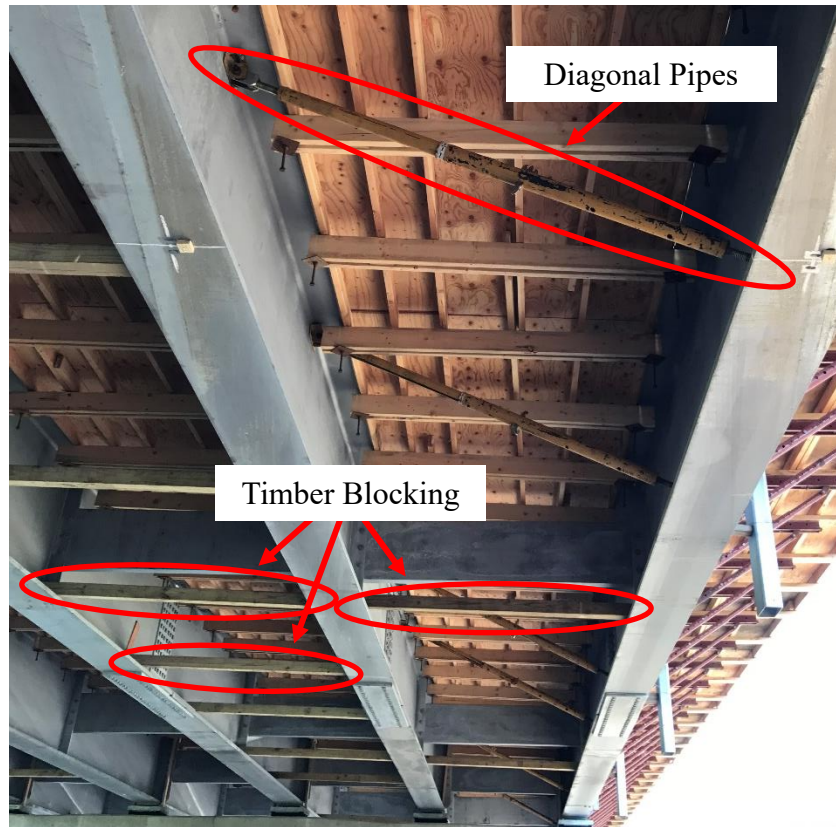


Figure 21. Updated bracing of the Maple Bridge

The bracing plan called for only timber blocking in the interior bays. A full instrumentation was also performed for the pouring of the deck. As a result, data were obtained for an unbraced dry run, a braced dry run, and a braced deck pour.

Unbraced Dry Run

For the unbraced Maple Bridge dry run, 8 tiltmeters, 26 strain gages, and 16 deflection transducers were included in the instrumentation of the Maple Bridge. The typical gage layout at each instrumented cross-sectional location is shown in Figure 22.

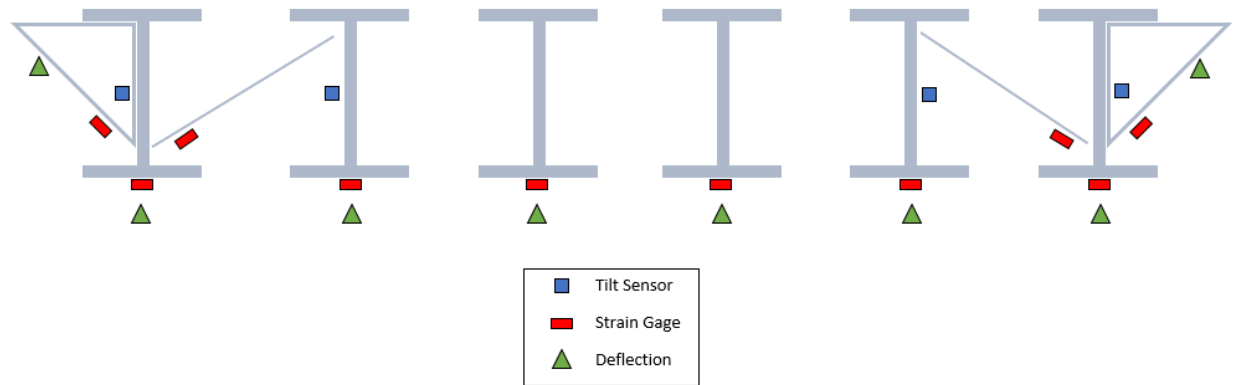


Figure 22. Typical unbraced dry run gage layout for the Maple Bridge

Note that this figure shows the yet-to-be-placed bracing and subsequent brace gage locations. The cross-sectional locations that were instrumented along the length of the bridge are shown in Figure 23.

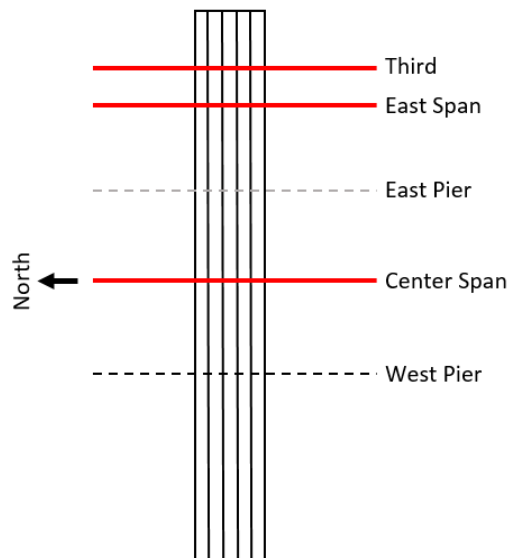


Figure 23. Maple Bridge instrumented unbraced dry run cross-sectional locations

Note that the location labeled Third corresponds to $1/3$ of the span length and was selected based on the results from the Cedar Fork Bridge project.

Braced Dry Run

For the braced Maple Bridge dry run, 8 tiltmeters, 18 strain gages, and 8 deflection transducers were included in the instrumentation. The cross-sectional locations that were instrumented along the length of the bridge are shown in Figure 24.

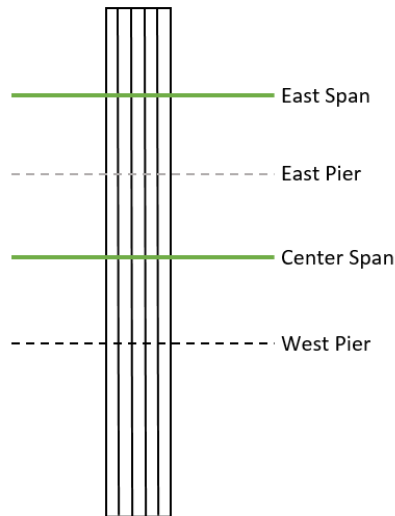


Figure 24. Maple Bridge instrumented braced dry run cross-sectional locations

Note that due to the results of the unbraced dry run, the Third ($1/3$ of the span length) location was not instrumented for the remaining runs due to the controlling values seen at the mid-spans. The typical gage layout at each instrumented cross-sectional location was the same as that shown for the unbraced dry run in Figure 22, with bracing instrumentation as shown.

Braced Deck Pour

For the braced Maple Bridge deck pour, 12 tiltmeters, 20 strain gages, and 16 deflection transducers were included in the instrumentation. The cross-sectional locations that were instrumented along the length of the bridge can be seen in Figure 25.

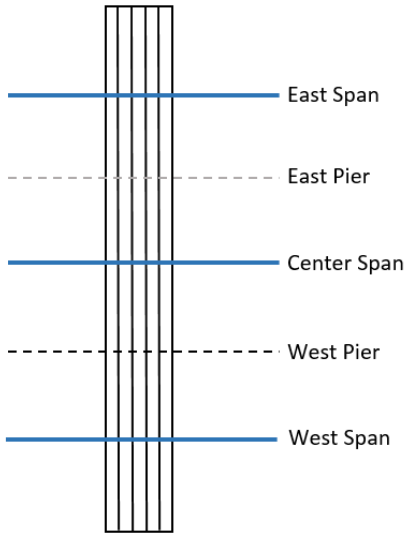


Figure 25. Maple Bridge instrumented braced deck pour cross-sectional locations

To compare the behavior of the end spans, this time both the east and west mid-spans were instrumented. For the east and center spans, the typical gage layout at each instrumented cross-sectional location was the same as that shown in Figure 22 for the unbraced dry run. For the west span, an instrumentation layout was chosen so that the rotation of the flange and web could be compared to determine if uniform rotation was experienced throughout the girder, while also providing data points for comparison with the east span results. This meant that tiltmeters were mounted on both the flange and the web of the north and south exterior girders, in addition to strain gages on the bottom flange, with deflections measured in the same locations as those on the east span. A comparison of these two layouts is shown in Figure 26.



Figure 26. Maple Bridge instrumentation for the east (left) and west (right) spans during the braced deck pour

Maple Bridge Deck Construction Results

A multitude of strain, rotation, and deflection data was collected from the instrumentation during both dry runs and the deck placement. Locations with gages present for all three data sets allowed for comparison of behavior with and without bracing. For example, in Figure 27, the center span rotation of the north exterior girder with respect to screed location is shown for the unbraced dry run, the braced dry run, and the braced deck pour by the three lines.

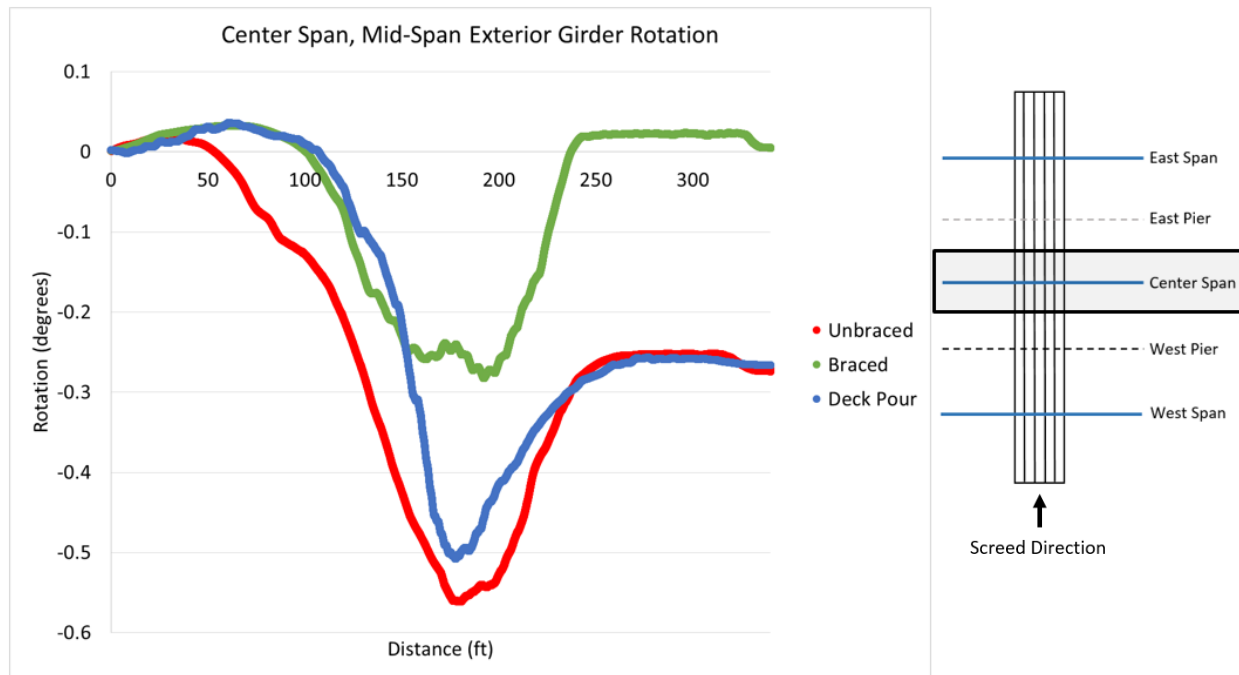


Figure 27. Maple Bridge rotation of the north exterior girder (center span) during all three runs

The gages were effectively zeroed out prior to all three data collection efforts, so the effects of the dry run were not included in the deck pour data. Note that the total screed weight was approximately 11 kips, with the heavier end, which houses the motor, on the north side. This same information for the east span is shown in Figure 28.

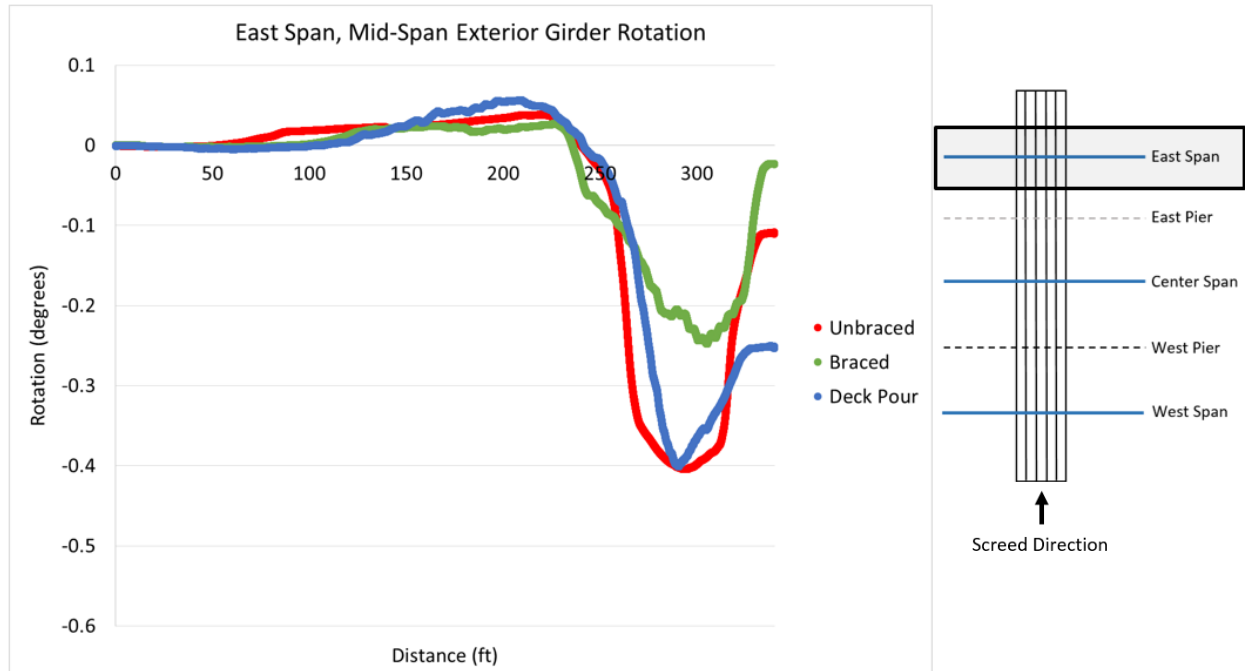


Figure 28. Maple Bridge rotation of the north exterior girder (east span) during all three runs

Note that for both of these graphs, the maximum girder rotation is seen when the screed is directly over the gage location. For both the center and east spans, the girder rotation for the unbraced dry run was roughly double that of the braced dry run, showing that the bracing significantly reduced the rotation of the exterior girders. In addition, the maximum rotation of the exterior girders for both locations for the unbraced dry run and braced deck pour were approximately equal.

One difference between the two locations is the so called residual rotation, or the rotation after the screed has moved off of the bridge. For the center span, the residual rotation of the unbraced dry run and the braced deck pour are similar and non-zero (approximately 0.27°). For the east span, however, the unbraced and braced dry runs behave similarly with respect to the residual rotation. The maximum rotation experienced at any instrumented location during the deck placement was approximately 0.56° , which occurred at mid-span of the center span.

These same comparisons can be made using the deflection data gathered. Figure 29 shows the deflection of the north formwork bracket at mid-span of the east span.

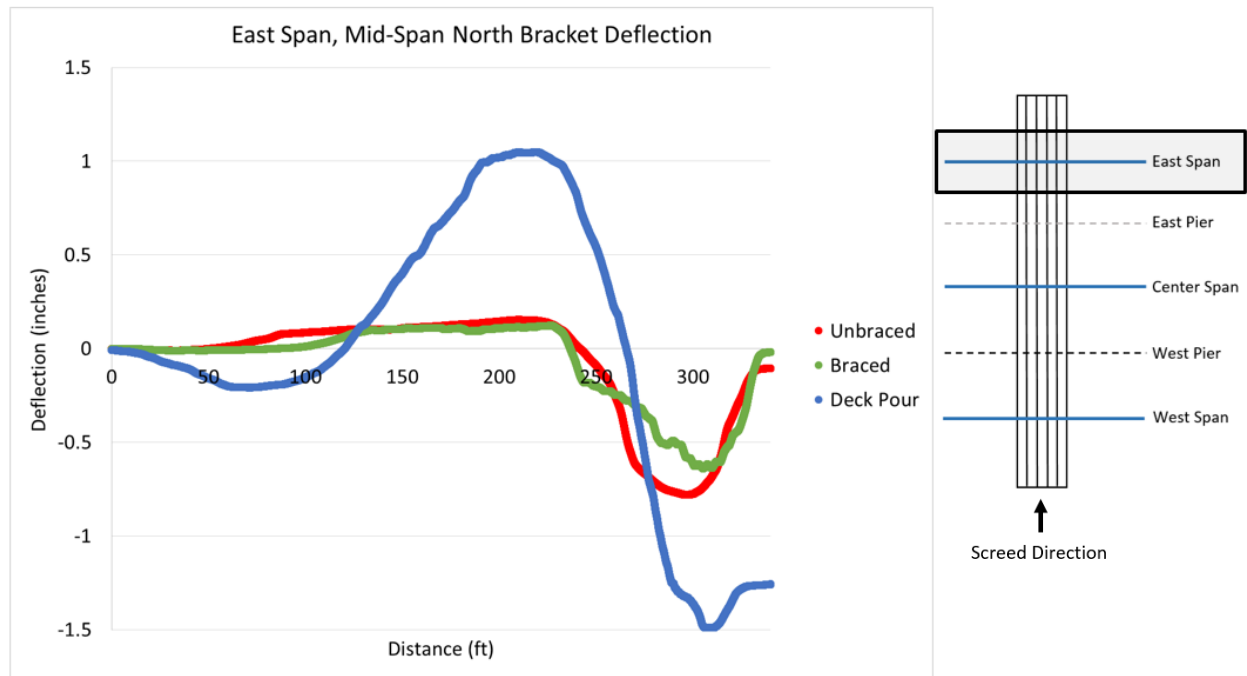


Figure 29. Maple Bridge deflection of the north formwork bracket (east span) during all three runs

The deflection data for this instrumented location are similar in behavior to that of the rotation of the exterior girder at the east span in that there is very little residual deflection for the unbraced dry run. The deflection data differs from that of the rotation data in that the addition of the bracing did not significantly impact the deflections. The unbraced and braced dry runs exhibit very similar behavior, with significantly more deflection caused by the deck pour due to the dead load from the concrete and the live loads associated with the deck placement crew and equipment other than the screed. It is also worth highlighting the uplift that is seen in the east span deflection data when the screed was over the center span, proving the continuity and elasticity of the girders.

The data can also be used to compare the behavior of the east and west spans. Figure 30 shows the deflections of the formwork brackets and girders for the east span during the deck pour.

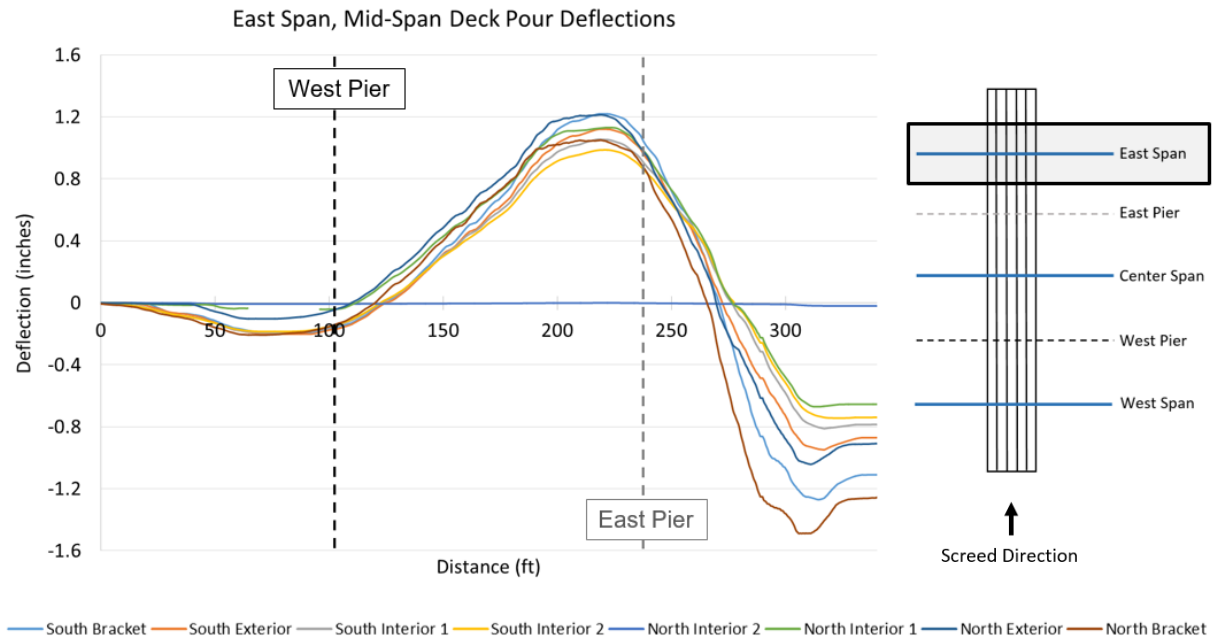


Figure 30. Maple Bridge deflections of brackets and girders (east span) during deck placement

The deflection transducer at the North Interior 2 location for the east span was faulty, and thus the zero data shown is not indicative of the actual deflection experienced at this girder.

The data for the west span are shown in Figure 31.

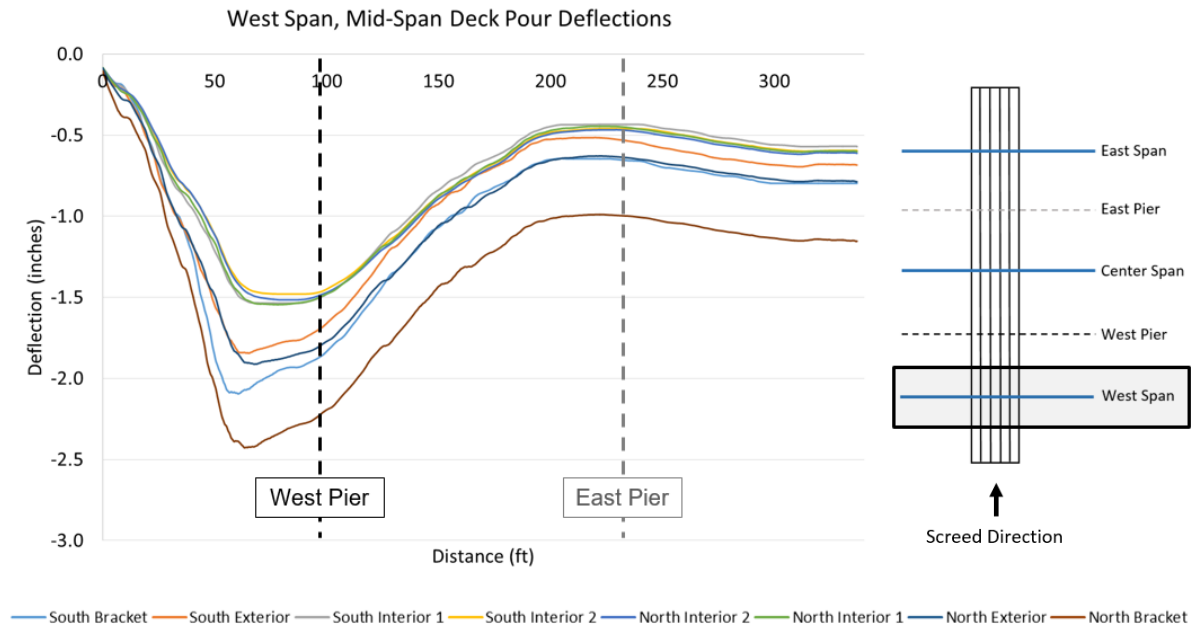


Figure 31. Maple Bridge deflections of brackets and girders (west span) during deck placement

In all cases, the response in the north bracket and exterior girder was always greater than that of the south bracket and exterior girder. This was due to the location of the engine on the north end of the screed, creating greater reaction loads on the north rail compared to that of the south rail.

Comparing Figure 30 and Figure 31, the maximum deflection experienced as a result of the screed load over the gages was approximately equal (approximately 2.5 in. for the north bracket location) when one accounts for the uplift experienced in the east span. In addition, the residual deflection for both spans was approximately equal, with a maximum deflection of approximately 1.2 in. at the north formwork bracket. These results appear to show that the east and west spans behaved similarly, despite initial variances in stiffness and load during deck placement due to the presence, or lack thereof, of the fresh concrete.

The deflection data also allow for the analysis of differential deflections to better understand how the girders along any given cross-sectional location are moving with respect to one another. Figure 32 shows the maximum recorded deflection of the formwork brackets and girders at mid-span of the east span for the two dry runs and the actual pour.

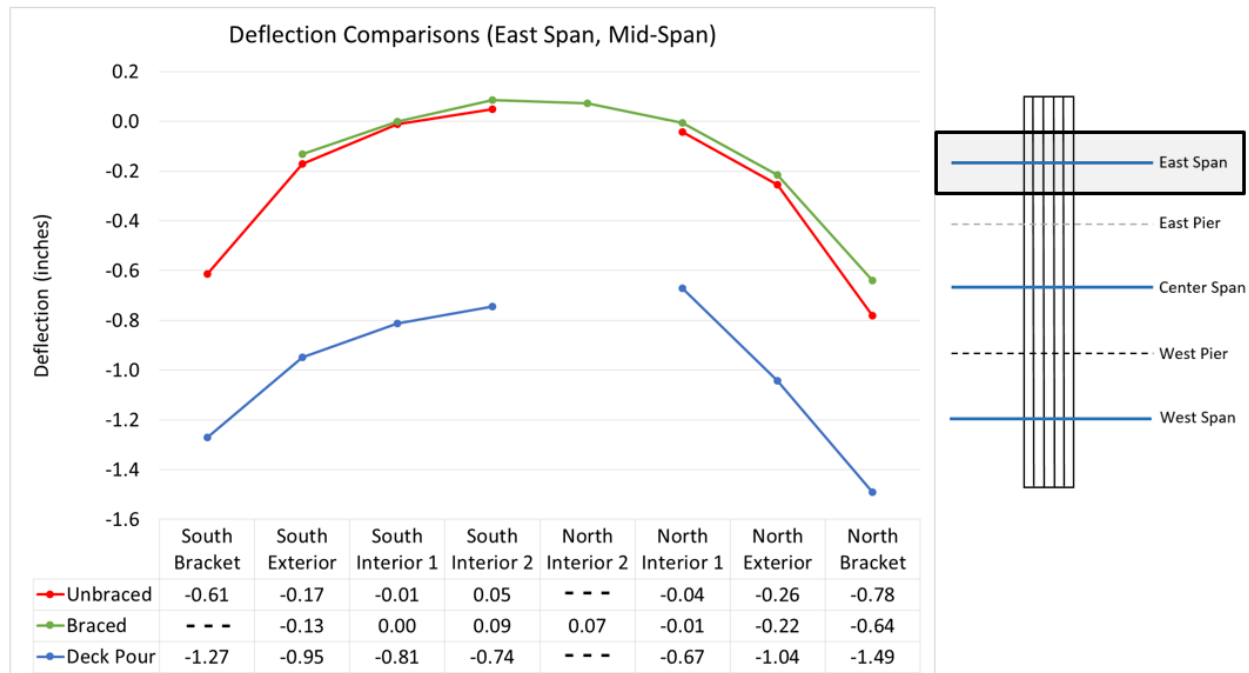


Figure 32. Maple Bridge deflections of brackets and girders (east span) during all three runs

Note that a faulty transducer is the reason for missing data points in the graphs (Indicated with - - in the table cells below the graph). For both dry runs and the deck placement, the deflected shape of the bridge cross-section was the same: differential deflection occurred such that the exterior girders deflected more relative to the interior girders. The type of bracing that was chosen, and successfully reduced girder rotation, did not also provide differential deflection restraint.

While the girders and brackets deflected as much as 1.49 in. during the deck placement, the system did begin to return to its original position after the screed load was off the bridge, although residual deflections were still present. Figure 33 shows deflection data for the east span instrumented locations.

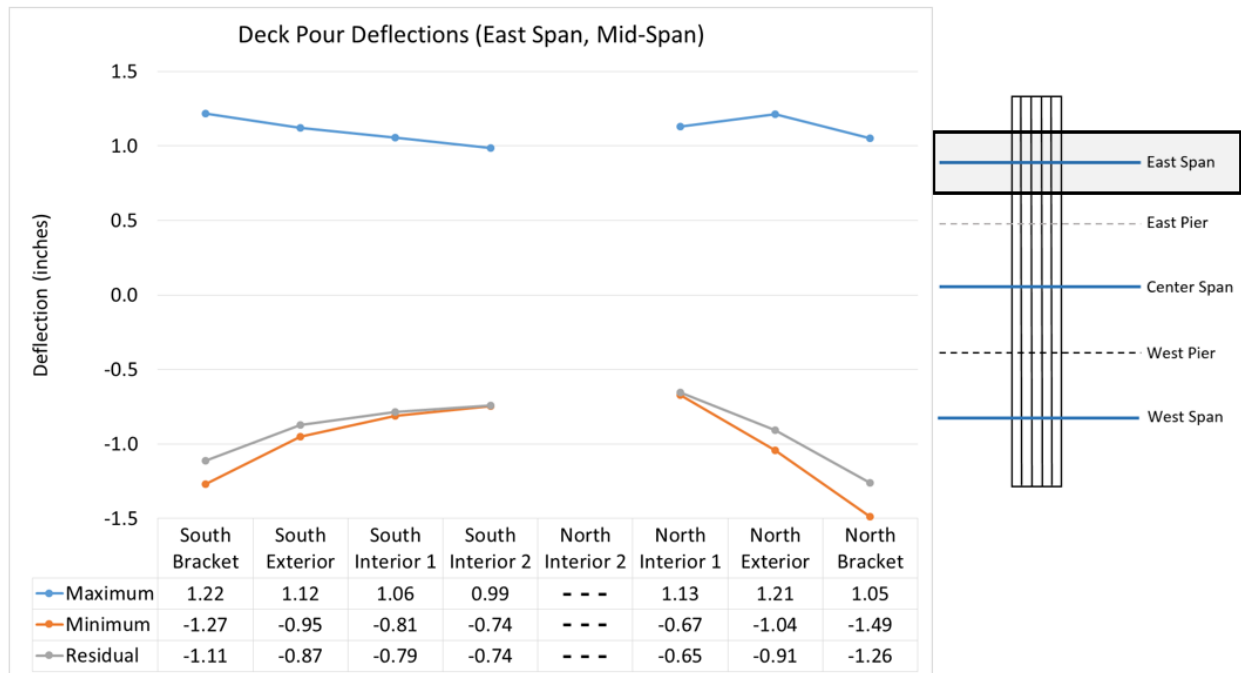


Figure 33. Maple Bridge deflection data for brackets and girders (east span) during deck placement

This figure shows the maximum deflection (largest uplift or smallest downward deflection and, in this case, the uplift experienced when the screed was on the center span), the minimum deflection (largest downward deflection), and the residual deflection (the deflection that remained in the beams after the screed was fully off from the bridge). The residual deflection is indicative of the permanent deformed shape of the bridge. From this figure, one can see that the all locations moved at least 1.73 in. total during the duration of the deck pour. This again shows the behavior of the bridge and its ability to respond to loads on other spans. Moreover, the east span had residual deflections that were relatively close in magnitude to the greatest downward deflection experienced. This is a result of the uplift that occurred prior to the screed reaching the east span (as also shown in the previous Figure 30).

Figure 34 shows the deflection data for the west span during deck placement.

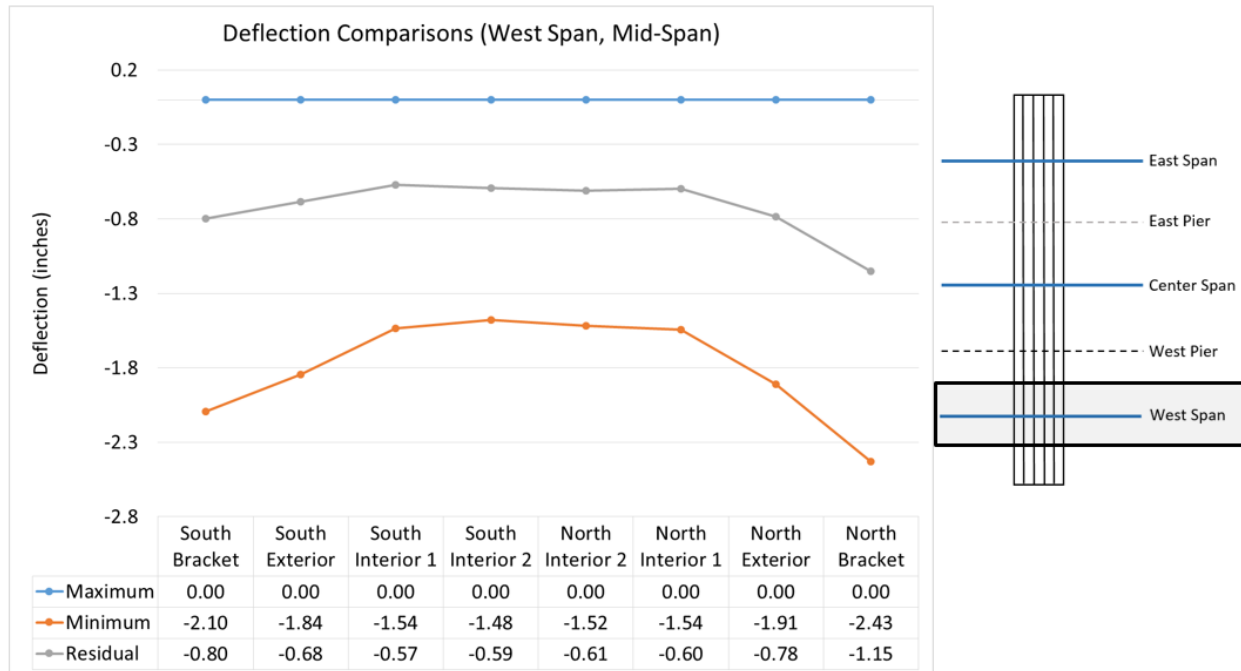


Figure 34. Maple Bridge deflection data for brackets and girders (west span) during deck placement

For this location, note that the maximum deflection is zero due to the screed starting out on this span (as also shown in Figure 31). The residual deflections at the west span were significantly less than the greatest downward deflection experienced, in this case due to the uplift that was seen after the screed load was on this span. The deflection results for both the east and west spans are similar in both deflected shape and in the trend of greater deflections on the north compared to the south.

The actual deflections from the field placement of the deck can also be compared to the design deflections specified in the bridge plans. The design deflections for this bridge are shown in Figure 35.

Note that the circled deflections correspond to the deflections associated with the deck placement and, thus, are the appropriate numbers for comparison. The design standards show a maximum deflection of 1 in. on the outer spans and 2 in. on the middle span for all girders. The actual field deflections were greater than 1 in. on the outer spans, although the residual deflections were closer to the design standards. However, differential deflections were seen. These are key discrepancies between the anticipated behavior of the bridge as specified in the design plans and the actual response of the bridge during deck placement in the field.



Figure 35. Maple Bridge dead load design deflections

BNSF Railway Bridge Construction Project

The BNSF Railway Bridge was a bridge construction project over the BNSF railroad in southwestern Iowa. This three-span, five-girder bridge project, shown in Figure 36, has a width of 30 ft and an overall length of 260 ft.



Figure 36. BNSF Railway Bridge

The bridge was instrumented prior to deck placement using strain gages, tiltmeters, and deflection transducers to measure strain, rotation and deflection throughout the duration of the deck pour. Due to the railroad presence under the bridge, the center span was not able to be instrumented. Rather than instrumenting both end spans, this bridge was heavily instrumented on one end span to capture all effects associated with the 45° skew. The screed traveled perpendicular to the roadway for deck placement, as shown in Figure 37.

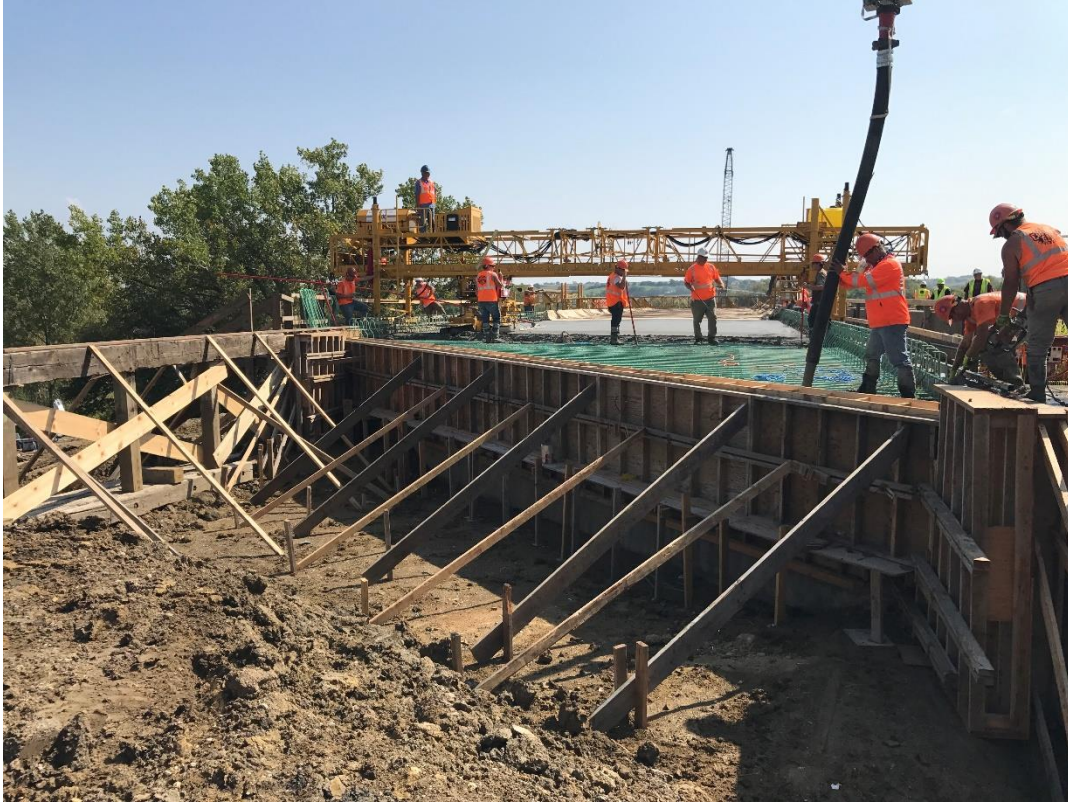


Figure 37. Screed orientation for the 45° skew BNSF Railway Bridge

While not called for in the plans, the contractor placed temporary bracing in the form of timber blocking in the exterior bays. Each timber strut was placed midway between the diaphragm/pier locations, as shown in Figure 38.

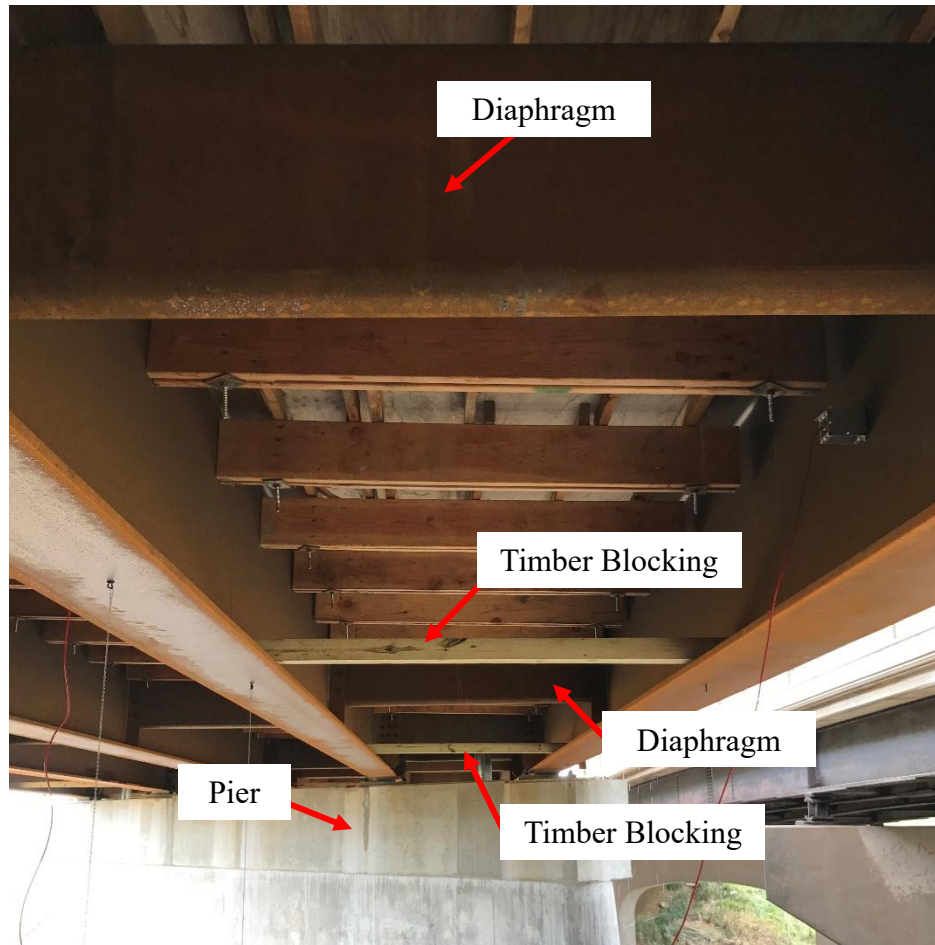


Figure 38. Temporary timber blocking locations in the exterior bays of the BNSF Railway Bridge

The presence of the bracing led to an updated instrumentation plan to instrument locations that would experience the greatest rotation (i.e., midway between diaphragms or blocking, as close to mid-span as possible). This instrumentation plan is discussed in the next section.

BNSF Railway Bridge Instrumentation Plan

A total of 8 tiltmeters, 13 deflection transducers, and 2 strain gages were included in the instrumentation of the BNSF Railway Bridge. The cross-sectional locations that were instrumented along the length of the bridge are shown in Figure 39.

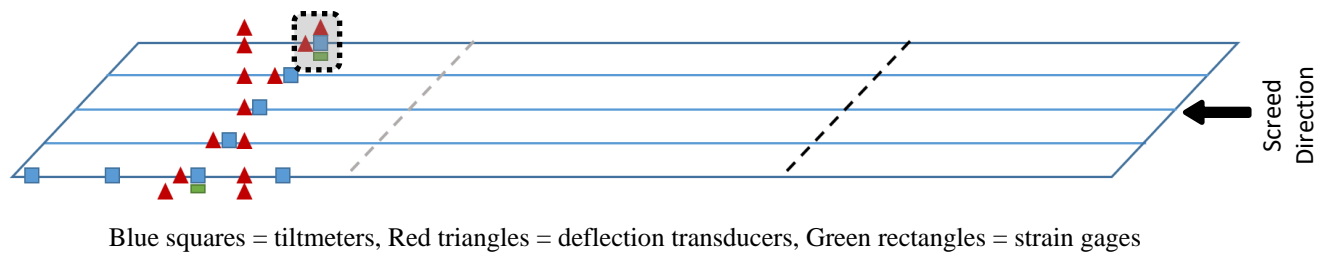


Figure 39. BNSF Railway Bridge instrumentation plan

As shown, special focus was placed on instrumenting a full cross-section at a location both along the skew and along a line perpendicular to the bridge. The actual field instrumentation present for the outlined region in Figure 39 is shown in Figure 40.



Figure 40. BNSF Railway Bridge exterior girder field instrumentation

The two chains in the image are from the deflection transducers, and the two red cables are associated with the attached tiltmeter and strain gage.

BNSF Railway Bridge Deck Construction Results

The 45° skew associated with this bridge was of great interest for data collection purposes to determine any heightened effects associated with differences in screed and roadway orientation. The deflection data obtained from a cross-section perpendicular to the roadway and along the skew can be seen in Figure 41 and Figure 42, respectively.

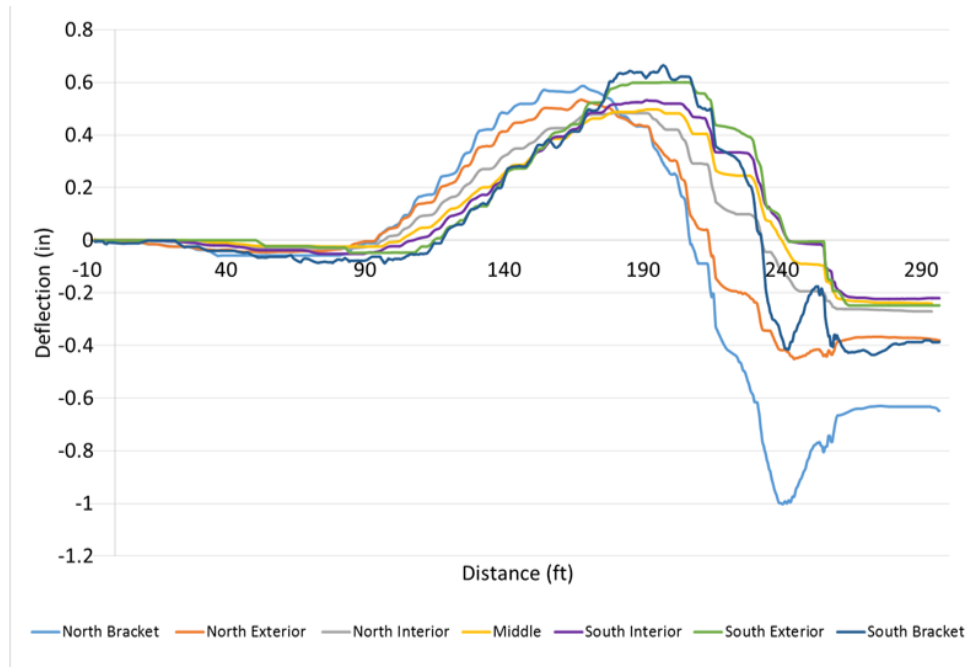


Figure 41. BNSF Railway Bridge deflection data for cross-section perpendicular to roadway orientation

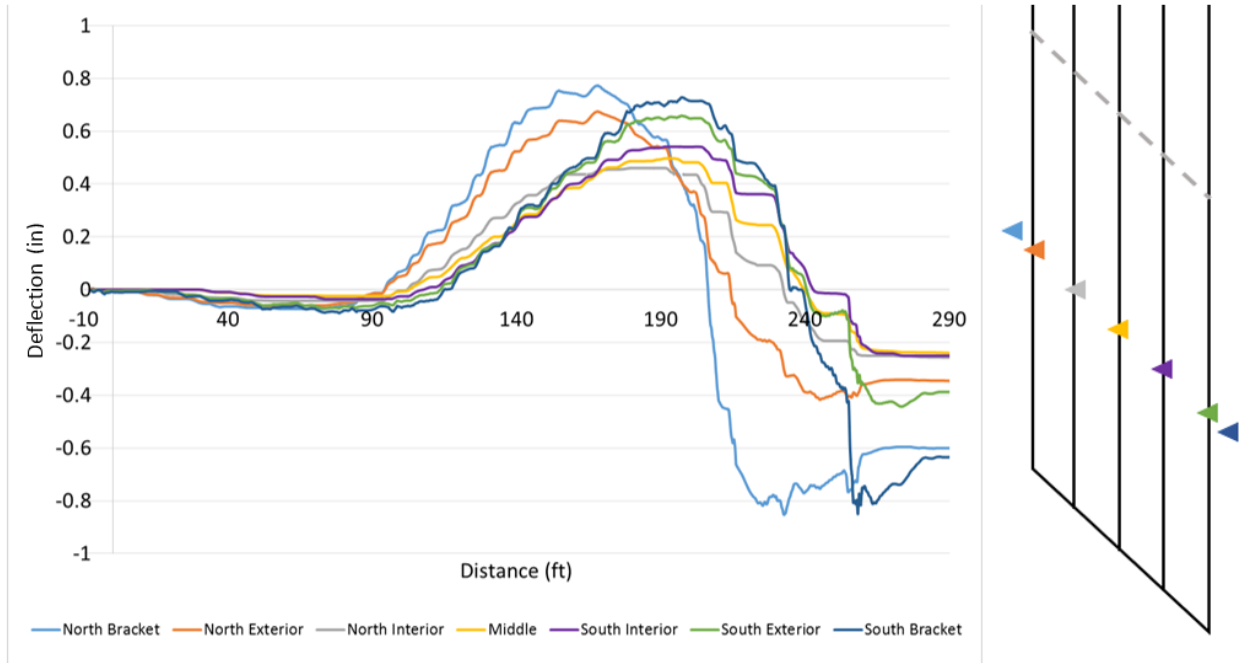


Figure 42. BNSF Railway Bridge deflection data for cross-section along skew

As can be seen when comparing these two figures, there is significantly greater differential deflection occurring for the cross-section that is perpendicular to the roadway.

This difference in differential deflection performance can be better illustrated by considering the maximum deflections occurring relative to other cross-sectional locations. These data are presented in Figure 43 and Figure 44.

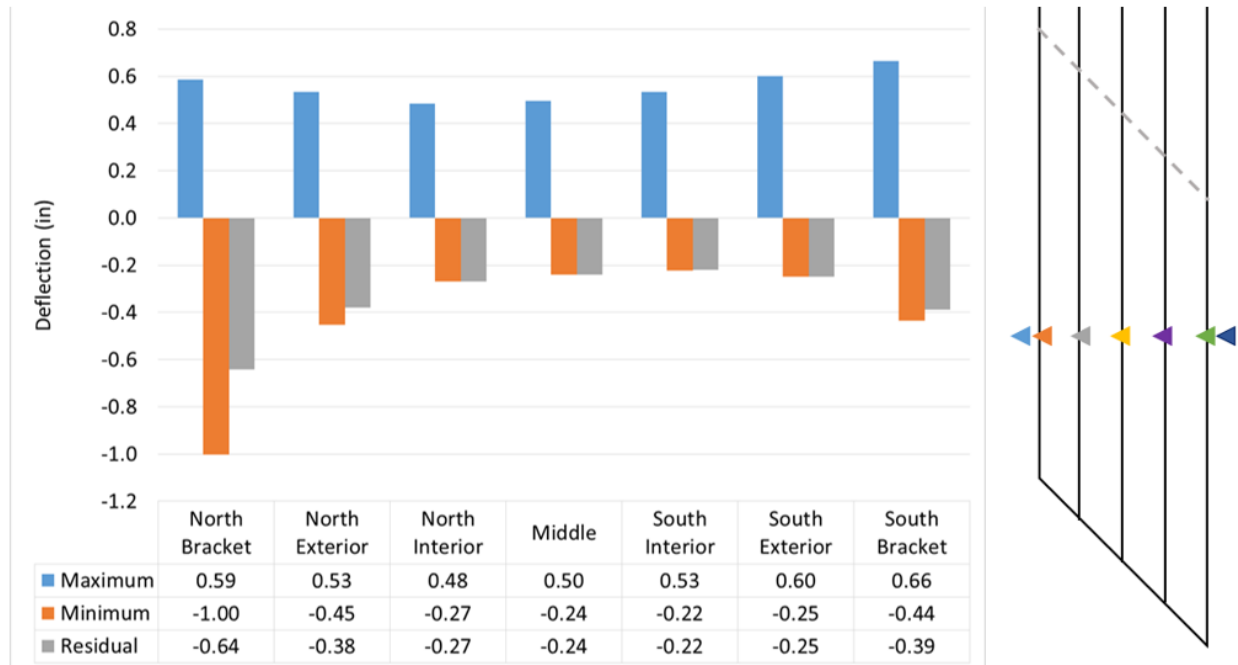


Figure 43. Selected deflection data for cross-section perpendicular to roadway of BNSF Railway Bridge

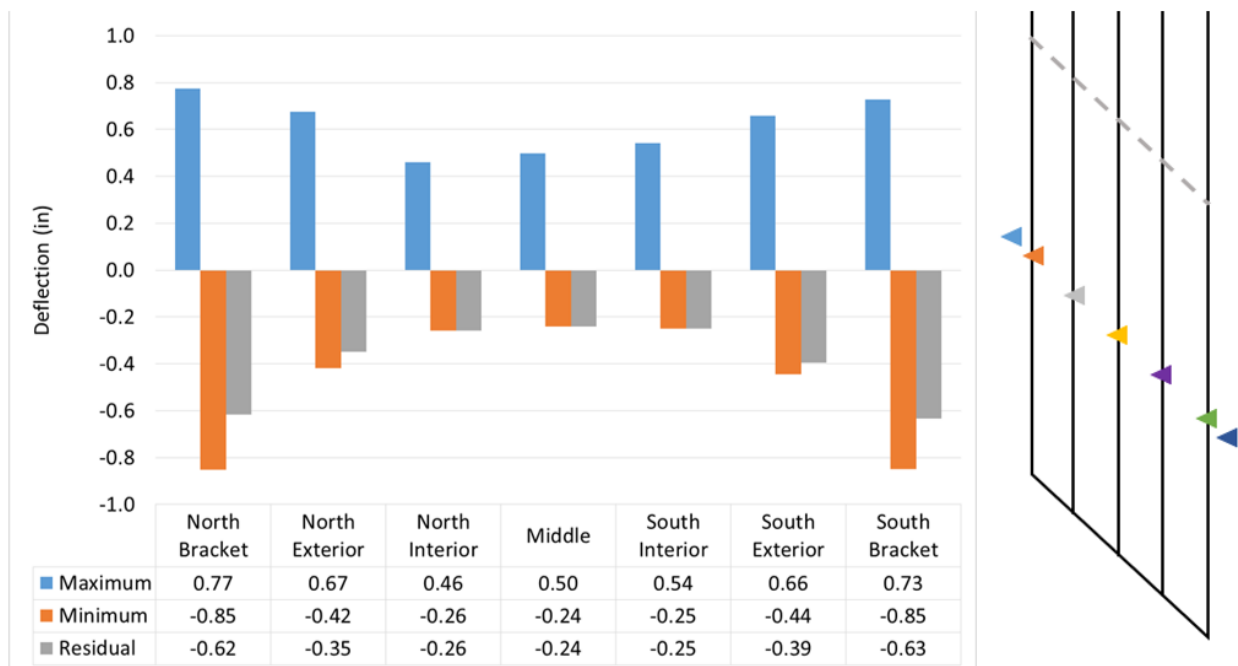


Figure 44. Selected deflection data for cross-section along skew of BNSF Railway Bridge

For these charts, the maximum deflection value indicates the greatest upward deflection detected during deck placement; the minimum value indicates the greatest downward deflection detected;

and the residual value indicates the amount of deflection sustained after the deck placement was completed and the screed load was off the bridge.

These figures illustrate the “permanent” or residual differential deflections that are experienced as a result of the screed load, as well as show the significant effect of skew on the overall deflected shape of the bridge, and thus of the deck. It is worth noting that the term permanent is used somewhat ambiguously due to an abbreviated length of data collection past deck placement. It is possible that the bridge shape returns further to its deflected shape a greater length of time after placement is completed, although it is anticipated that this would not account for the entirety of the residual differential deflections experienced.

This same presentation of data can be done for the rotation values, which showed similar behavior for the cross-section parallel to skew. In addition to instrumenting the cross-section, additional tiltmeters were placed along the exterior girder, as shown previously in the instrumentation plan. The data obtained from these gages are shown in Figure 45 and Figure 46.

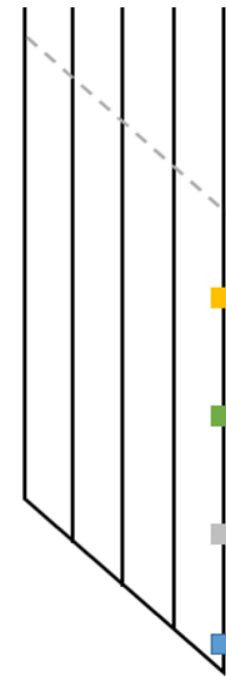
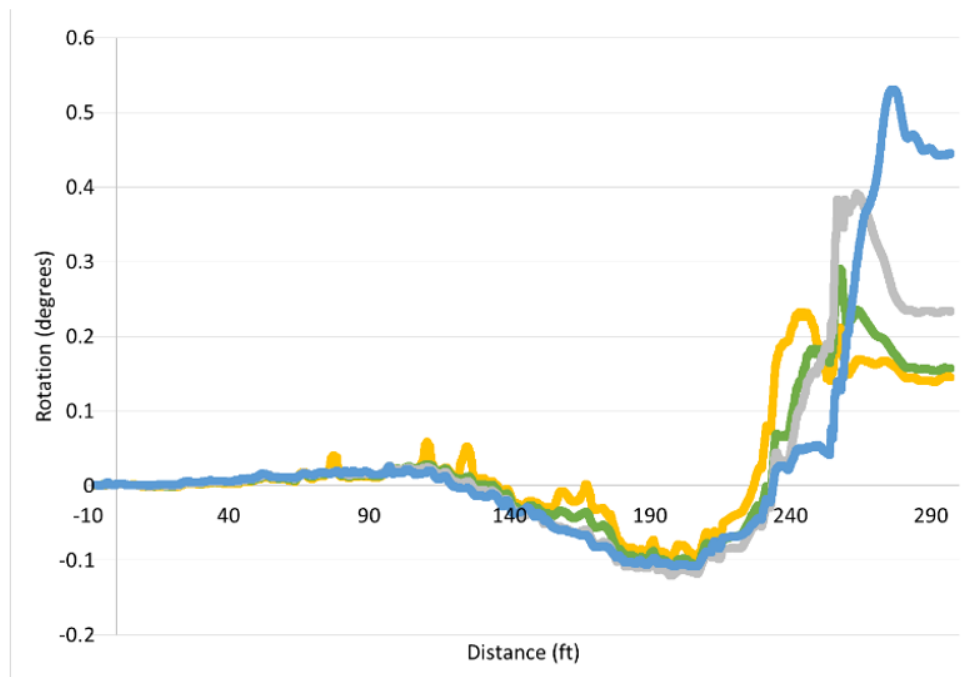


Figure 45. BNSF Railway Bridge rotation data for south exterior girder

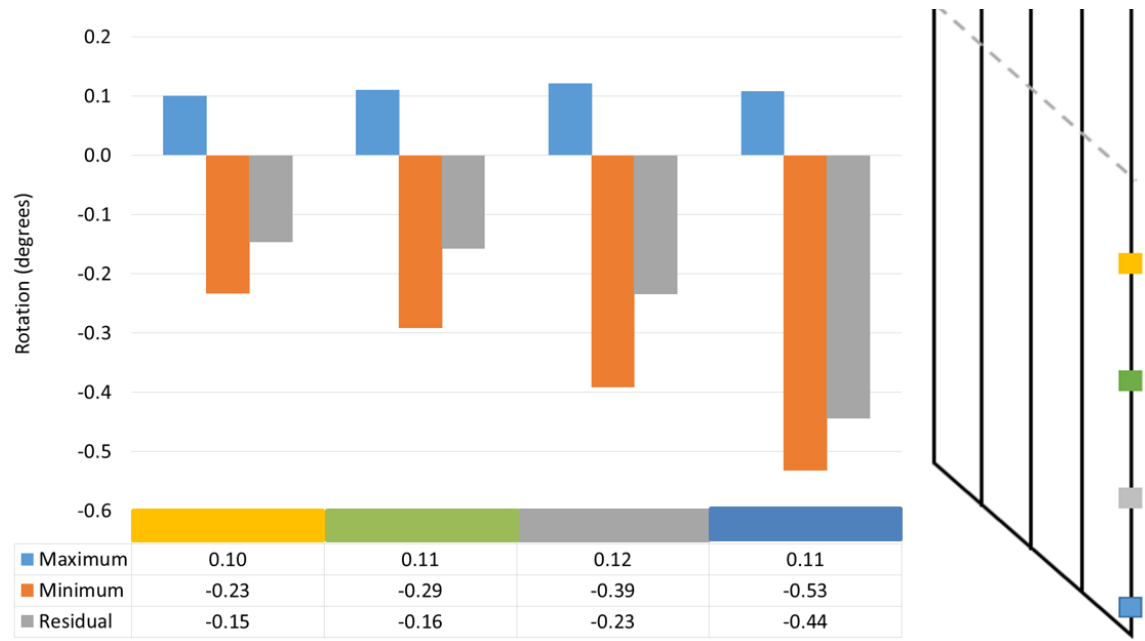


Figure 46. Selected rotation data for south exterior girder of BNSF Railway Bridge

As can be seen from these data, significantly greater rotation was experienced at the end of the girder. This location of the bridge coincides with the portion of the deck placement in which the screed load is off the bridge on one side and still loading the other side. This unequal distribution of the screed load when associated with a large skew leads to increased girder rotation, as evident from the data presented here.

CHAPTER 4. ANALYTICAL STUDY

To provide supplemental data while also validating the field observations, the researchers created analytical models that incorporated a variety of variables thought to affect girder rotation. The scope of this chapter is to provide an understanding of the effects caused by these loads when applied over the portion of overhang on the exterior girder in terms of deflection and rotation using finite element analysis (FEA) by correlating the results with the field data.

Upon calibration, the researchers conducted a parametric study to improve the understanding of the structural behavior of bridges when different loads, such as concrete weight and screed weight, are acting on them. Actual field testing provides a realistic estimation of the rotation and deflection of girders and overhang, respectively. The FEA, however, plays an important role in providing estimation of the contributing mechanisms, while also allowing for the study of various other parameters. This is not feasible during field investigations due to the nature of testing, project timeframe, site-specific issues, construction schedule, and other restrictions.

The three-dimensional (3D) FEA was performed using the structural analysis and design software for bridges, CSiBridge. The numerical study included the investigation of effects of different combinations of bracing, including cases of using no timber block, only timber block, only temporary bracing, and temporary bracing with timber block—on three different bridges.

This chapter provides a detailed discussion of the finite element models (FEMs) along with comparisons of the FEA results with the field investigations. FEA models for the Maple Bridge in Ida County and the BNSF Railway Bridge in Adams County were developed and used to compare with results from their field investigations, while a 160 ft bridge with 0° skew from Iowa DOT bridge standards (Iowa DOT 2016) was also modeled and studied for various configurations.

Finite Element Modeling Techniques

Each FEM was prepared using different types of objects/elements that are available in CSiBridge (Computers and Structures, Inc. 2016). A detailed overview of each object is provided in Table 4.

Table 4. Summary of object types used in FEA

Object Type	Structural Component(s)	Notes
Shell	Girder web, flange, formwork	3 or 4 node formulation that combines membrane and plate-bending behavior
Frame	Connection plates, wood joists, exterior hangers, bracing, diaphragms, connecting rods, columns, cap beams, timber blocks	3D beam columns formulation, which includes the effects of biaxial bending, torsion, axial deformation, and biaxial shear deformations
Link	Bearing connections at abutments and columns	Two-joint connecting links

The basic geometry of each of the bridges was created by using the bridge modeling wizard. By providing initial dimensions, such as depth of girders, span length, diaphragm sizes, bearing types, connection plates, cap beams, and columns, basic geometry was developed. All of the other structural details such as formwork, wood joists, hangers, overhang formwork, and other constraints were added manually for each of the bridges per the actual site specific dimensions and loading scenarios. The structural models were prepared for a stage that was under construction with no hardened concrete. Thus 3/4 in. thick formwork and 2×6 wood joists were modelled. The shell element was used to model steel girders and formwork. The girder web was meshed into different parts to facilitate the modeling of the exterior hanger to represent the realistic structural model. Moment releases were assigned at the connection region of the formwork and girder flange. Similarly, moment releases were assigned at the connection of wood joists and the girder flange. All other objects such as wood joists, hanger elements, diaphragms, cap beams, columns, bracing, and wood blocks were modeled using frame elements.

The critical part of the numerical analysis was to develop a modeling technique that would capture the effects of overhang construction on exterior girder deflection and rotation. The deflection under the overhang assembly was also important considering the nature of issues faced in the exterior girder rotation. When continuous diaphragms are placed at regular intervals, the overhang construction introduces a rigid body rotation of the exterior girders. The modeling of the exterior hanger was carried out to mimic the rigid body rotation of the exterior girder. The best way to address this issue was to mesh the girder webs at points where the horizontal channel and diagonal meet at the girder web. The constraints were assigned, because in reality, the horizontal channels were supported by the girder web only in the horizontal and vertical direction. Thus, body constraints only in X and Y directions for each pair of nodes of girder and horizontal channels were assigned. Similarly, the diagonal legs were supported by the girder webs and constraints in X and Y directions were assigned at the pair of nodes of the girder web and diagonals. The hanger assembly was installed every 36 in.; thus, the overhang assembly was modeled at every 36 in. in the FEM.

The steel bolts for the overhang were connected to the horizontal channel of the overhang assembly at a 45° angle as shown in Figure 47.

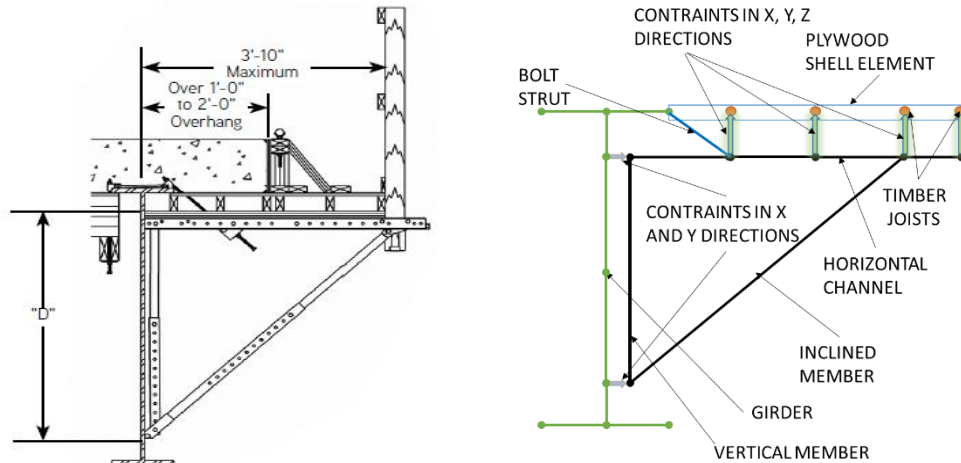


Figure 47. Overhang details per construction documents (left) and FEA model (right)

The horizontal channels of the overhang assembly were meshed into four parts to facilitate the connection of formwork and horizontal timber joists running in the longitudinal direction of the bridge. The horizontal timber joists were spaced at 16 in. apart. The formwork and horizontal joists were drawn at the same elevation as that of the girder flange. Further, constraints in the X, Y, and Z direction were assigned to the pair of nodes of the horizontal channel and formwork as well as the timber joists. A steel rod/bolt strut connects from the top flange to the horizontal channel at 45°. Figure 47 provides a description of the overhang assembly connection with the girder. The section details of the horizontal channel and the vertical and diagonal legs of the bracket assembly are shown in Figure 48.

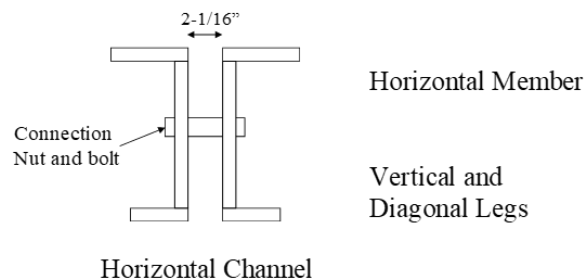


Figure 48. Section properties of horizontal channel and vertical and diagonal legs

This procedure was used for modeling the bracket assembly in the FEA of the three bridge case studies.

Finite Element Analysis of Maple Bridge

The Maple Bridge has a total span length of 340 ft comprising three spans—of 120 ft, 136 ft, and 102 ft—and a width of 43 ft 2 in. The 8 in. concrete deck is supported by six steel girders spaced at 7 ft 4-13/16 in. apart. The steel girders are supported over fixed bearings at integral abutments and one pier, with expansion bearings on the second pier. The spliced girders were W44×230

and W44×290. Diaphragms at the abutment are C12×20.7, and pier and intermediate diaphragms are MC18×42.7. A 54 in. overhang length was modeled. Table 5 provides a summary of the data used in preparation of the model for the Maple Bridge (shown in Figure 49).

Table 5. Section properties of objects used in Ida County Maple Bridge FEM

Section	Properties
Girder	Shell element W44×230, W44×290
Formwork	Shell element 3/4 in. thick
Wood joist	Frame element 2×6
Timber block	Frame element 4×4
Bracket assembly	
Horizontal channel	Frame element, per Figure 48
Vertical channel	Frame element 1-7/8 in. hollow tube
Coil rod	Frame element 1/2 in.
Bearings	
Abutment	Link element, U1, U2, U3 restrained
Pier 1	Link element, U1, U2, U3 restrained
Pier 2	Link element, U1, U2 restrained

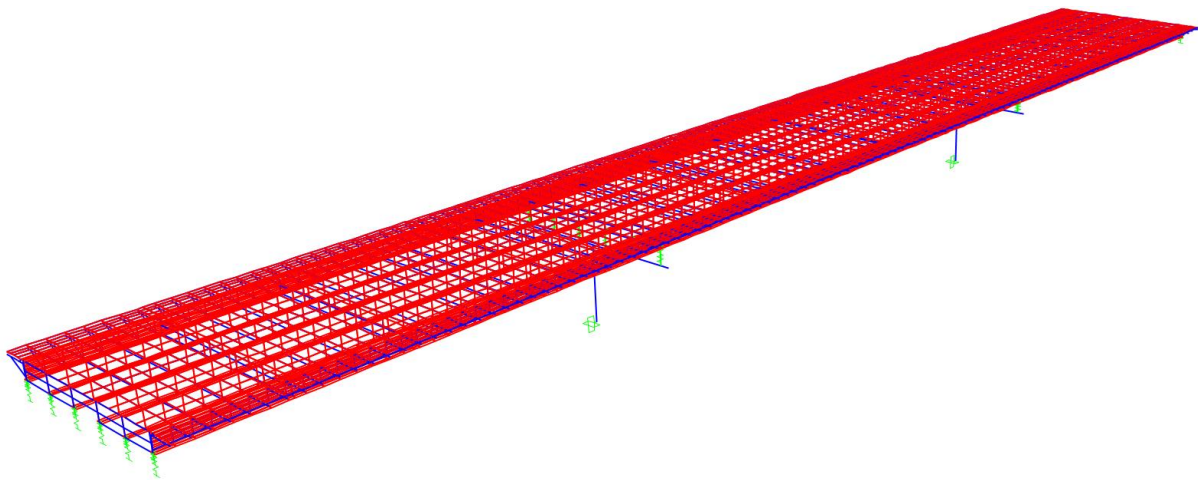


Figure 49. Maple Bridge model

The field investigation of the bridge was completed for a dry run test; thus, the FEM was analyzed for a dry run test and compared with the dry run test field readings. The final values of rotation and deflection were obtained by deducting rotation and deflection due to self-weight and rail weight of the structure from the total deflection and rotation due to self-weight, rail weight, and screed load. Table 6 provides a summary of loads assumed in the preparation of the FEA of the Maple Bridge.

Table 6. Description of loads in the FEA model of the Maple Bridge

Load	Description
Self-weight of girders, diaphragms, formwork, bracket assembly	Directly calculated by the program
Rail weight	75 plf 2 ½ in. from edge of the concrete deck
Screed weight	12 kips on the north side 6 kips on the south side

The dimensions of the finishing machine are shown in Figure 50.

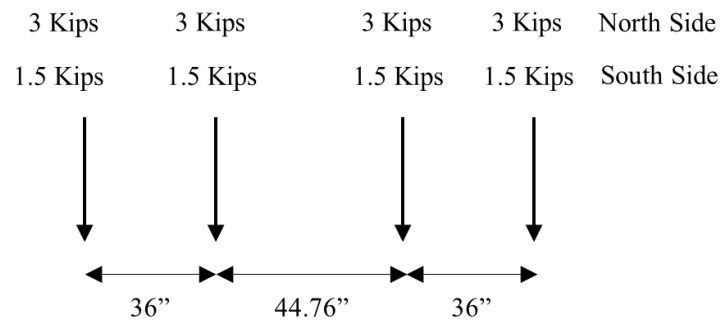


Figure 50. Screed weight and dimensions

Three different cases were studied for the analysis of the Maple Bridge unbraced dry run test:

- Case A: No timber blocking
- Case B: With timber blocking
- Case C: With temporary bracing and timber blocking

These are graphically depicted in Figure 51 and labeled Case A, B, and C in the graphs that follow.

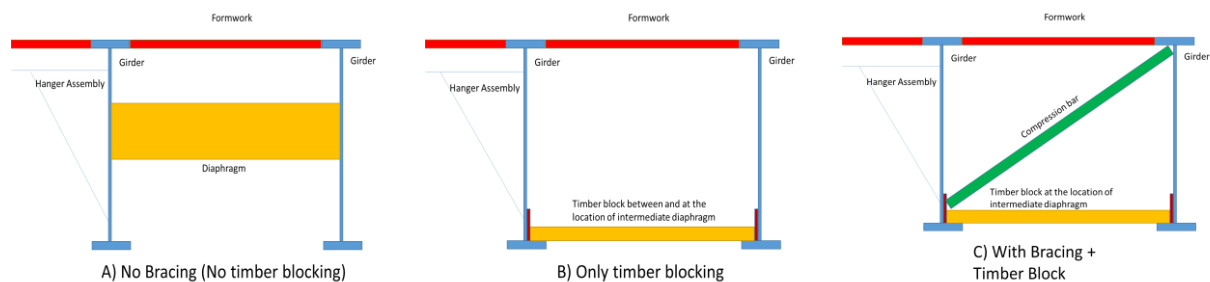


Figure 51. Bracing cases analyzed for the Maple Bridge

The cases were then compared with the data obtained from the Maple Bridge unbraced dry run test. The cases were primarily studied to investigate the effects of different systems such as timber blocks and temporary bracing on the rotation and deflection of the exterior girders. Different types of bracing systems are available to contractors. Some contractors follow traditional practices of installing 4×4 timber blocks along with the shims that lock the timber block with girders between permanent diaphragms.

Bracing plans were modified during construction of the Maple Bridge, so, for Case B with timber blocking for this part of the study, the numerical models were prepared by adding timber blocks in the exterior and first interior bay from each side of the cross-section.

Temporary bracing systems have different requirements, however, #4 transverse tie bars and a tight fit adjustable pipe was suggested as a temporary bracing for Case C of this numerical study. One temporary brace was used when the diaphragm spacing was less than 20 ft and two temporary braces spaced at equal distances were used when the diaphragm spacing exceed 20 ft. The temporary brace was included only in the exterior bays. At the intermediate diaphragm location, only a transverse tie bar was included in the analysis. A temporary brace was also included just beyond the abutments at each abutment location in the exterior bay.

Finite Element Analysis Results and Comparison with Field Investigations (Maple Bridge)

As part of the field investigations, sensors were installed mostly in the second and third span of the Maple Bridge to capture the actual deflection and rotation as the screed traversed from Span 1 to Span 3. Overall, FE analysis predicted results that were in good agreement. The maximum values of deflection and rotations were extracted for each span and are shown in Figure 52 through Figure 57.

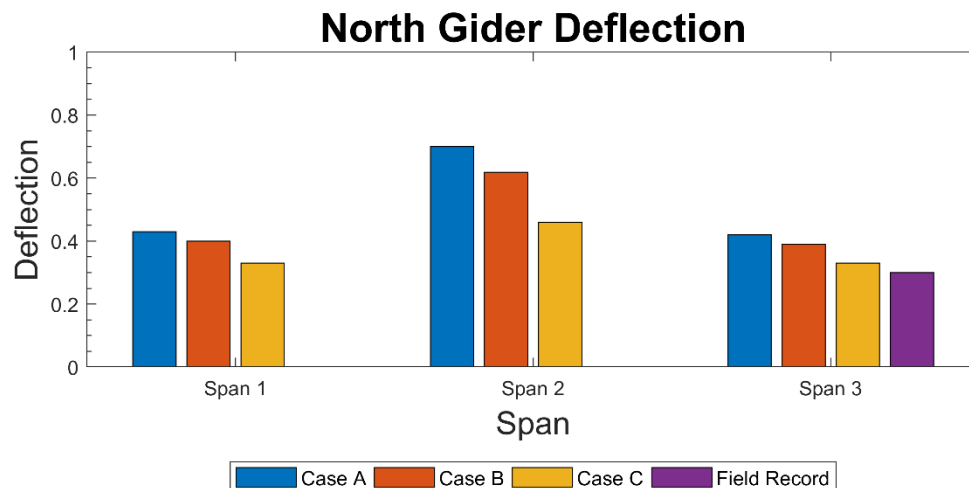


Figure 52. Maple Bridge north girder deflection

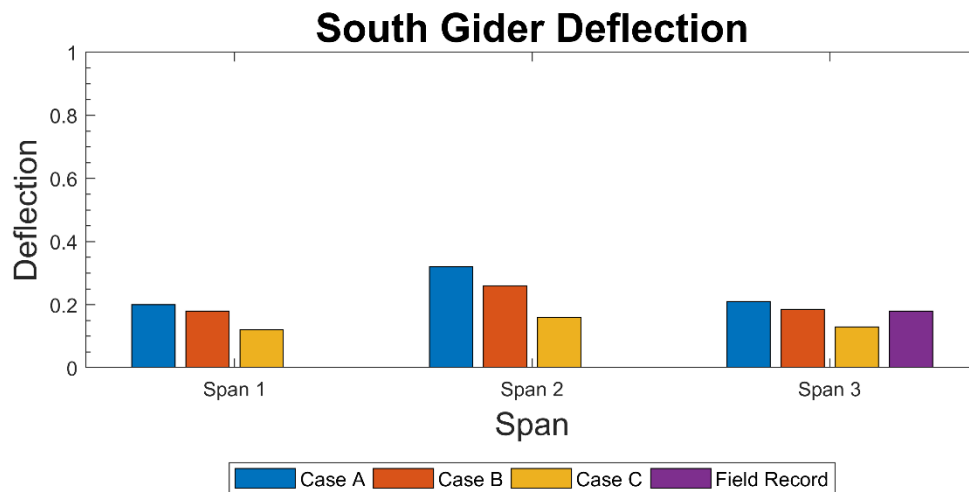


Figure 53. Maple Bridge south girder deflection

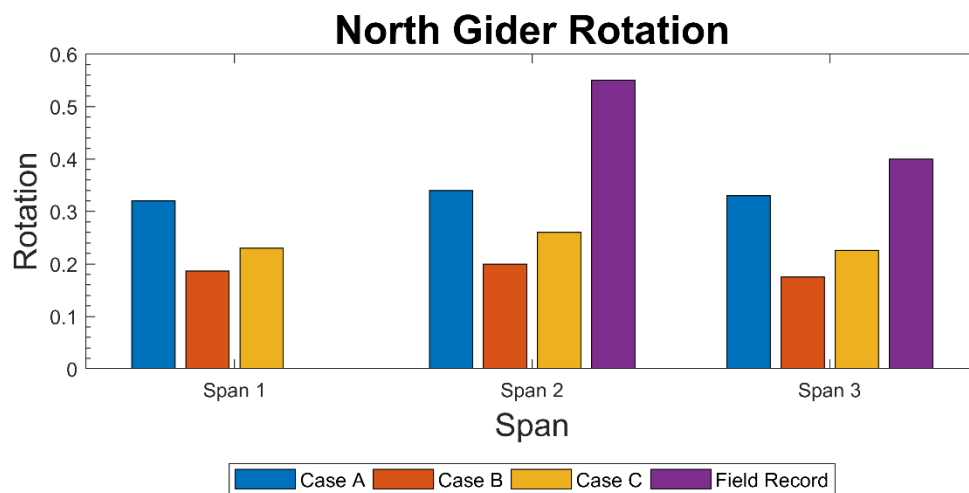


Figure 54. Maple Bridge north girder rotation

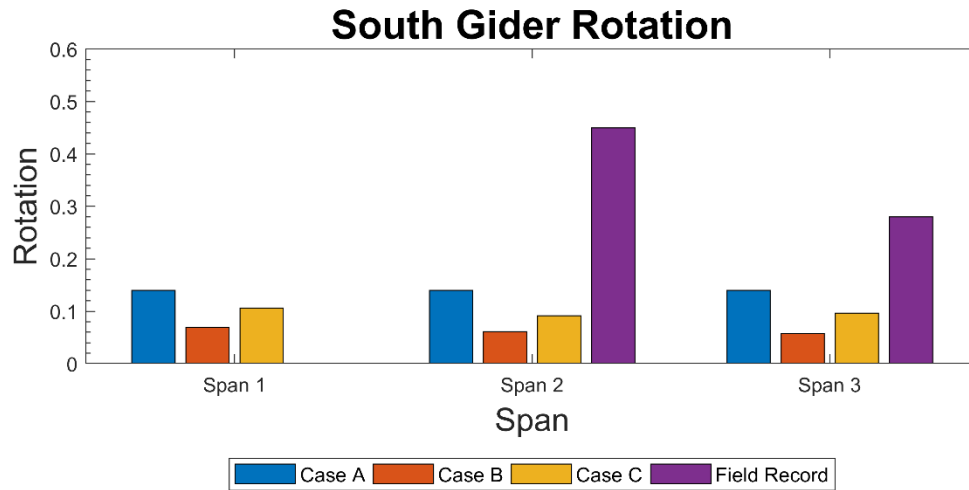


Figure 55. Maple Bridge south girder rotation

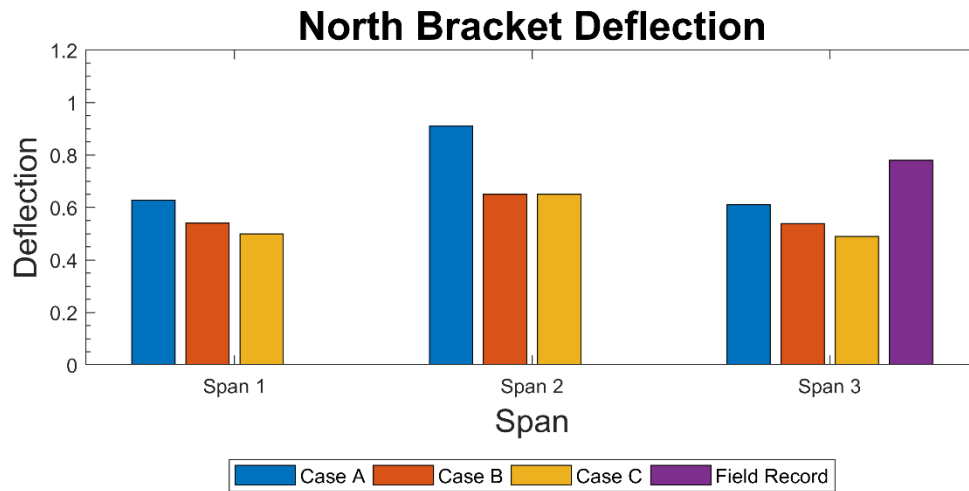


Figure 56. Maple Bridge north bracket deflection

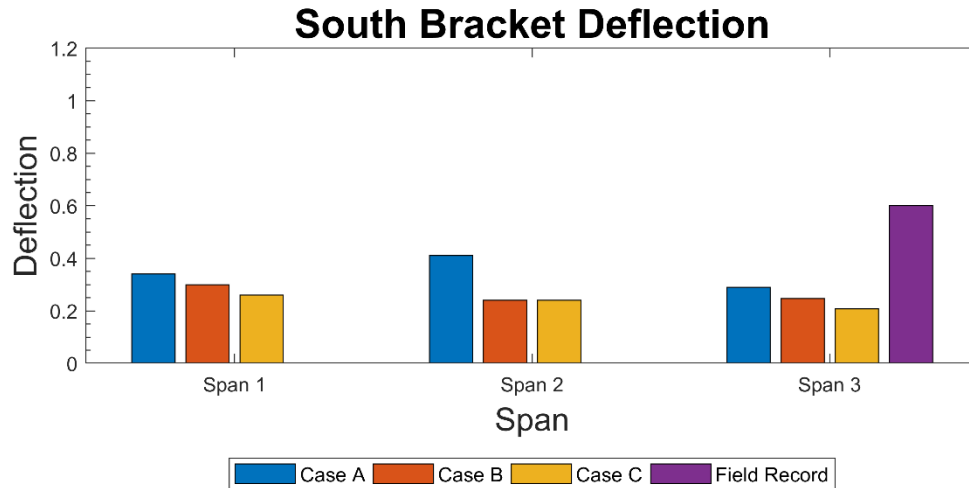


Figure 57. Maple Bridge south bracket deflection

The deflection at Span 3 for the north girder was estimated at 0.45 in., 0.4 in., and 0.35 in. for Case A, B, and C, respectively. The deflection recorded in the field was 0.3 in. Similarly, the deflection at Span 3 for the south girder was estimated 0.21 in., 0.18 in., and 0.13 in. for Case A, B, and C, respectively. The field investigation recorded a value of 0.18 in. The results suggest that adding different bracing components helps reduce the deflection of the girder to a very minimal extent.

For deflection under the bracket, the FEM underestimated the deflection values in Span 3 when compared with the field investigation results for both the exterior girders by 0.15 in. to 0.40 in. The addition of different bracing components did not significantly reduce the bracket deflection. The results also suggest that, by adding timber blocking (Case B) and bracing (Case C), deflections under the bracket are reduced by only a nominal magnitude of 0.05–0.10 in. when compared to no timber block (Case A).

Rotation of both exterior girders was underestimated by the FEM by a magnitude of about 0.15° to 0.30° when Case A and field investigations were compared. Addition of bracing components such as timber block and temporary bracing further reduced the rotation of the exterior girder. This is because the bottom flange is supported against rotation by the compression force generated in the timber block (Case B). In this study, the timber blocks were used for the exterior as well as the first interior bay from either side of the bridge cross-section. Thus, the entire system and, most importantly, the proper shimming between the timber blocks and girders can effectively reduce exterior girder rotation. For Case C, where temporary bracing as well as timber blocks were added to the model, both components got involved in resisting the rotation of exterior girders. Thus, it was concluded that the FEM provided results that had good agreement with the field investigation results.

Finite Element Analysis of BNSF Railway Bridge

The BNSF Railway Bridge is located in Adams County, near Nodaway, on 260th Street over the railway. The bridge has a total span length of 260 ft—comprising three spans, of 78 ft, 104 ft, and 78 ft—and a width of 43 ft 2 in. The 8 in. concrete deck is supported by six steel girders spaced at 6 ft 9 in. apart. It is a 45° skewed bridge with diaphragms spaced at 19 ft 4 in. parallel to the skew. The steel girders are supported over fixed bearings on the first and second spans. The girders were W40×167 and W40×199 at the spliced location. Diaphragms at abutments are C12×20.7, and pier and intermediate diaphragms are MC18×42.7. The permanent diaphragms were parallel to the skew. A 54 in. bracket overhang length was considered for the BNSF Railway Bridge. The model is shown in Figure 58.

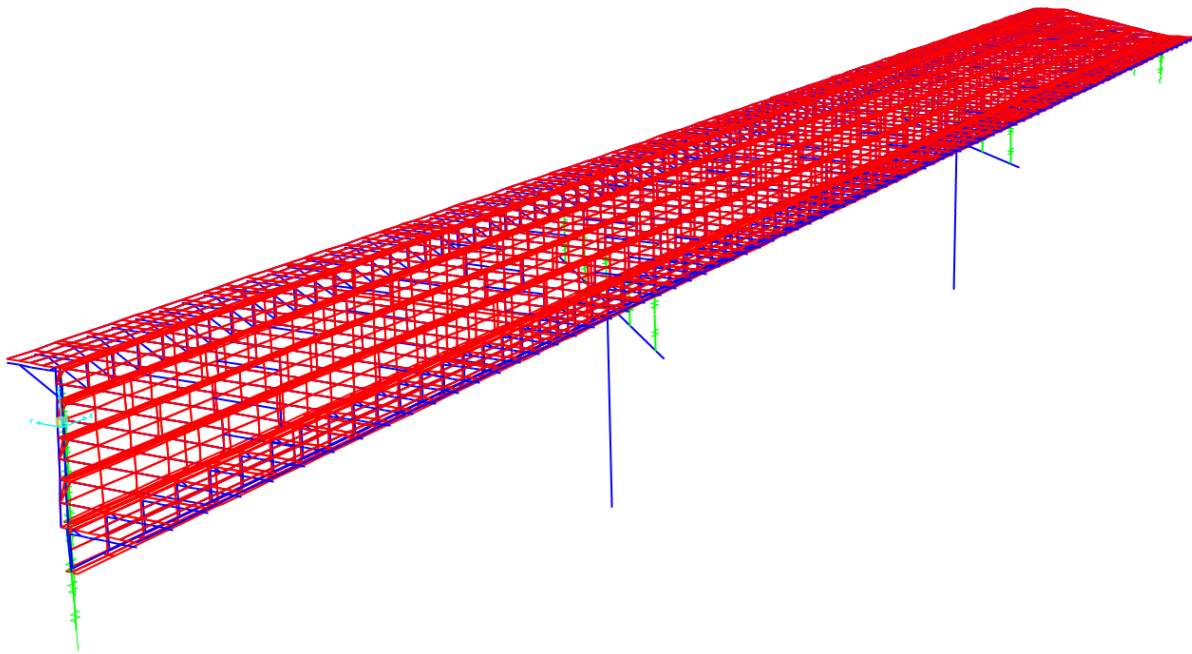


Figure 58. BNSF Railway Bridge model

The field investigation of the bridge was completed for a wet condition; thus, different cases of screed load along with wet concrete load were analyzed and compared with the field readings. The final values of rotation and deflection were obtained by deducting rotation and deflection due to self-weight and rail weight of the structure from total deflection, and rotation due to self-weight, rail weight, wet concrete load, and screed load. Table 7 provides a summary of loads assumed in the preparation of the BNSF Railway Bridge FEA model.

Table 7. Load cases for the BNSF Railway Bridge

Load Case	Description
Case 1	Span 3, centerline of the bridge
Case 2	Span 3, mid-span of south girder
Case 3	End of the rail on north side
Case 9	Span 3, mid-span of north girder
Case 4	Span 2, centerline of the bridge
Case 5	Span 2, mid-span of north girder
Case 6	Span 2, mid-span of south girder
Case 7	End of Span 2, north girder
Case 8	End of Span 2, south girder

Modeling techniques as explained previously were followed for all of the load cases that were analyzed.

Load Cases 1, 2, 3, and 9 were assumed such that the loading scenarios would provide minimum (downward) deflection within the third span. Load Cases 4, 5, 6, 7, and 8 were assumed such that these cases would provide maximum (upward) deflection within the third span.

For the BNSF Railway Bridge, a comparison was made between the bridge installed with timber blocking and without it. In the case of the model with timber blocks, timber blocks were added between permanent diaphragms only in the exterior bays from either side of bridge cross-section. Figure 59 provides a summary of the sensors installed for the field investigation.

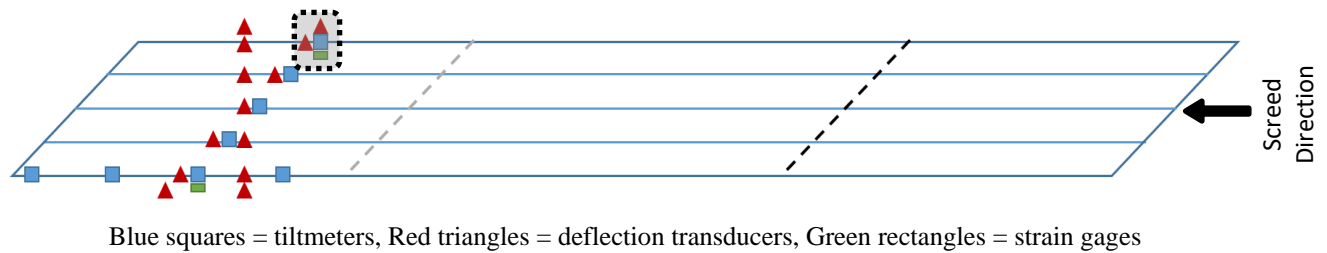


Figure 59. Instrumentation plan of the BNSF Railway Bridge

The third span was fully instrumented perpendicular to the roadway and parallel to the 45° skew. The instrumentation of the second span was not possible due to the railroad below the bridge. The deflection readings taken from sensors as well as the FEM perpendicular to the roadway are termed the cross-section deflection. The deflection and rotation readings taken from sensors as well as the FEM parallel to the 45° skew are termed the diagonal deflection and the diagonal rotation, respectively. The south girder was instrumented between each permanent diaphragm to measure rotation; thus, the points were named 1/8th, 3/8th, 5/8th and 7/8th.

Finite Element Analysis Results and Comparison with Field Investigation (BNSF Railway Bridge)

As part of the field investigations, sensors were installed mostly in the third span for the BNSF Railway Bridge to estimate the actual deflection and rotation as the screed traverses from Span 1 to Span 3. Based on the combination of loading cases studied, the maximum as well as minimum values of deflection and rotation were extracted for the third span and are shown in Figure 60 through Figure 67. From Figure 60, it can be seen that, for the interior girders, the positive cross-section deflection (upward) in Span 3 for all cases is in the range of 0.45 in. to 0.55 in.

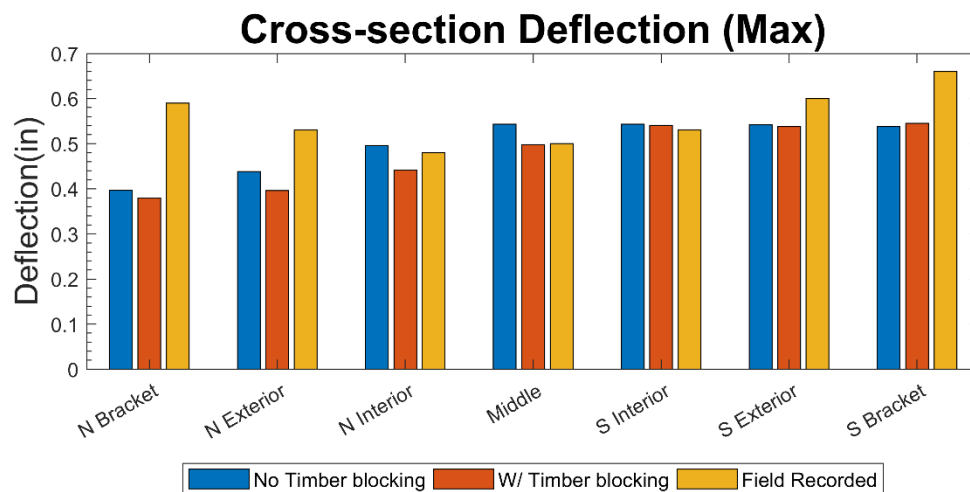


Figure 60. BNSF Railway Bridge maximum cross-section deflection

The positive deflection (upward) for the exterior girders (north and south) as well as the brackets (north and south) recorded in the field was higher than that estimated by the FEM by 0.1 in. to 0.2 in.

Figure 61 shows that the FEM overestimated the minimum cross-section deflection (downward) at all locations compared to what was recorded in the field.

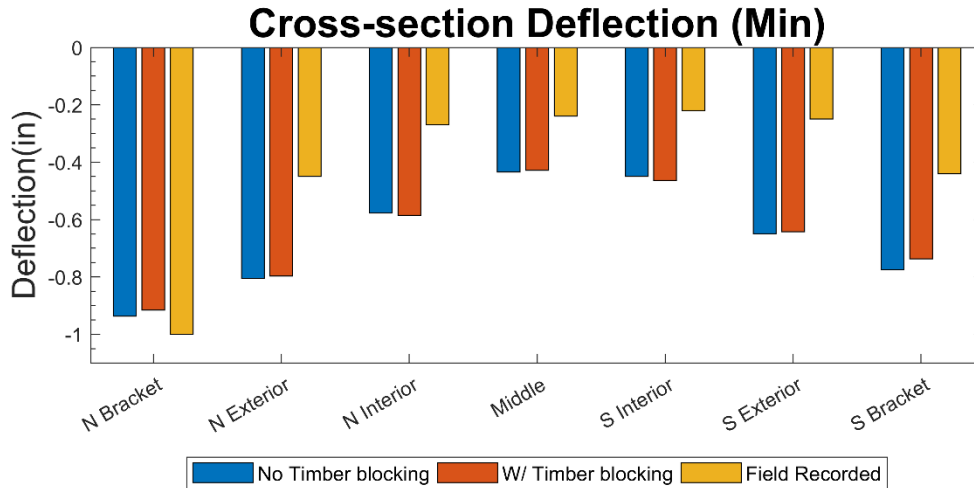


Figure 61. BNSF Railway Bridge minimum cross-section deflection

A similar trend can be seen for diagonal deflection for both the maximum and minimum scenarios from Figure 62 and Figure 63, respectively.

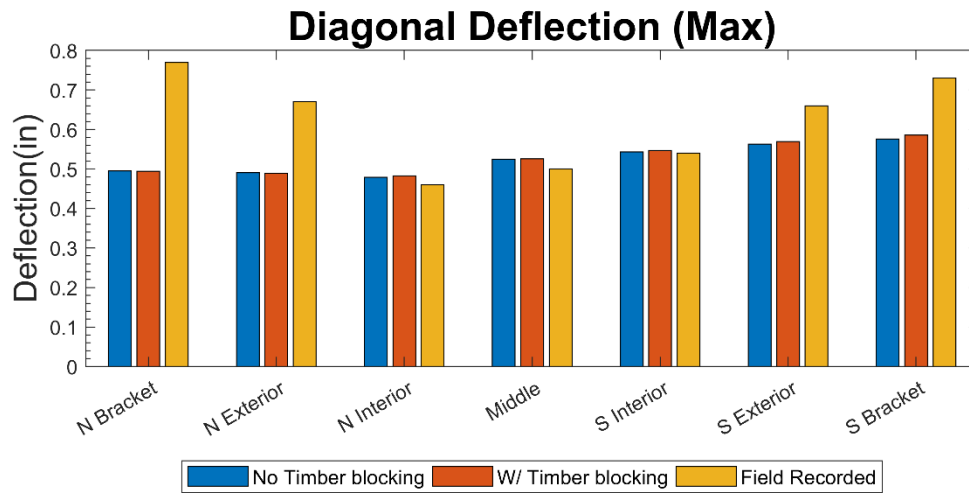


Figure 62. BNSF Railway Bridge maximum diagonal deflection

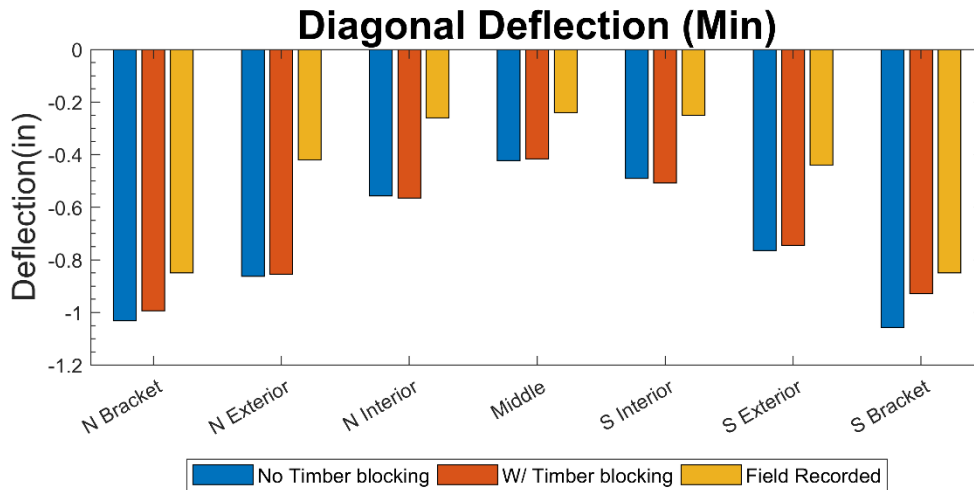


Figure 63. BNSF Railway Bridge minimum diagonal deflection

Figure 64 and Figure 65 show maximum diagonal rotation and minimum diagonal rotation, respectively.

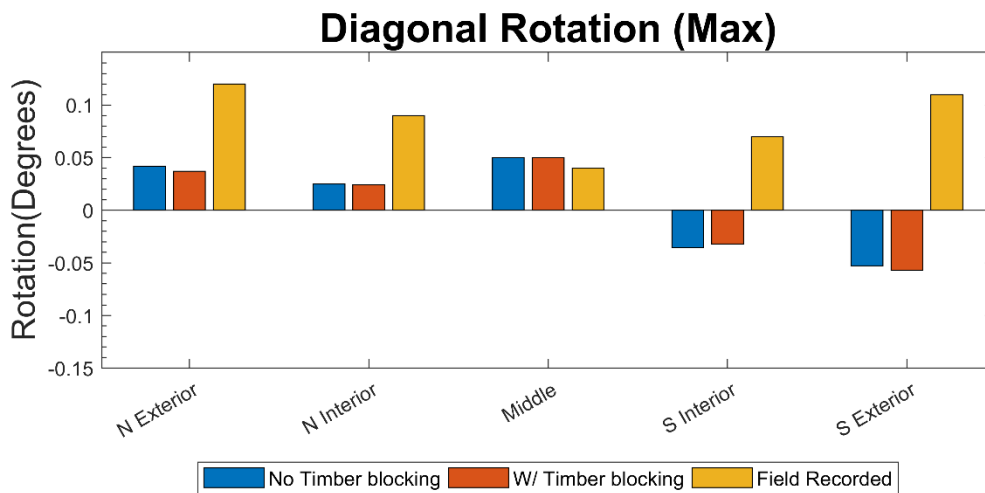


Figure 64. BNSF Railway Bridge maximum diagonal rotation

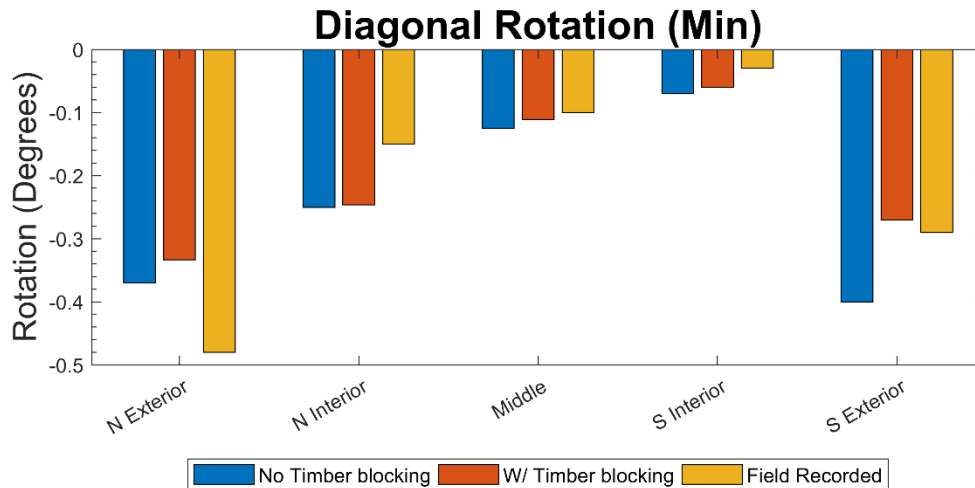


Figure 65. BNSF Railway Bridge minimum diagonal deflection

The minimum diagonal rotation for the north and south girders recorded in the field were 0.48° and 0.29° , respectively. The FEM for no timber blocking and with timber blocking for the north girder estimated 0.37° and 0.34° , respectively. Similarly, for no timber blocking and with timber blocking for the south girder, the FEM estimated 0.4° and 0.27° , respectively. The range for maximum diagonal rotation per the field investigation was recorded between 0.04° and 0.14° . Both cases of no timber blocking and with timber blocking of the BNSF Railway Bridge FEM slightly underestimated the maximum diagonal rotation seen in the field. Figure 66 and Figure 67 show the maximum and minimum values of rotation estimated at different points along the length of the south girder.

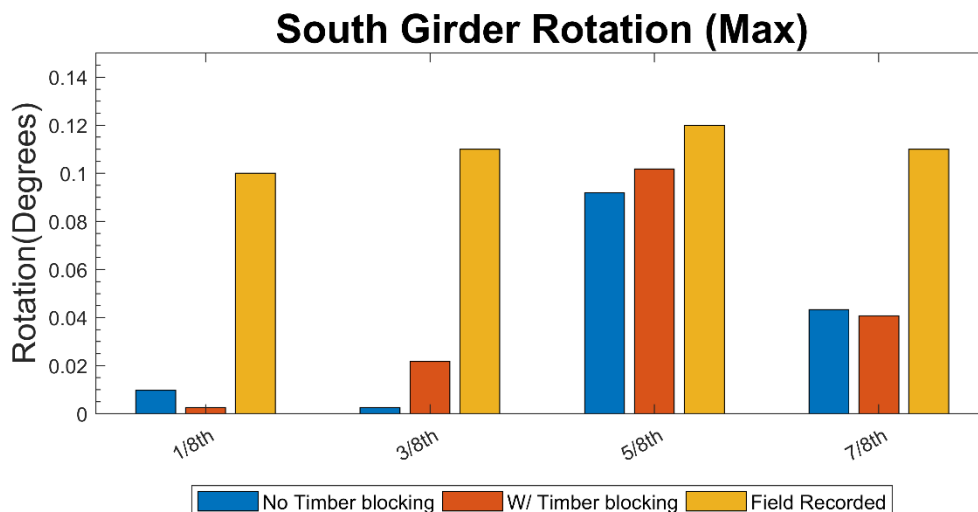


Figure 66. BNSF Railway Bridge maximum south girder rotation

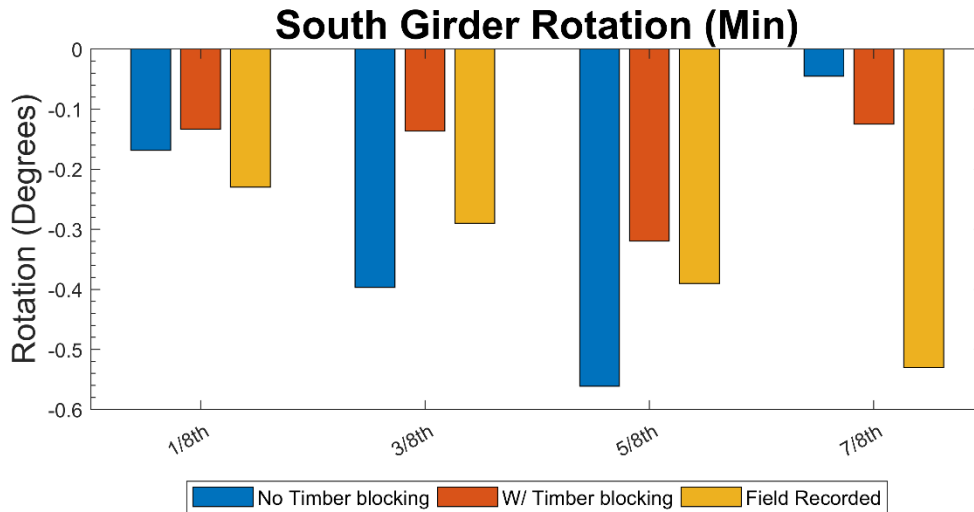


Figure 67. BNSF Railway Bridge minimum south girder rotation

From Figure 67, it can be seen that the minimum rotation at all points, except the 7/8th point, was overestimated by the no timber block FE model.

The rotations were reduced significantly at midspan of the third span for the FEM with timber blocking. Several values of the rotation and deflection were within the acceptable range for the FEM and that recorded in the field. However, the combination of different loading conditions may not have captured all the maximum and minimum effects to correlate with the field investigations.

Iowa DOT 160 ft Standard Bridge

To study the effects of loads on exterior girders, a numerical study was performed to investigate situations with different combinations of timber blocks, temporary bracing, and the orientation of temporary bracing and load location. In this analysis, a 160 ft Standard Bridge having the shallowest girder, which is W30×99, was used. The model is shown in Figure 68.

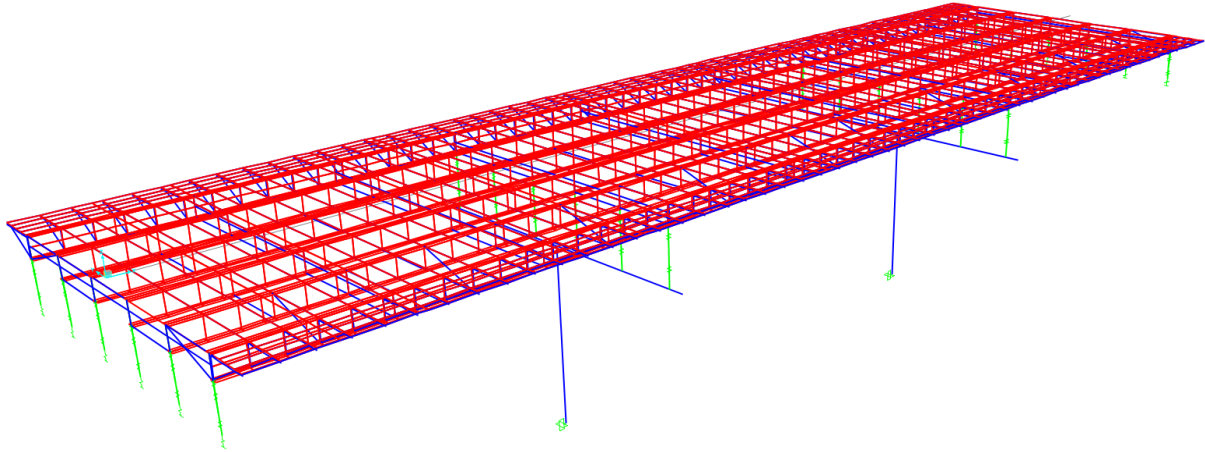


Figure 68. Iowa DOT 160 ft Standard Bridge model

An integral abutment bridge with a fixed bearing on the first pier and an expansion bearing on the second pier was assumed. Initially, the analysis was carried out for four cases: no timber block, with timber block, with temporary bracing, and with temporary bracing + timber blocks. Further, two cases—no timber block and with temporary bracing + timber blocks—were studied to investigate the effect of load location and orientation of the cross-frame (see Figure 69).

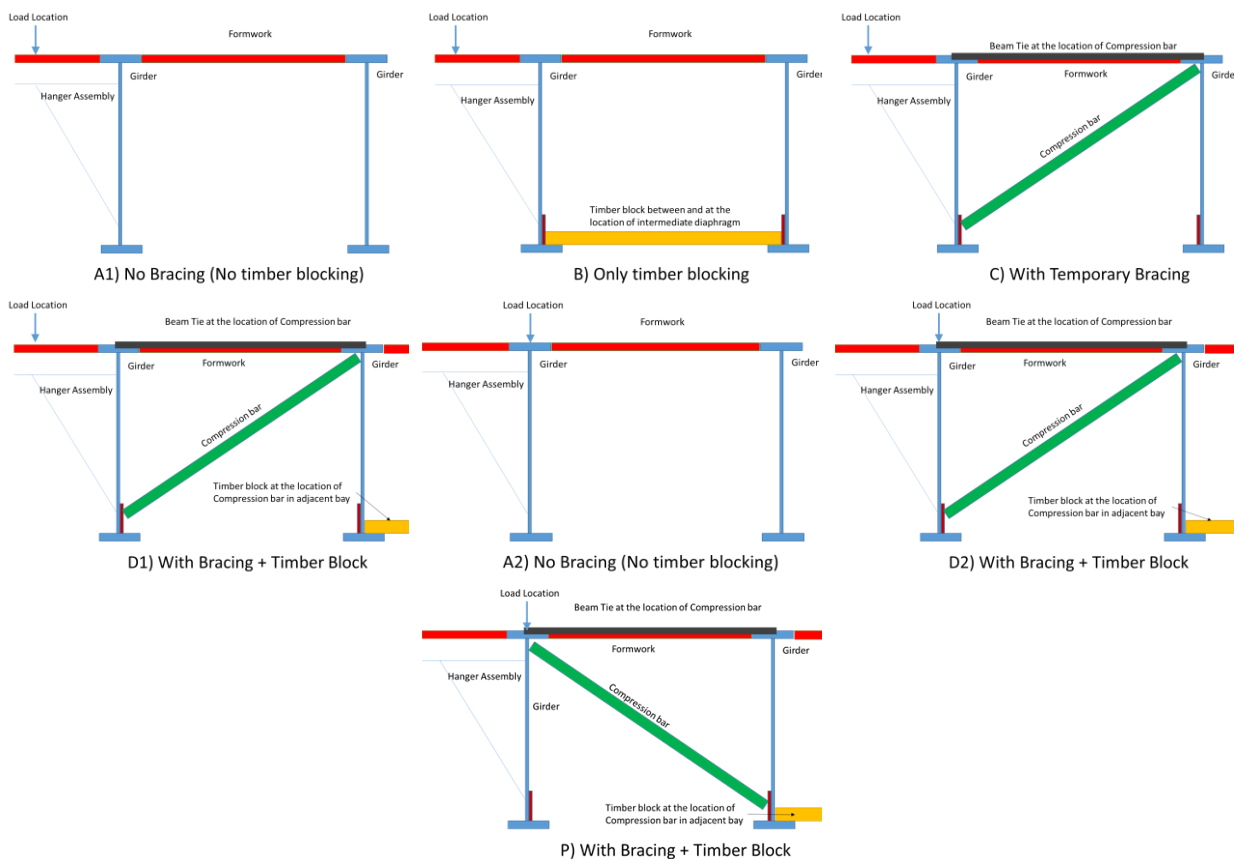


Figure 69. Cases investigated for 160 ft Standard Bridge

For Case A1, no bracing or timber blocks were added. For Case B, timber blocks were added between two diaphragms and at the locations of permanent diaphragms in the exterior as well as the first interior bay from either side of the bridge cross-section. For Case C, only temporary bracing was added in the exterior bays. For Case D1, timber blocking and temporary bracing was studied as follows: in the exterior bay, timber blocks were not present where the temporary bracing was present and, at the permanent diaphragm locations, timber blocks were added at the bottom flanges of the girders; in the first interior bay, timber blocks were added between permanent diaphragms and at the permanent diaphragm locations. Note that no temporary bracing was added in the interior bays in any of the cases.

Case A1 and D1 were further extended to study the effect of load location and called Case A2 and D2. In Case A2 and D2, rail load and screed weight were applied at the centerline of the exterior girder. Case P was studied to understand the effects of load location and change in the cross-frame orientation along with timber blocks. In Case P, the combination of a timber block and a compression bar remained similar to Case D1; however, the orientation of the compression bar was changed. The compression bar in Case P was connected from the top of the exterior girder to the bottom of the first interior girder.

The previous Figure 69 provides a graphic depiction of all the cases.

The vehicle load was applied at the middle span of each span and a wet concrete load was assigned ahead of the finishing machine to estimate the maximum girder rotation and deflection for each span. Live loads as described in Table 8 were assigned to the rest of the surface of the formwork.

Table 8. Load cases for the 160 ft Standard Bridge

Load	Description
Self-weight of girders, diaphragms, formwork, bracket assembly	Directly calculated by the program
Rail weight	75 plf 2 ½ in. from edge of the concrete deck 75 plf at centerline of girder (Case A2, D2, and P)
Weight of Concrete	100 psf, up to 15 ft ahead of the screed location
Live Load	50 psf all over the portion of the deck 50 psf live load is present on the walkway
Screed Weight,	9 kips on the north side 3 kips on the south side
Deflection caused by vehicle	Total deflection (GW+FW+RW+VL+LL +CL) – Deflection due to (GW + FW + RW)

GW = girder weight, FW = formwork weight, RW = rail weight, VL = vehicle load, LL = live load, CL = concrete load

In the discussion that follows, Case A1, B, C, and D1 are compared first and then the comparisons are extended to Case A1, A2, D1, D2, and P. Figure 70 through Figure 72 show the loading conditions that were assumed for this set of analyses.

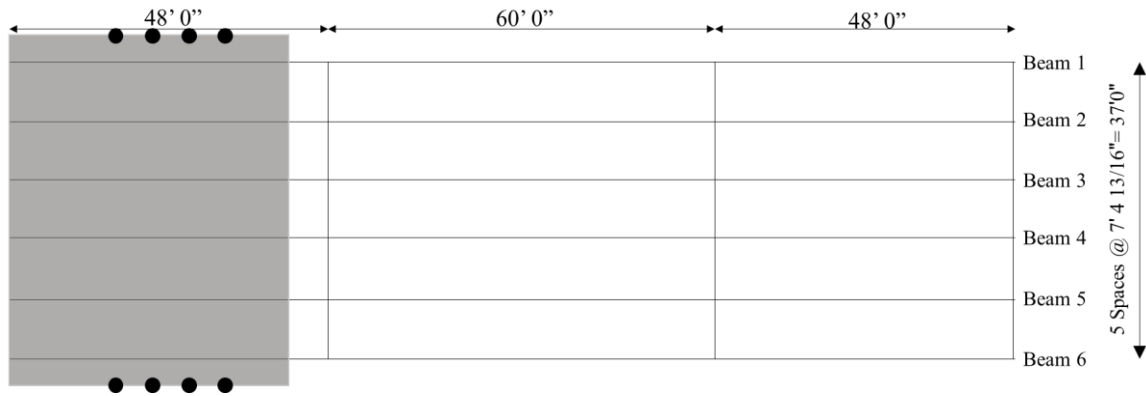


Figure 70. Span 1 vehicle and wet concrete load for 160 ft Standard Bridge

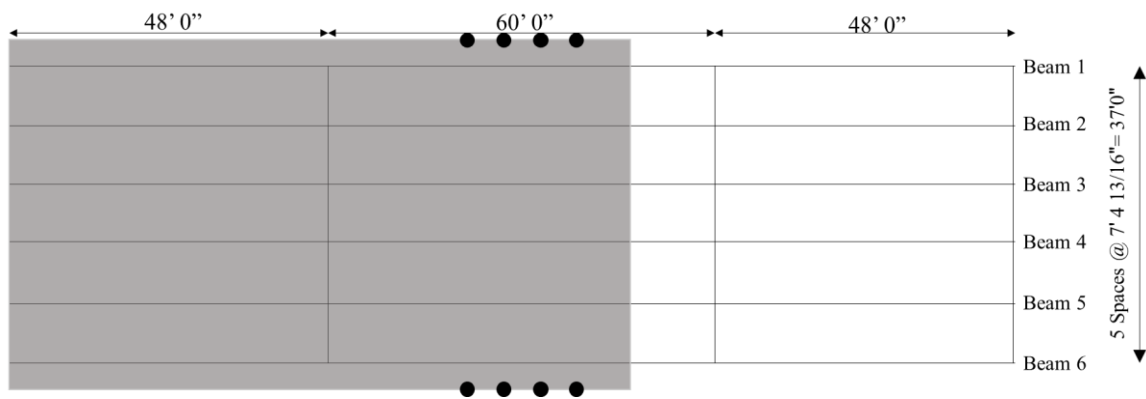


Figure 71. Span 2 vehicle and wet concrete load for 160 ft Standard Bridge

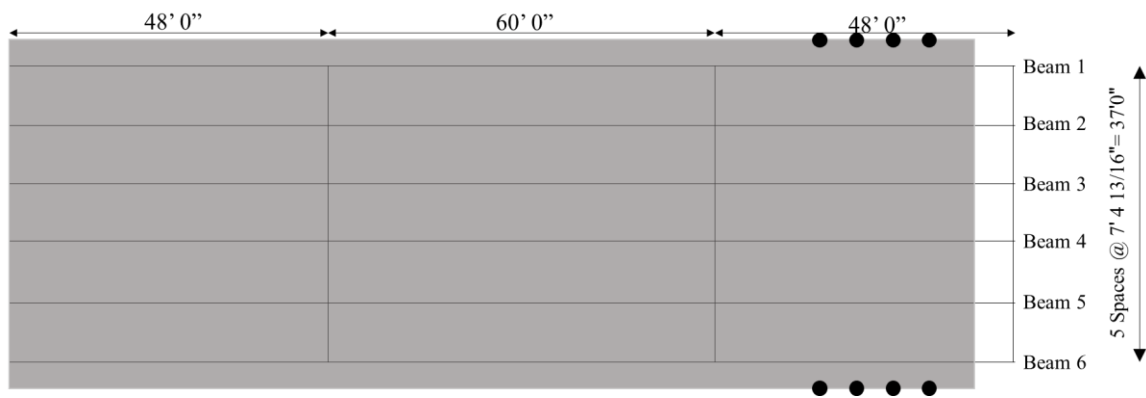


Figure 72. Span 3 vehicle and wet concrete load for 160 ft Standard Bridge

For the first set of analysis, different configurations of bracing systems were found to have no significant effect on the deflection of the north and south girder (Figure 73 and Figure 74).

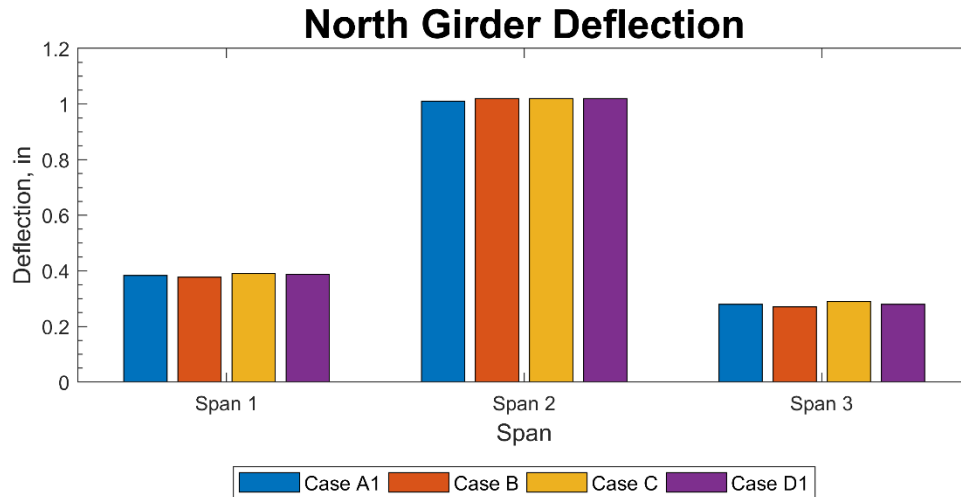


Figure 73. 160 ft Standard Bridge north girder deflection

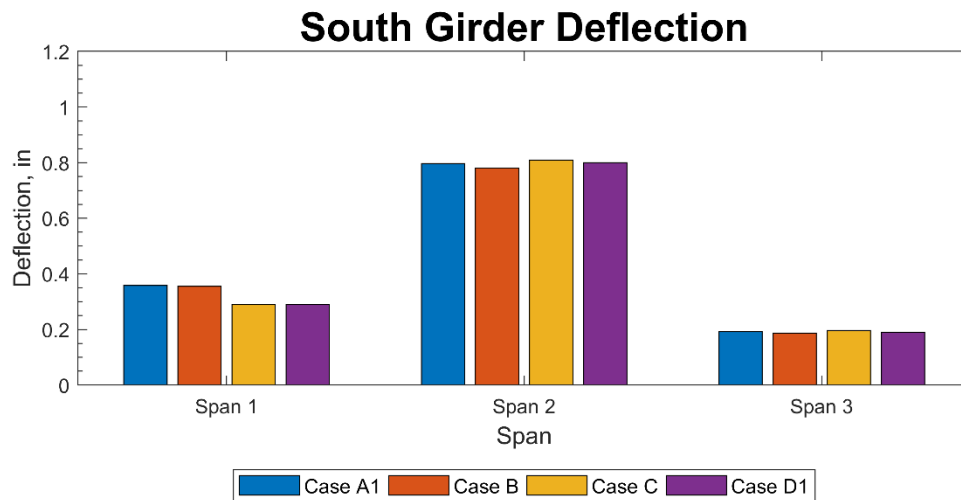


Figure 74. 160 ft Standard Bridge south girder deflection

However, rotation was greatly reduced as bracing components were introduced one by one (Figure 75 and Figure 76).

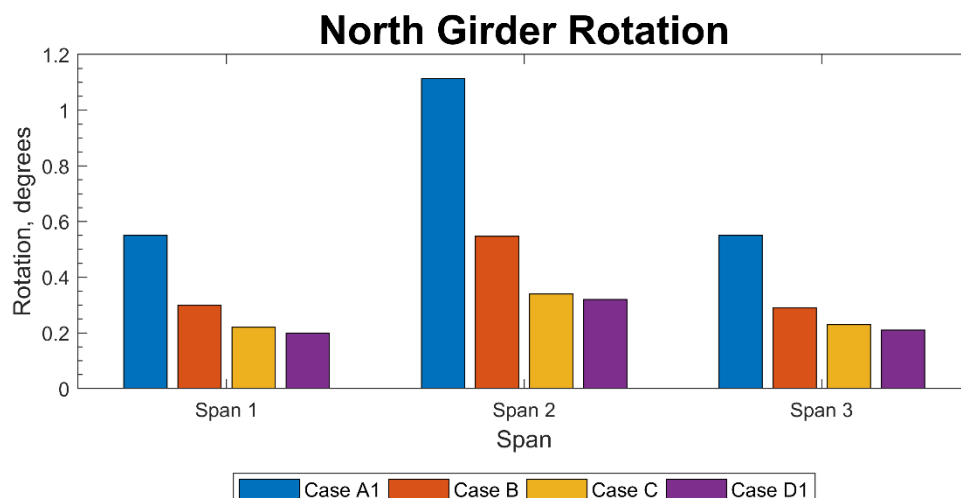


Figure 75. 160 ft Standard Bridge north girder rotation

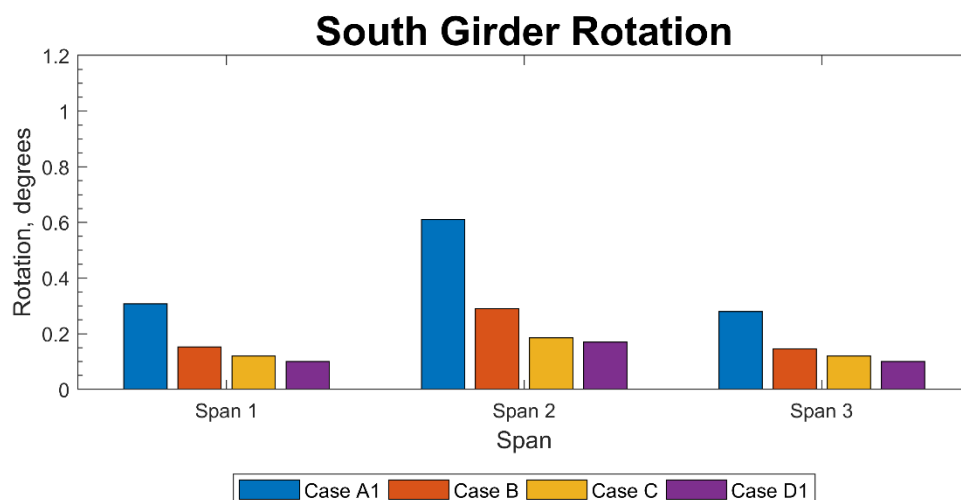


Figure 76. 160 ft Standard Bridge south girder rotation

For the first span of the north girder, rotations of 0.55° , 0.30° , 0.22° , and 0.20° were calculated from the numerical studies for Case A1, B, C, and D1, respectively. Similarly, for the first span of the south girder, rotations of 0.31° , 0.15° , 0.12° , and 0.10° were recorded for Case A1, B, C, and D1, respectively. For the second span, rotation values of 1.11° , 0.55° , 0.34° , and 0.32° for the north girder and 0.61° , 0.29° , 0.19° , and 0.17° for the south girder were obtained for cases A1, B, C, and D1, respectively. The primary differences in the rotation values for the north versus south girder are due to the magnitude of the screed wheel load. As mentioned earlier, adding the different components of bracing did not have any significant effect on the deflection of the exterior girders; however, it has some marginal effect on the deflection of the bracket (Figure 77 and Figure 78).

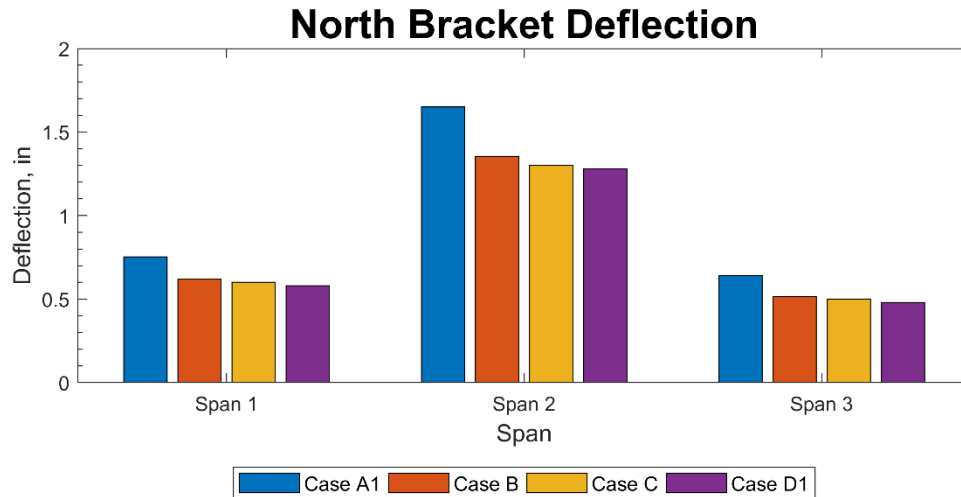


Figure 77. 160 ft Standard Bridge north bracket deflection

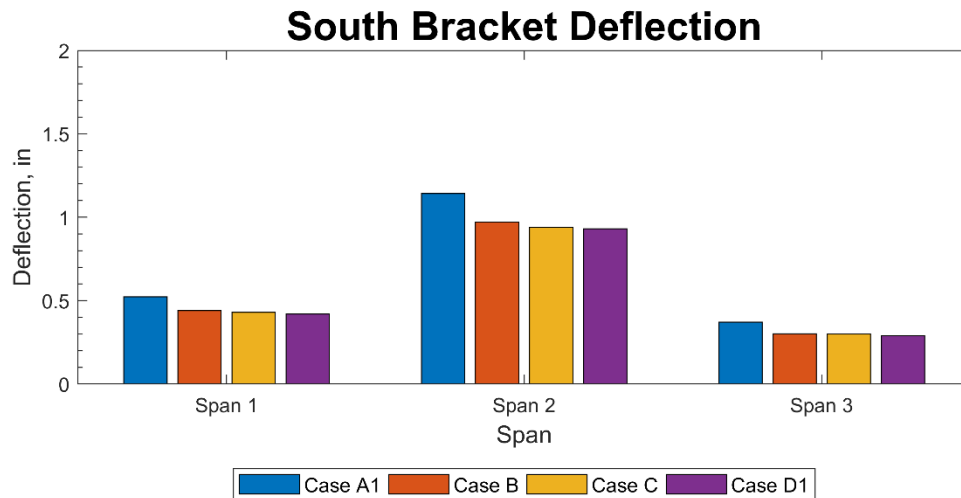


Figure 78. 160 ft Standard Bridge south bracket deflection

Due to reduced rotation, the deflection under the bracket is also reduced. The reduction in the deflection can be of concern from the design point of view, because it is sometimes preferred to limit the deflection of the bracket assembly instead of putting a limit on the rotation of the exterior girders. The temporary bracing along with the use of timber blocks offered the greatest performance improvement to minimize rotation.

The cases that provided the maximum and minimum values of rotation for exterior girders were further investigated (see Figure 79 through Figure 84). A similar pattern was observed for deflection, where changing different configurations of bracing components did not have any significant effect on the deflection of the south and north girders (Figure 79 and Figure 80).

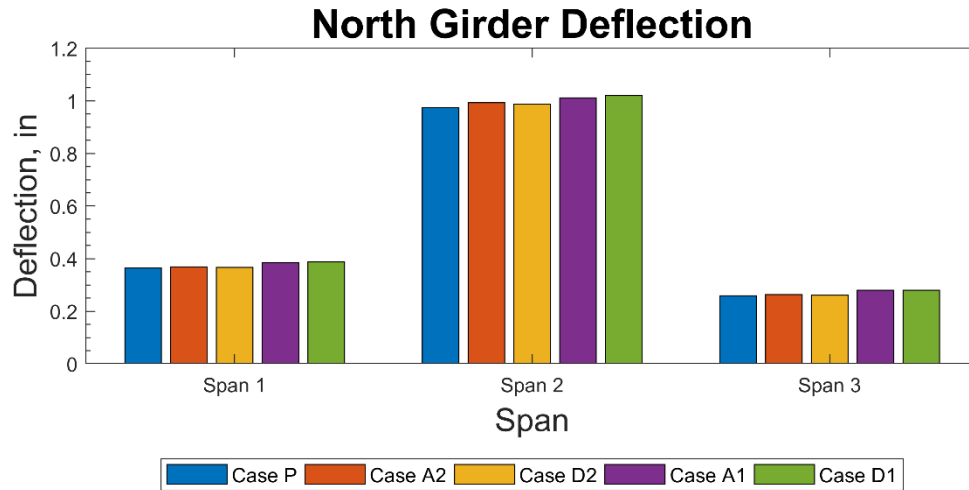


Figure 79. 160 ft Standard Bridge north girder deflection

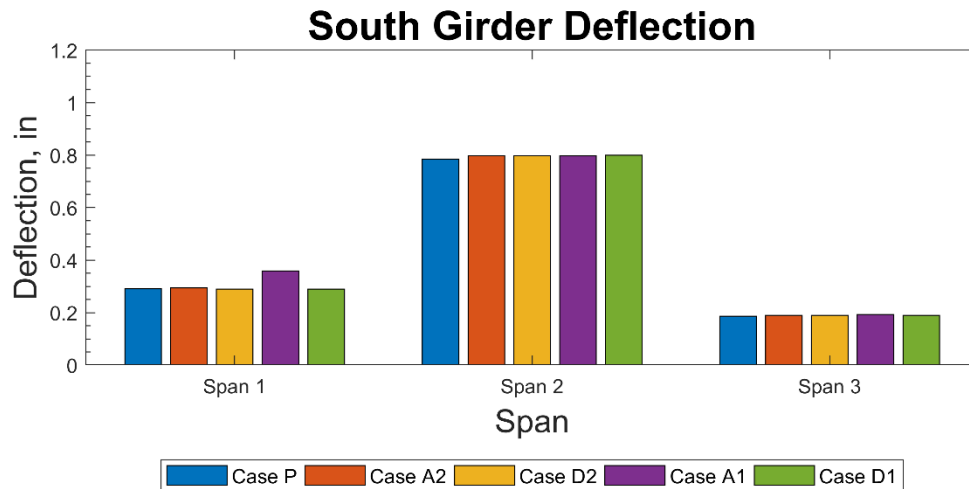


Figure 80. 160 ft Standard Bridge south girder deflection

However, the rotation of the exterior girder along with the deflection under the bracket was reduced for Case P, A2, and D2 compared to Case A1 (Figure 81 and Figure 82).

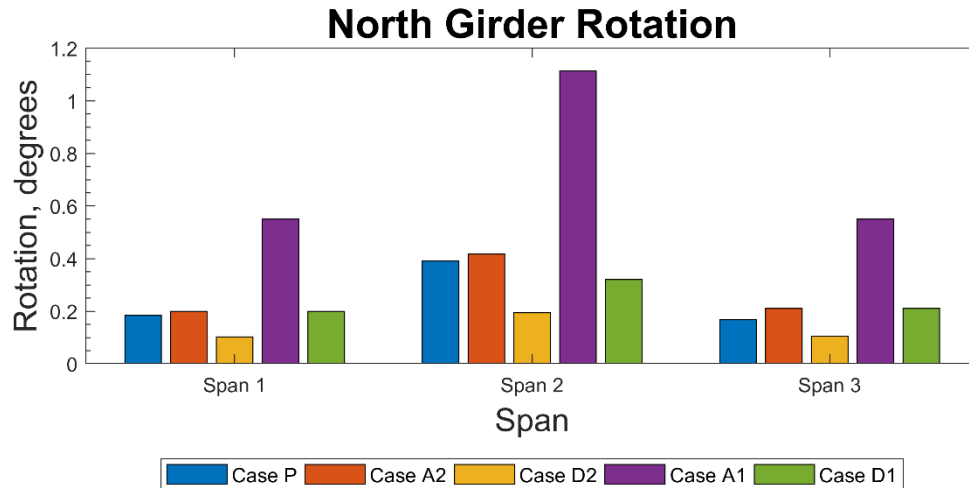


Figure 81. 160 ft Standard Bridge north girder rotation

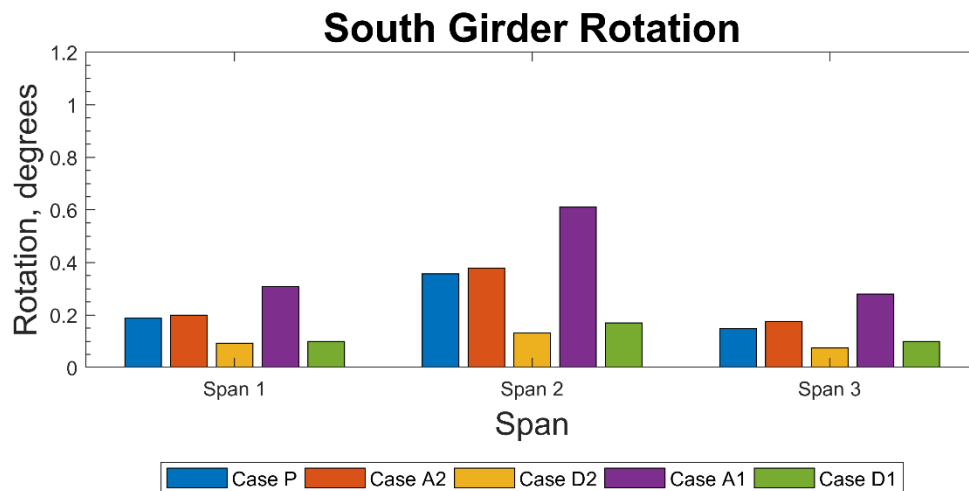


Figure 82. 160 ft Standard Bridge south girder rotation

Changing the location of the wheel load was found to reduce rotation significantly. This can be confirmed by comparing Case A2 and A1. Similarly, changing the orientation of the diagonal strut along with applying the load at the centerline of the exterior girder, as included in Case P, did not make a significant difference when compared to Case D1. This, however, can minimize the effects to a limited extent due to the location of the load application. Case D2 provided the lowest values of rotation and bracket deflection (Figure 83 and Figure 84).

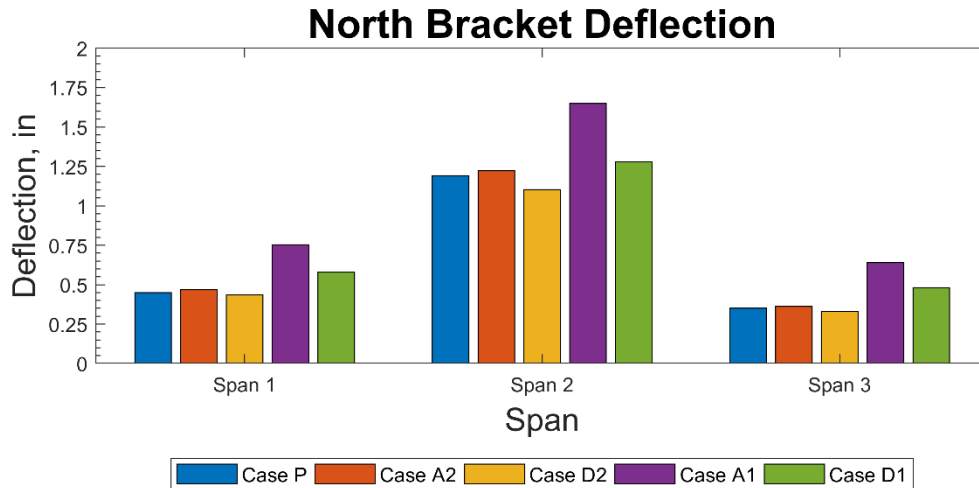


Figure 83. 160 ft Standard Bridge north bracket deflection

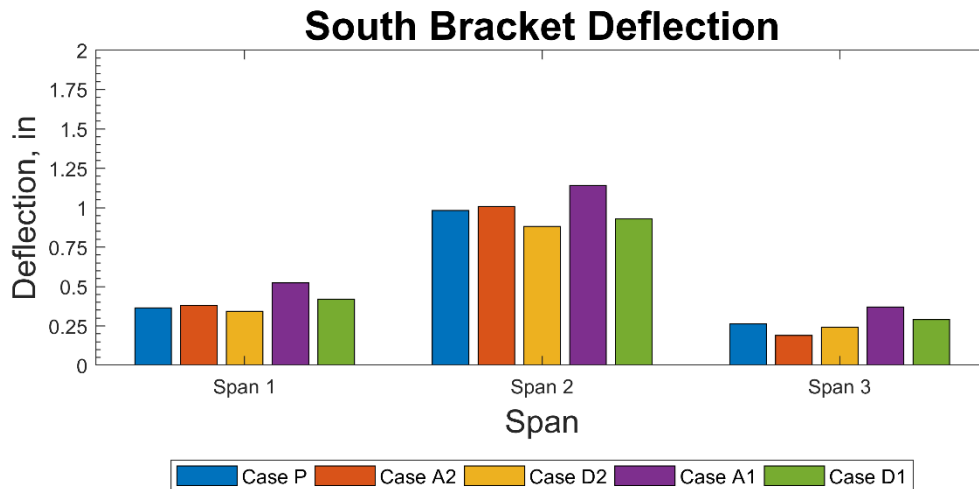


Figure 84. S160 ft Standard Bridge south bracket deflection

This could be due to the fact that, when the orientation of the diagonal strut is reversed, the bottom flange of the girder is not supported and the stiffness provided by the transverse ties as well as the diagonal strut are less than that provided by the temporary bracing system, as included in Case D2.

CHAPTER 5. PARAMETRIC STUDY

To investigate the parameters that affect the rotation and deflection of exterior girders, as well as the deflection of the brackets, the researchers performed a parametric study involving six different parameters. The goal of the parametric study was to identify the parameters for which the rotation and deflection of the exterior girders and brackets were most sensitive. The six parameters identified to study were brace strength, skewness angle, diaphragm spacing, girder spacing, span ratio, and girder flange thickness.

For the parametric study, the researchers modeled and used the Iowa DOT 260 ft Standard Bridge. The modeling of the bridge was completed similar to the procedure described for the analytical case study bridges, except for the timber blocking and temporary bracing. Timber blocks and compression struts of the temporary bracings were modeled using compression-only elements by providing the axial stiffness of the members. This modeling technique is expected to simulate the actual situation of the bridge, as these members are expected to participate when subjected to a compression load. Figure 85 provides an overview of the bridge modeled using the CSiBridge software package.

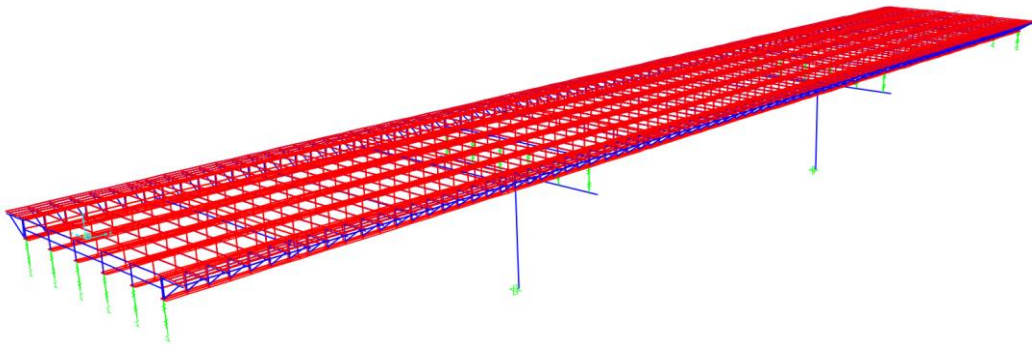


Figure 85. Iowa DOT 260 ft Standard Bridge model

Table 9 summarizes the loading details considered in this investigation.

Table 9. Loads considered for parametric study on the 260 ft Standard Bridge

Load	Description
Self-weight of girders, diaphragms, formwork, bracket assembly	Directly calculated by the software
Rail weight	75 plf 2 ½ in. from edge of the concrete deck
Weight of Concrete	100 psf, up to 15 ft ahead of screed location
Live Load	50 psf all over the portion of deck
	50 psf live load on walkway
Screed Weight,	6 kips on the north side
	6 kips on south side
Deflection caused by vehicle	Total deflection (GW+FW+RW+VL+LL +CL) – Deflection due to (GW + FW + RW)

GW = girder weight, FW = formwork weight, RW = rail weight, VL = vehicle load, LL = live load, CL = concrete load

Three load cases were studied for each of the six parameters. The load cases were applied at the mid-span of the interior and each exterior span as shown in Figure 86 through Figure 88.

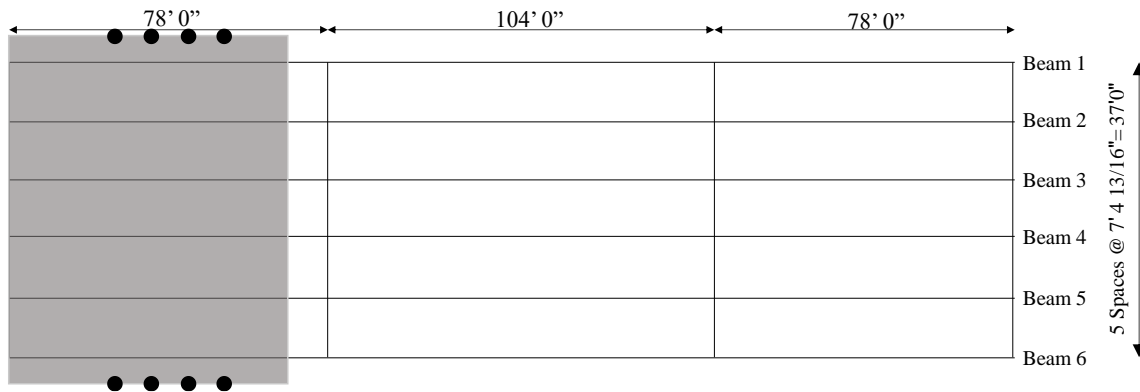


Figure 86. Span 1 vehicle and wet concrete load for 260 ft Standard Bridge

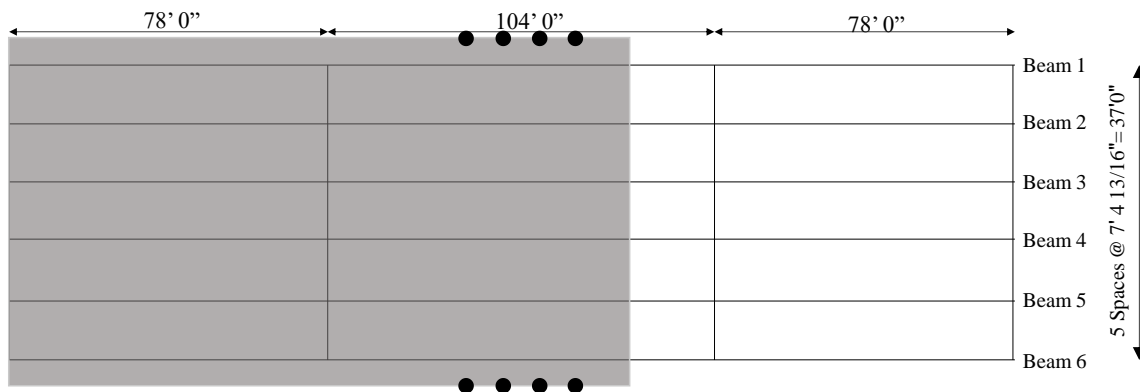


Figure 87. Span 2 vehicle and wet concrete load for 260 ft Standard Bridge

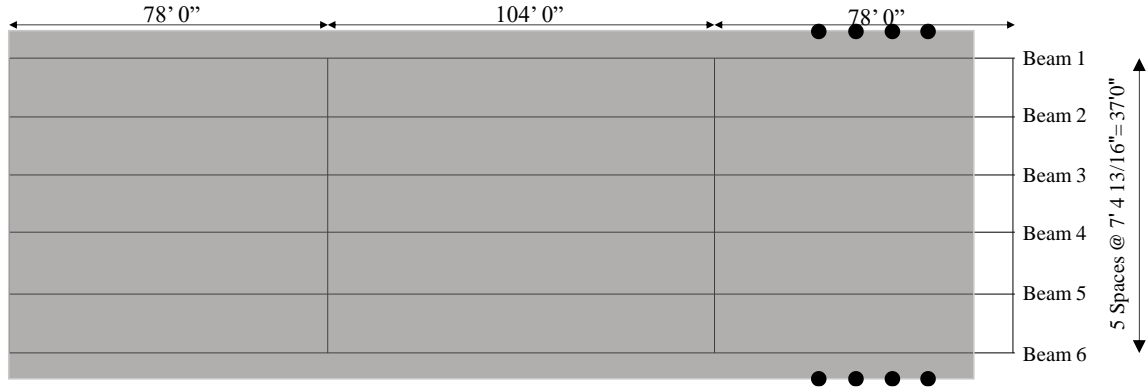


Figure 88. Span 3 vehicle and wet concrete load for 260 ft Standard Bridge

The three bracing conditions were investigated similar to the Ida County Maple Bridge.

Brace Strength

A series of diaphragms act together with the longitudinal girders to form a system that behaves as a unit. An effective brace resists twist of the cross-section. Diaphragms are placed at the ends, across the interior supports, and intermittently along the span. Diaphragms are placed to transfer the lateral loads from the bottom of the girder to the deck and from the deck to the bearings, providing stability to the bottom flange when it is subjected to the compression load and stability to the top flange when it is in compression before the deck hardens. Diaphragms also help prevent distortion during bridge construction and distribute dead and live loads uniformly to the bridge system. The American Association of State Highway and Transportation Officials (AASHTO) *Load and Resistance Factor Design (LRFD) Bridge Design Specifications* suggest that diaphragms for rolled beams and plate girders should be as deep as possible. However, the minimum depth of diaphragms should be half of the girder depth for rolled steel girder bridges and three quarters of the girder depth for plate girder bridges. The basic equation for buckling strength of the torsionally braced beams under a uniform moment with continuous torsional bracing is given by the following:

$$M_{cr} = \sqrt{M_o^2 + \overline{\beta}_b EI_y}$$

where, M_o = buckling capacity of unbraced beam in kip-in and $\overline{\beta}_b$ = attached torsional brace stiffness in in-k/rad per in. length). Yura et al. (1992) developed an equation to calculate an effective brace stiffness, β_T , including the effects of stiffeners as follows:

$$\frac{1}{\beta_T} = \frac{1}{\beta_b} + \frac{1}{\beta_{sec}} + \frac{1}{\beta_g}$$

where, β_b is the stiffness of the attached brace, β_{sec} is the cross-section web stiffness, and β_g is the girder system stiffness. The AASHTO specifications do not explicitly provide guidance on

quantifying the spacing of diaphragms/bracing for regular steel bridges. Thus, in this parametric study, the effect of brace stiffness was evaluated on the deflection and rotation of exterior girders subjected to torsional loads. Structural sections C15×33.9 and W21×50 were assumed as intermediate diaphragms in this investigation. Using the two different sections, FEMs were developed. According to the standard rolled beam bridges, W21×50s were designed to be the intermediate diaphragms for the 260 ft Standard Bridge. Figure 89 through Figure 96 show the results obtained for the brace strength as the parameter of interest.

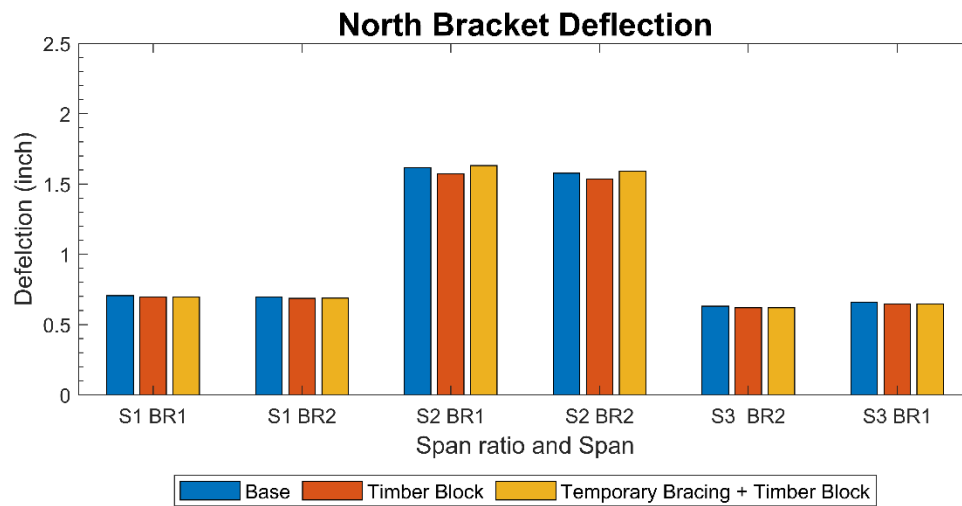


Figure 89. 260 ft Standard Bridge north bracket deflection (brace strength)

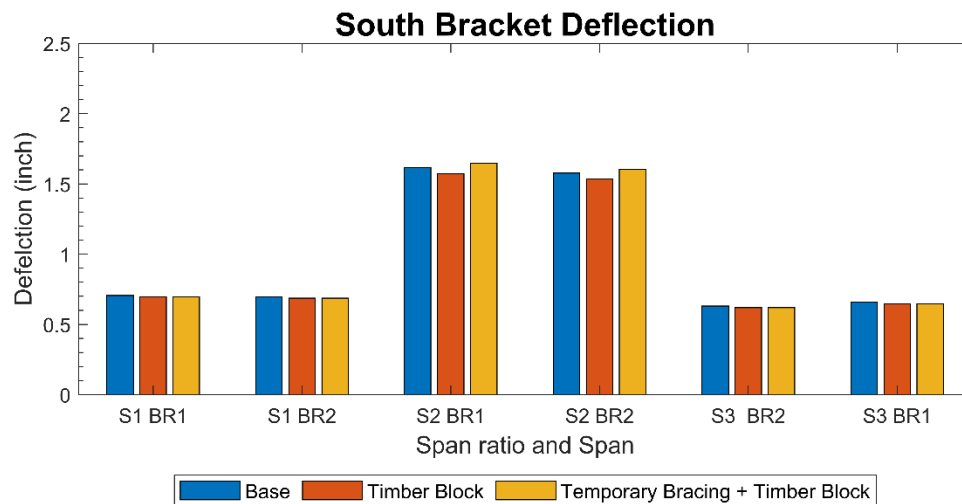


Figure 90. 260 ft Standard Bridge south bracket deflection (brace strength)

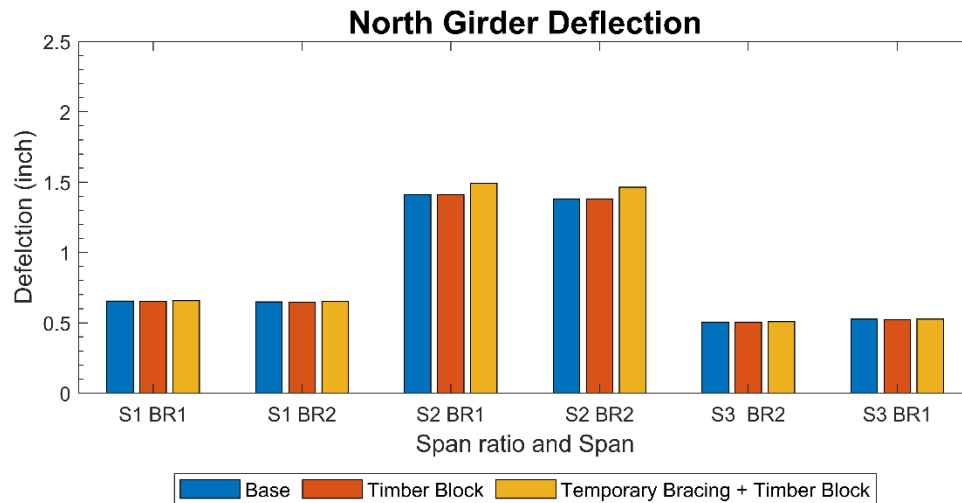


Figure 91. 260 ft Standard Bridge north girder deflection (brace strength)

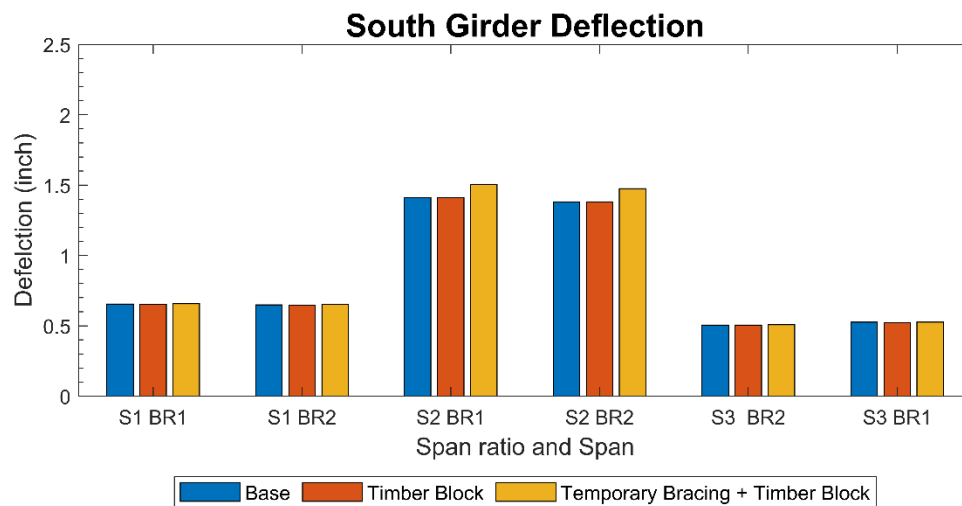


Figure 92. 260 ft Standard Bridge south girder deflection (brace strength)

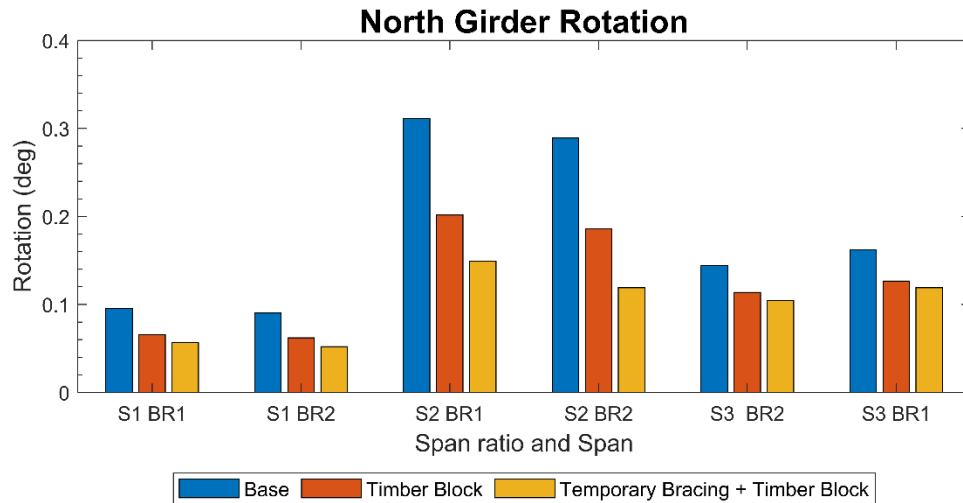


Figure 93. 260 ft Standard Bridge north girder rotation (brace strength)

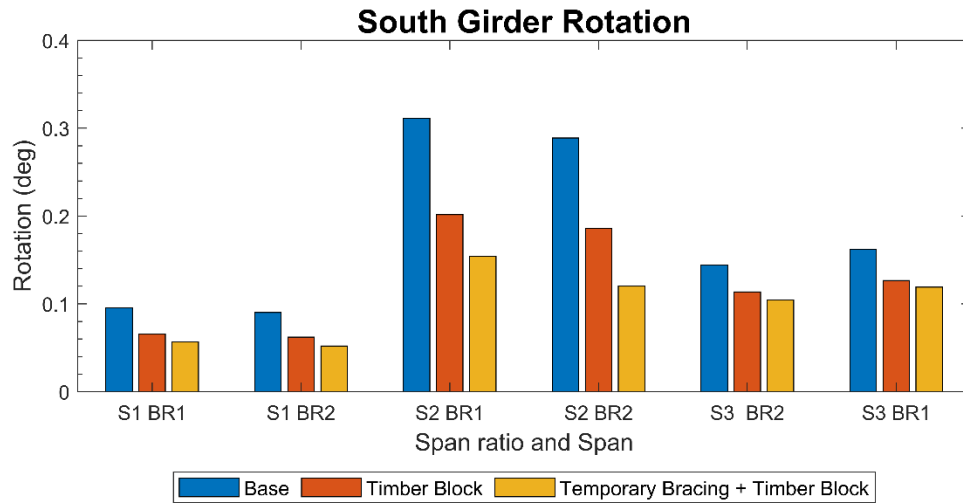


Figure 94. 260 ft Standard Bridge south girder rotation (brace strength)

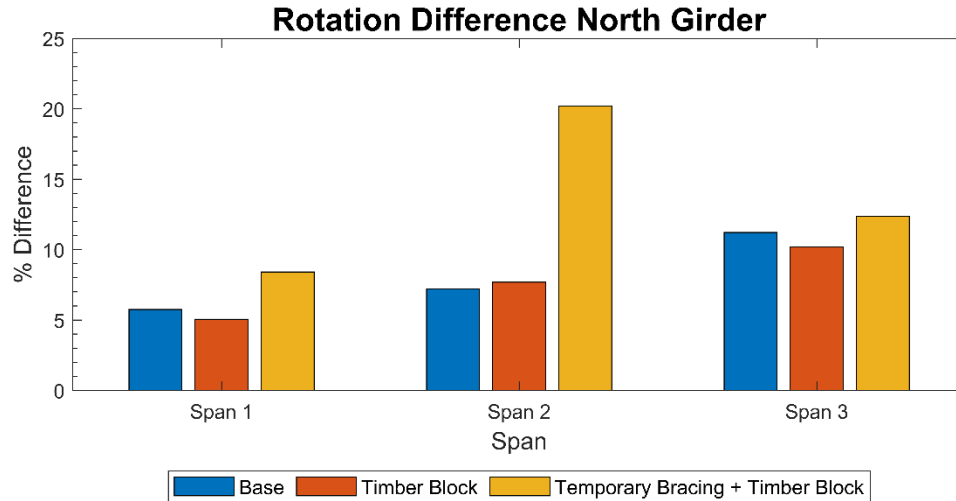


Figure 95. 260 ft Standard Bridge rotation difference for north girder (brace strength)

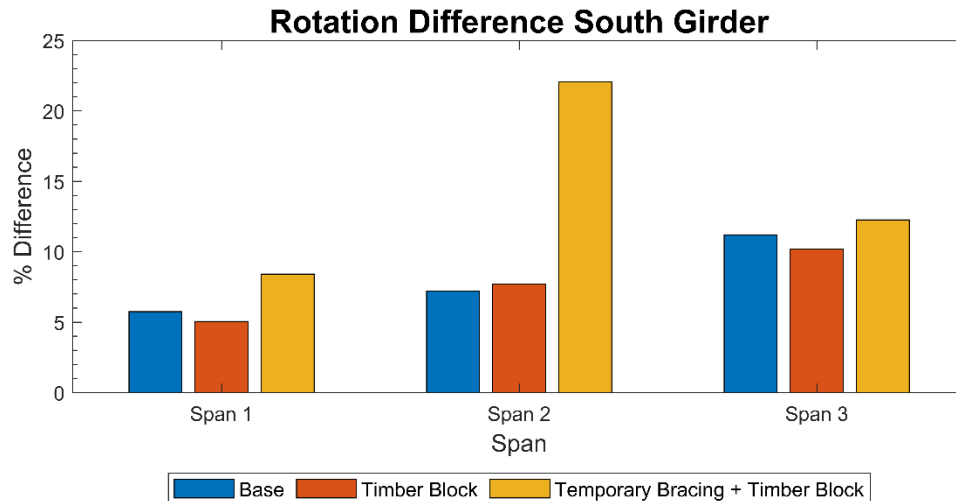


Figure 96. 260 ft Standard Bridge rotation difference for south girder (brace strength)

It was found that utilizing W21×50 as the intermediate diaphragm had no significant effect on the deflection of girders and brackets when compared with the same bridge modeled using C15×33.9. However, rotation was affected when W21×50s were utilized as the permanent diaphragms. The greatest difference was seen for Span 2 for Case C (temporary bracing + timber blocking). In general, Case C was affected most when W21×50 was utilized instead of C15×33.9.

Skew Angle

Two bridges were studied while investigating the effect of skew on the deflection of girders and brackets, as well as on exterior girder rotation. A skew angle more than 20° often causes unsymmetrical loading and a drop in the lateral torsional stiffness when compared to bridges at

0° skew (Roddis et al. 2008). Thus, bridges with skew angles more than 20° were included in the current investigation. For this parameter, skew angles of 30° and 45° were considered. The framing plan for bridges with skew angles of 30° and 45° are shown in Figure 97 and Figure 98, respectively.

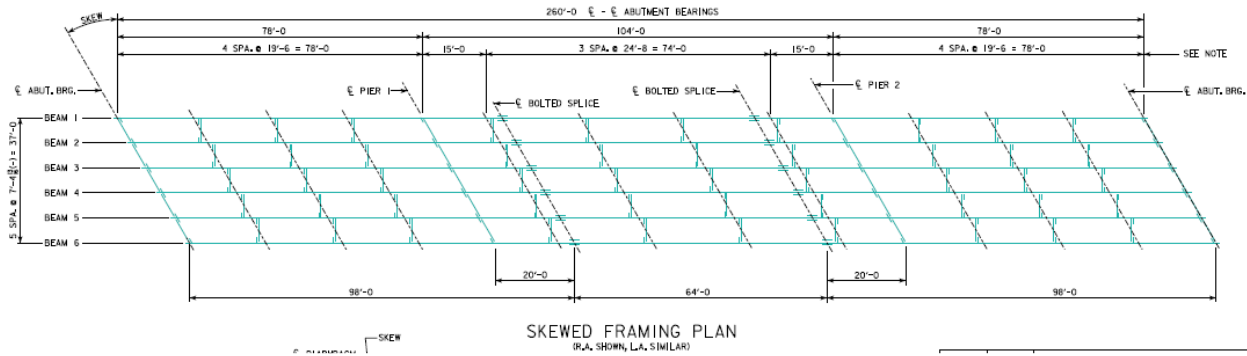


Figure 97. 30° skew 260 ft Standard Bridge framing plan

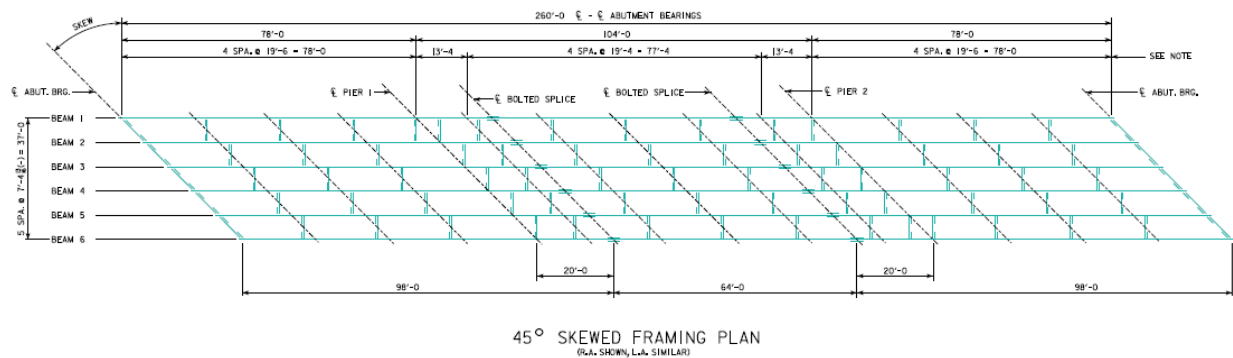


Figure 98. 45° skew 260 ft Standard Bridge framing plan

For this parameter, three load cases and three different bracing cases were studied. The screed load was applied perpendicular to the skewness. The load cases were investigated similar to the brace strength parameter, and loads were applied at mid-span of each span of the bridge with reference to the bridge centerline, as shown in Figure 99 through Figure 101.

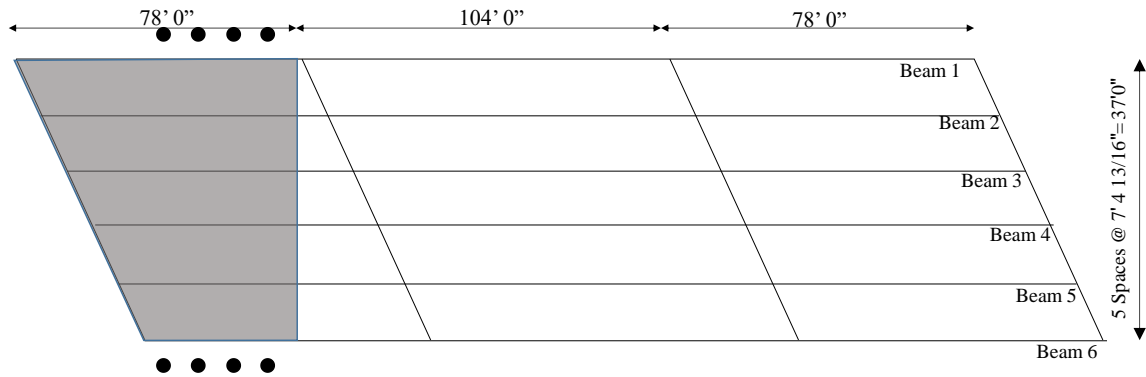


Figure 99. 260 ft Standard Bridge Span 1 vehicle and wet concrete load for skewed bridges

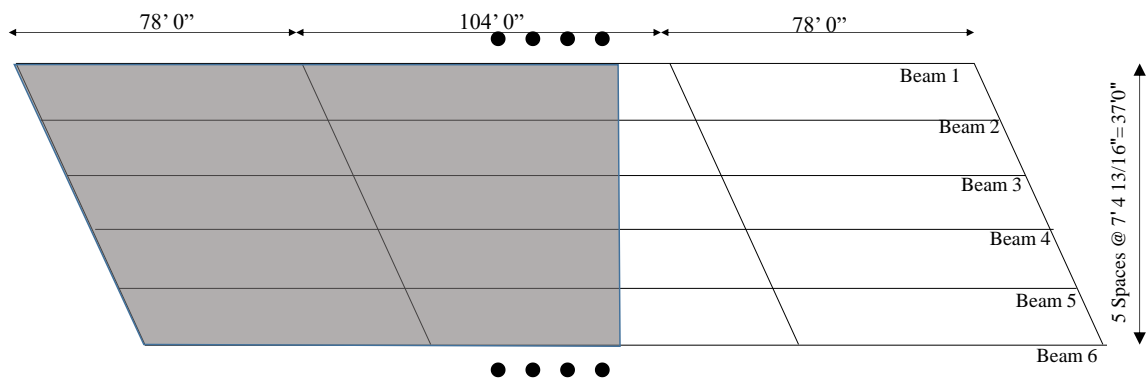


Figure 100. 260 ft Standard Bridge Span 2 vehicle and wet concrete load for skewed bridges

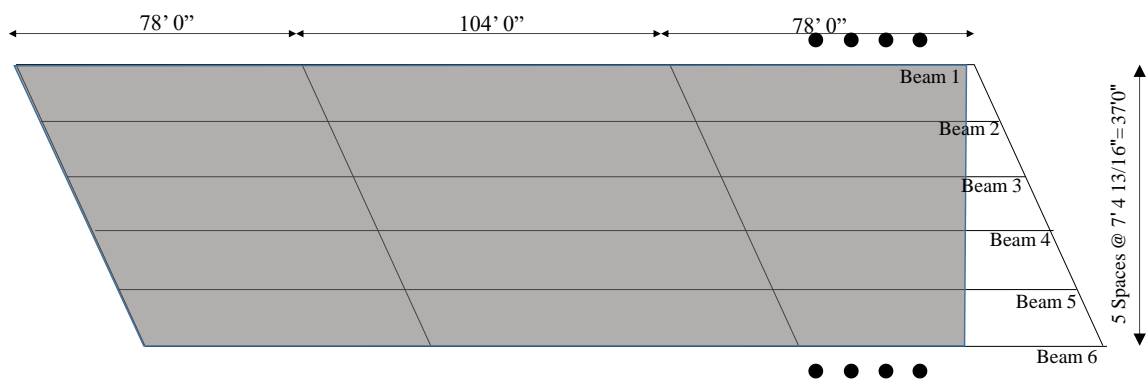


Figure 101. 260 ft Standard Bridge Span 3 vehicle and wet concrete load for skewed bridges

The main difference in the bridge framing plan of the two bridges was the spacing of diaphragms in the interior span. For the 30° skew bridge, the first intermediate diaphragm within the interior span was located at 15 ft 0 in. from either of the interior supports, and the intermediate diaphragms were spaced at three equal spaces between the first and last intermediate diaphragm of the interior span. For the 45° skew bridge, the first intermediate diaphragm within the interior

span was located at 13 ft 4 in. from either of the interior supports, and the intermediate diaphragms were spaced at four equal spaces between the first and last intermediate diaphragm of the interior span. Figure 102 through Figure 109 show the results obtained for the investigation of the skewness angle parameter.

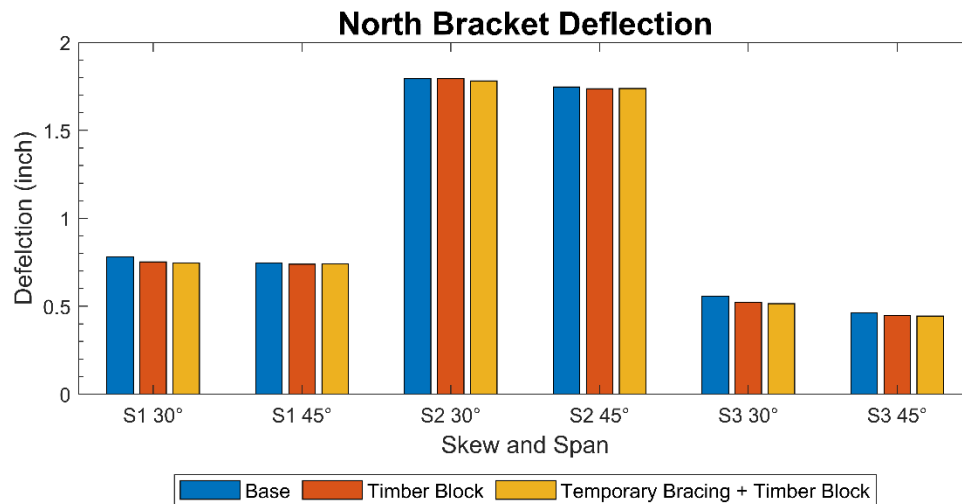


Figure 102. 260 ft Standard Bridge north bracket deflection (skew angle)

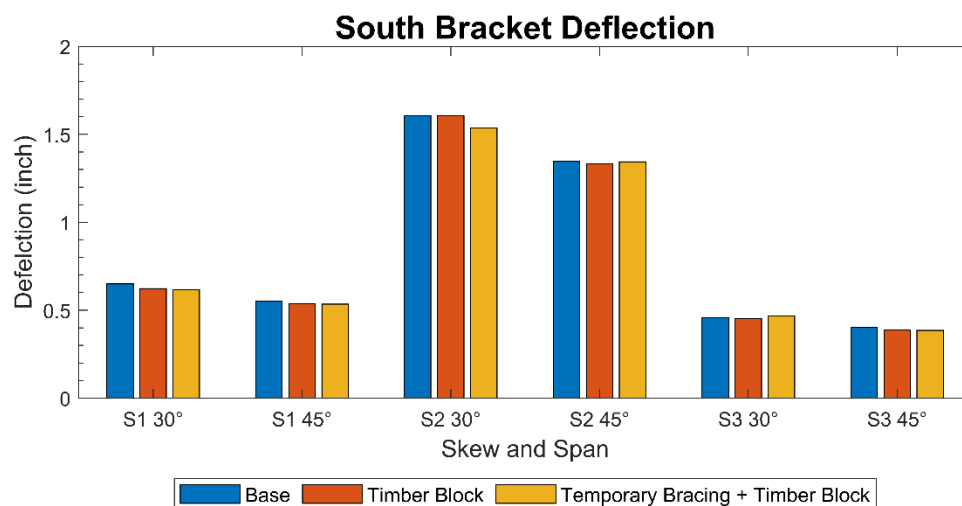


Figure 103. 260 ft Standard Bridge south bracket deflection (skew angle)

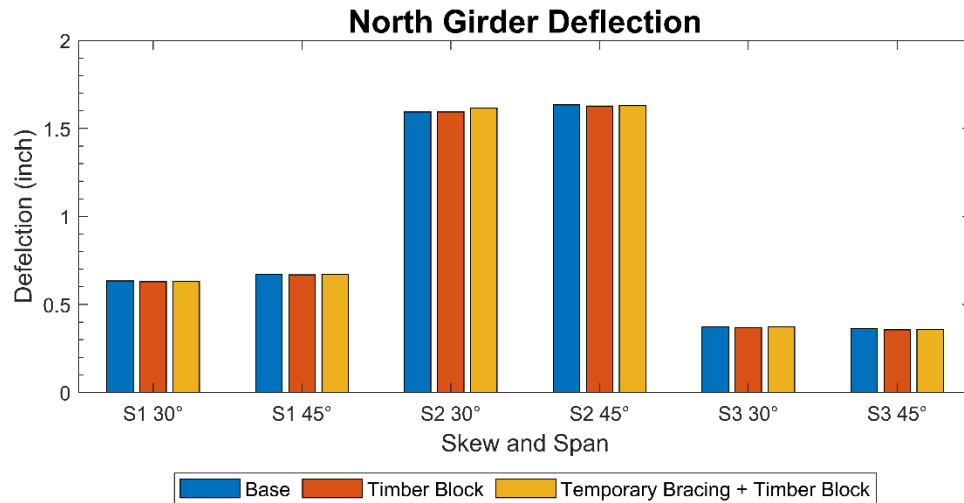


Figure 104. 260 ft Standard Bridge north girder deflection (skew angle)

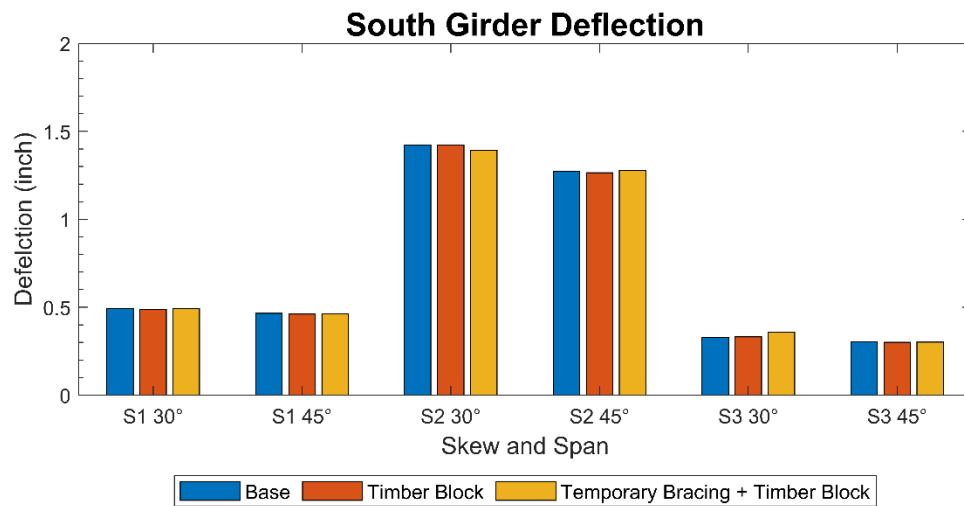


Figure 105. 260 ft Standard Bridge south girder deflection (skew angle)

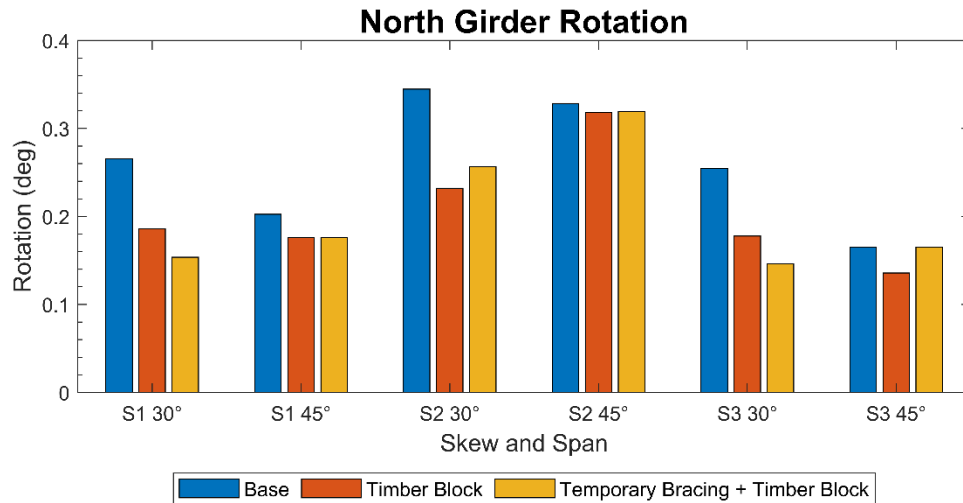


Figure 106. 260 ft Standard Bridge north girder rotation (skew angle)

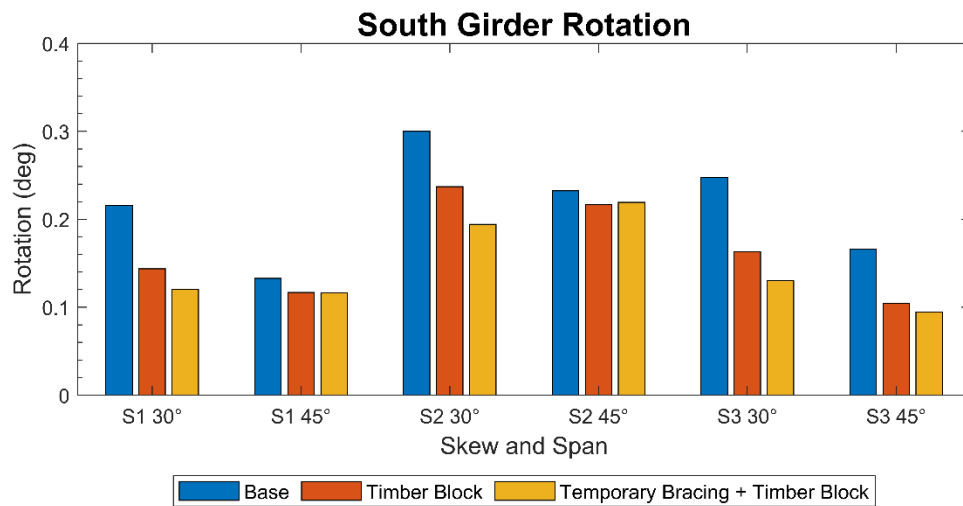


Figure 107. 260 ft Standard Bridge south girder rotation (skew angle)

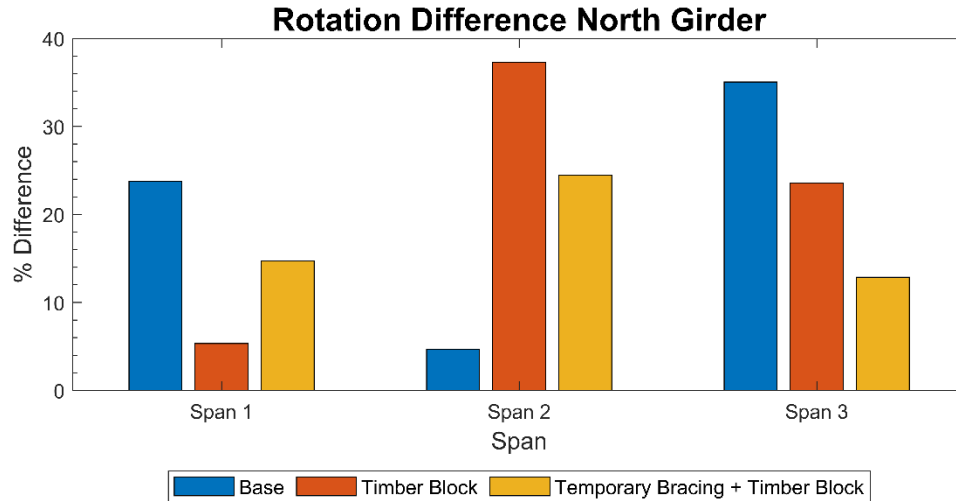


Figure 108. 260 ft Standard Bridge rotation difference for north girder (skew angle)

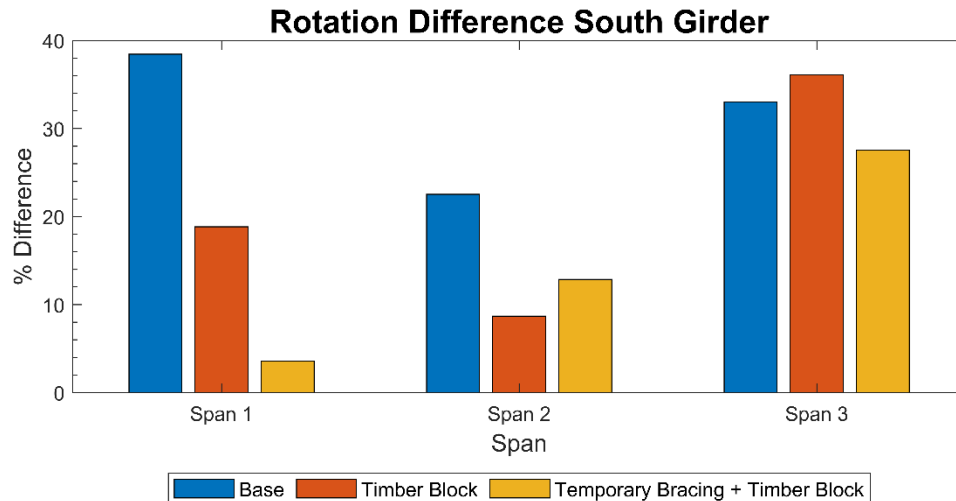


Figure 109. 260 ft Standard Bridge rotation difference for south girder (skew angle)

The skew angle influenced the deflection and rotation of the north and south girders. The unsymmetrical load distribution due to skewness increased the deflection and rotation of the north girder. When deflections were compared for bridges with a skew angle of 30° and 45°, deflection of the bracket was only slightly affected due to the skew angle. Rotation, on the other hand, increased as the skew angle increased. Table 10 summarizes the reduction due to temporary bracing system (Case C) when compared with the base case (Case A) for the same bridge.

Table 10. 260 ft Standard Bridge percentage of reduction in rotation with temporary bracing system during deck placement depending on skew angle

Skew angle	Case A	Case C	% Reduction in rotation
0°	0.29	0.12	58.9
30°	0.34	0.26	25.5
45°	0.33	0.32	2.9

Case A = no temporary bracing and Case C = temporary bracing + timber blocking

As shown, the temporary bracing system may become ineffective in reducing the rotation of the exterior girders when the skew angle increases. The temporary bracing system was highly effective in reducing the rotation of the 0° skew bridge. However, for a skew angle of 30° and greater, the temporary bracing system became increasingly ineffective.

Diaphragm Spacing

To investigate the effect of diaphragm spacing on rotation and deflection of the exterior girders, two bridge cases were studied with different diaphragm spacing. For the first bridge case, which was the 260 ft Standard Bridge, the diaphragms in the exterior spans were spaced at equal 19 ft 6 in. spacing. The interior span had a different configuration. The diaphragms were located at 15 ft 0 in. from either interior support, and the remaining diaphragms within the span were spaced at 24 ft 8 in. In the base case, there were three sets of permanent diaphragms within the exterior and interior spans. In the second bridge, a uniform 26 ft 0 in. spacing was assumed in all three spans. Thus, such configuration assumes two sets of permanent diaphragms in the exterior spans and three sets of permanent diaphragms in the interior span. Figure 110 through Figure 117 provide the deflection and rotation results for girders and brackets.

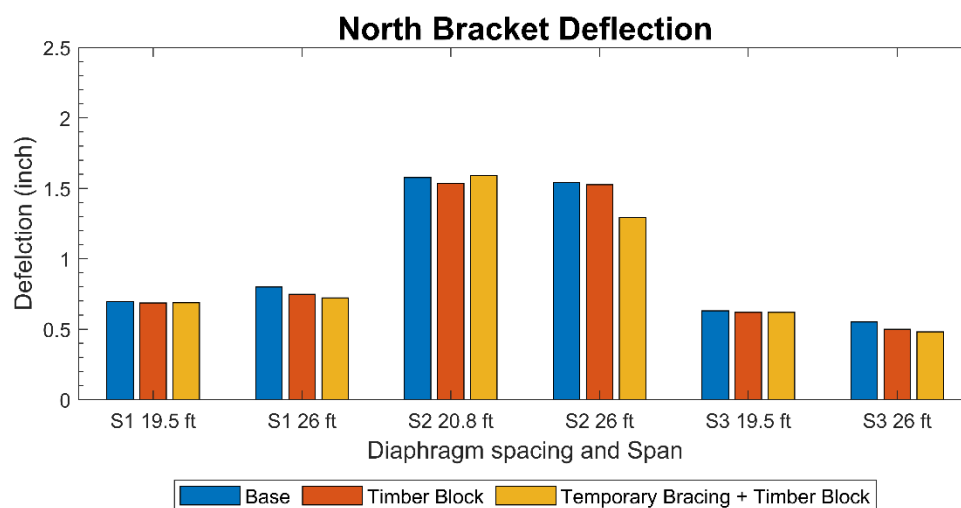


Figure 110. 260 ft Standard Bridge north bracket deflection (diaphragm spacing)

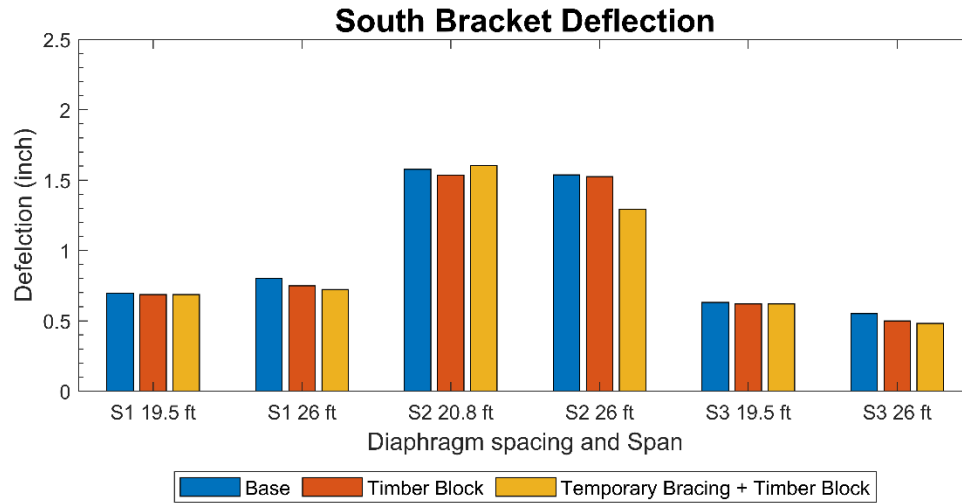


Figure 111. 260 ft Standard Bridge south bracket deflection (diaphragm spacing)

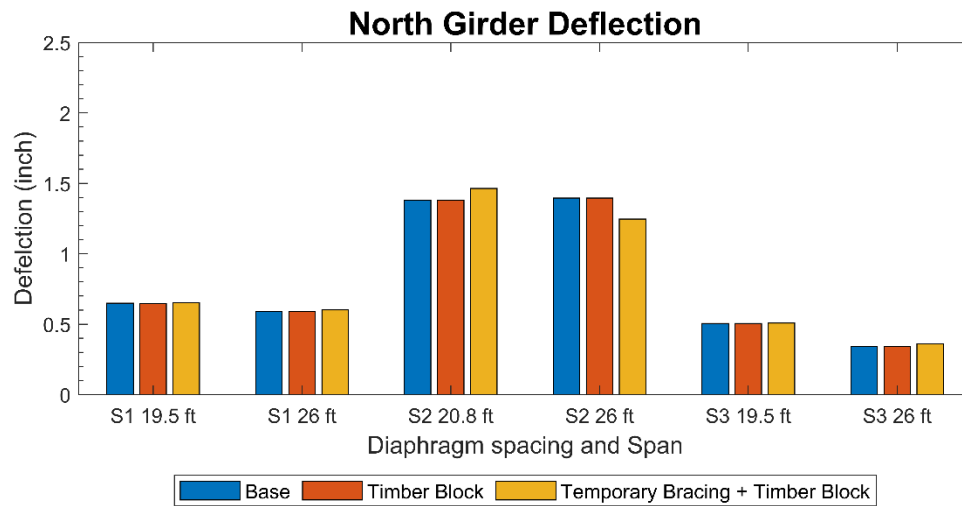


Figure 112. 260 ft Standard Bridge north girder deflection (diaphragm spacing)

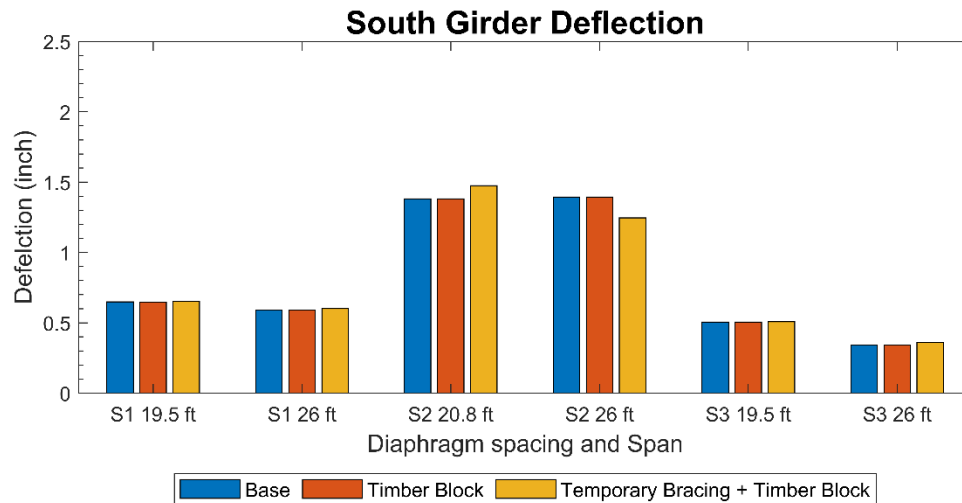


Figure 113. 260 ft Standard Bridge south girder deflection (diaphragm spacing)

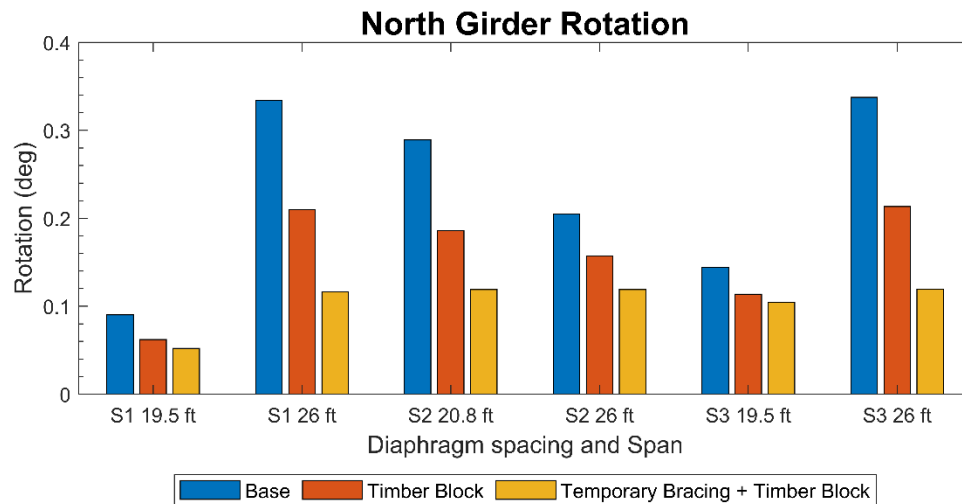


Figure 114. 260 ft Standard Bridge north girder rotation (diaphragm spacing)

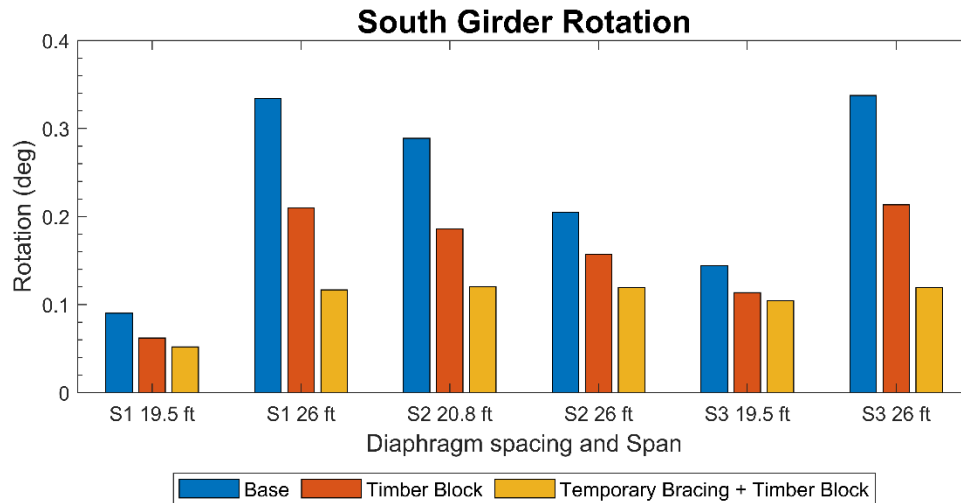


Figure 115. 260 ft Standard Bridge south girder rotation (diaphragm spacing)

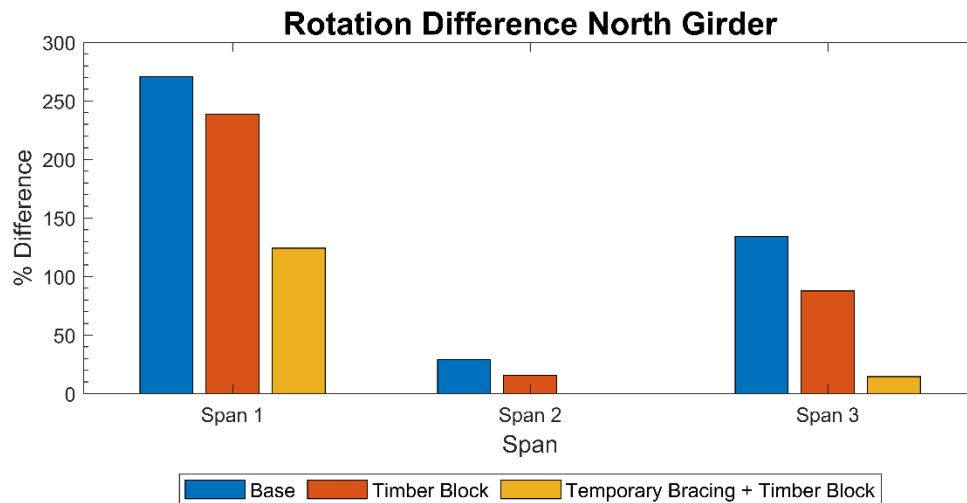


Figure 116. 260 ft Standard Bridge rotation difference for north girder (diaphragm spacing)

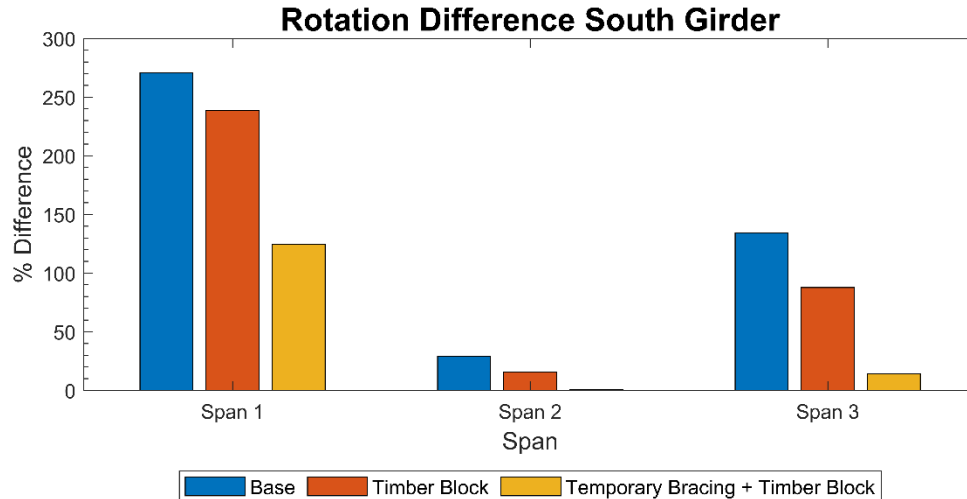


Figure 117. 260 ft Standard Bridge rotation difference for south girder (diaphragm spacing)

When the results of the two bridge cases were compared, it was observed that bracket deflection in the first span for a bridge with 26 ft diaphragm spacing was greater than that in the bridge with diaphragm spacing of 19 ft 6 in. However, for Span 2 and 3, a slight decrease was observed in bracket deflection. The deflections of the north and south girders were least affected due to the change in girder spacing. However, girder rotation in Span 1 of the second bridge was greater due to the increased diaphragm spacing. In the 260 ft Standard Bridge, the diaphragm spacing was not uniform, although it was closer together than in the second bridge. The rotation in the standard 260 ft bridge, where the diaphragm spacing was less than 26 ft, was greater than in the other case. This suggests that diaphragm spacing, as well as the number of diaphragms spaced at uniform distances, can affect the rotation of exterior girders when loads are applied on the deck overhang during construction. The use of timber blocks and temporary bracing was found effective in reducing rotation based on the FE simulations.

Girder Spacing

In this parametric study, girder spacing was varied to study its effect on the rotation and deflection of exterior girders. For the base case, which was the 260 ft Standard Bridge, the girder spacing was 7 ft 4-13/16 in. For the second bridge case that was studied in this parameter investigation, the girder spacing was increased to 9 ft 0 in. By increasing the girder spacing, the width of the bridge also increased. The width of the 260 ft Standard Bridge was 43 ft 2 in., while the width of the second bridge reached 51 ft 2 in. Increased girder spacing also increased the wet concrete load as well as the live load on the remaining portions of the bridge. The increased girder spacing also increased the length of the permanent diaphragms, which reduced the brace stiffness. Figure 118 through Figure 125 present the results in terms of the deflection and rotation results derived for the girder spacing parameter.

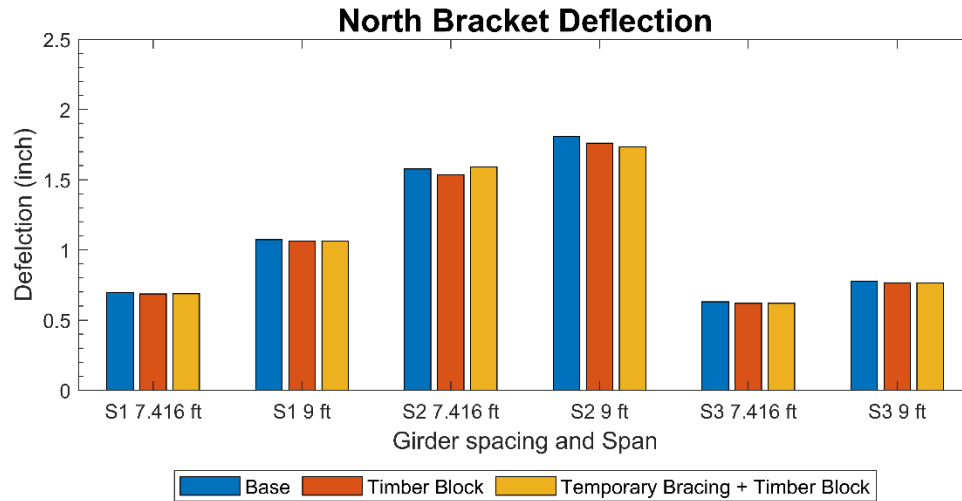


Figure 118. 260 ft Standard Bridge north bracket deflection (girder spacing)

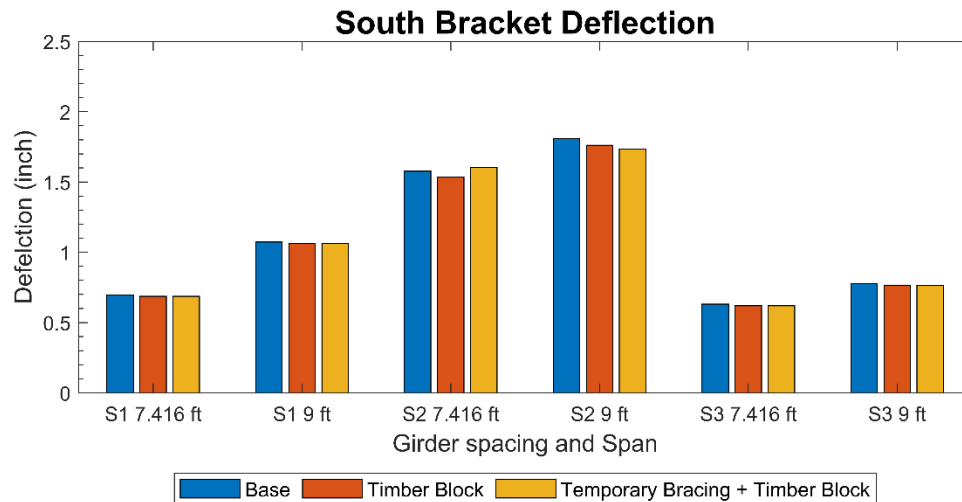


Figure 119. 260 ft Standard Bridge south bracket deflection (girder spacing)

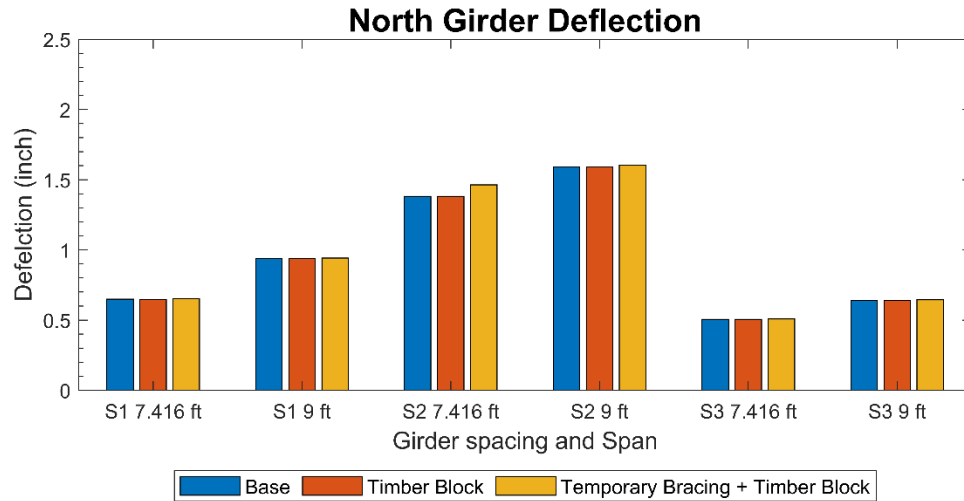


Figure 120. 260 ft Standard Bridge north girder deflection (girder spacing)

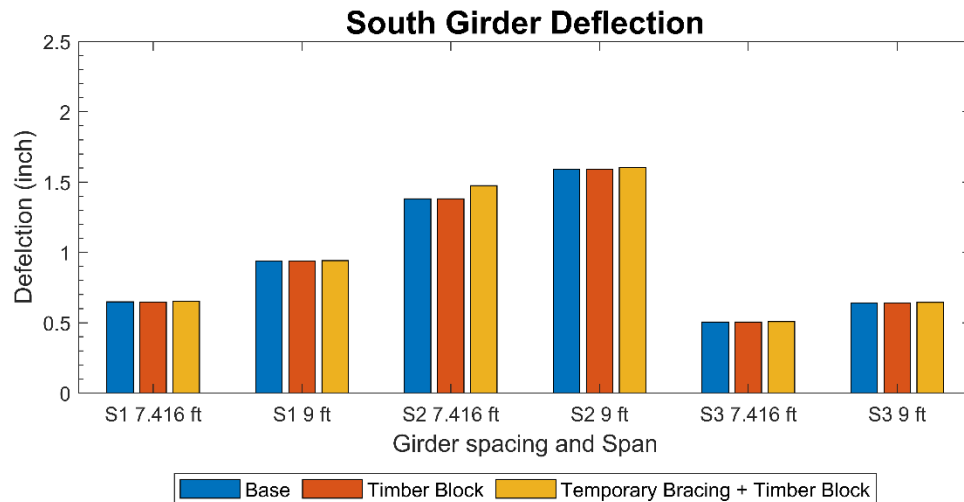


Figure 121. 260 ft Standard Bridge south girder deflection (girder spacing)

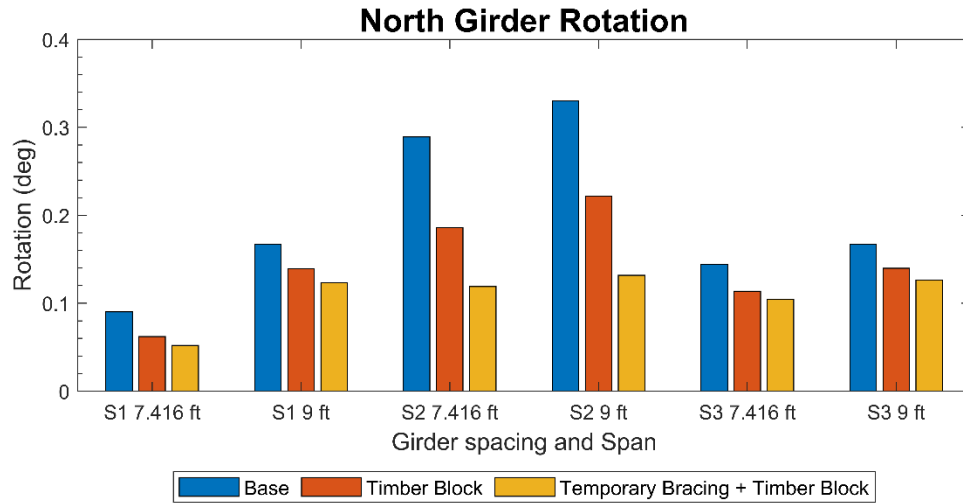


Figure 122. 260 ft Standard Bridge north girder rotation (girder spacing)

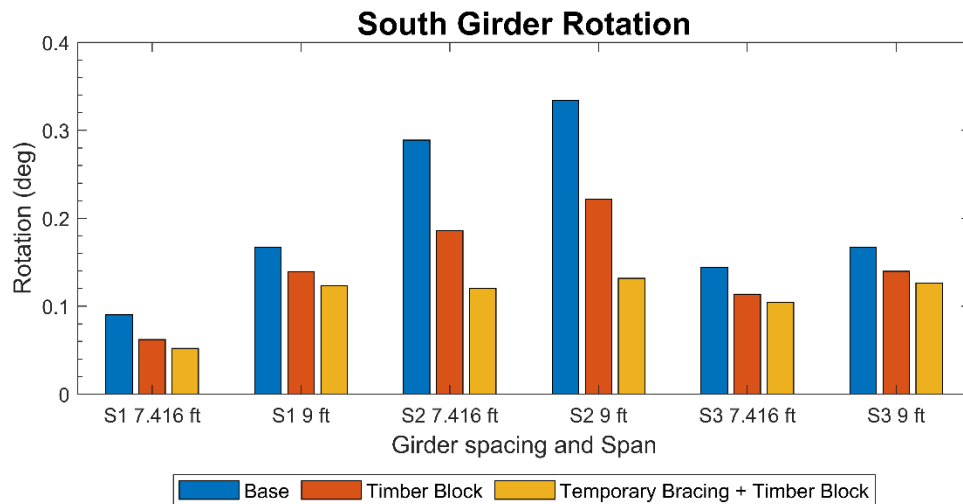


Figure 123. 260 ft Standard Bridge south girder rotation (girder spacing)

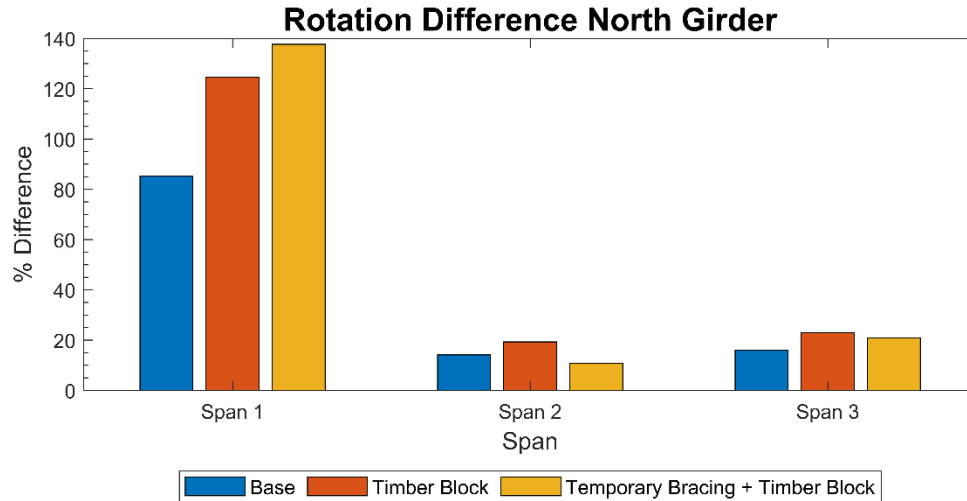


Figure 124. 260 ft Standard Bridge rotation difference for north girder (girder spacing)

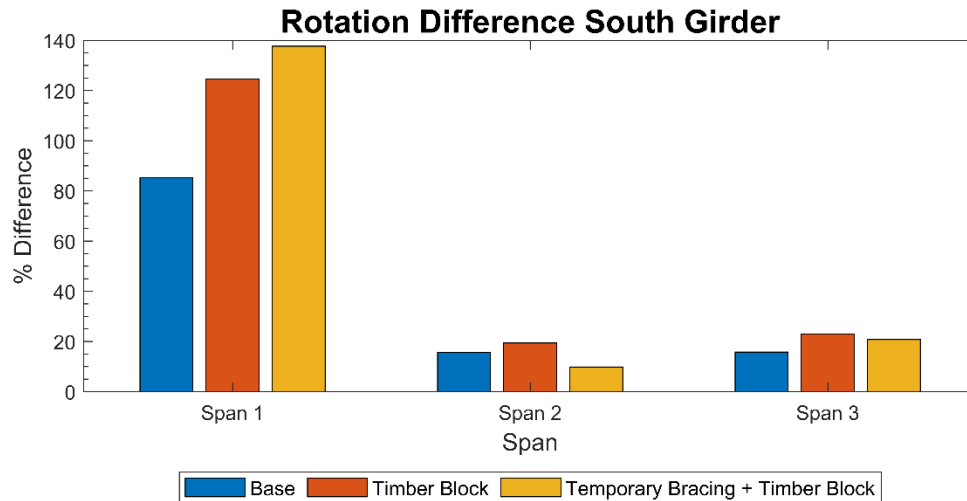


Figure 125. 260 ft Standard Bridge rotation difference for south girder (girder spacing)

Due to the increased girder spacing, deflection and rotation increased compared to the base case of the 260 ft Standard Bridge. The increased girder spacing increased the wet concrete load and reduced the brace and girder stiffness available to the system. The first span was the most affected span in terms of increased rotation. The timber block (Case B) and temporary bracing system (Case C) reduced the rotation. When rotation was compared between the two bridges, increased girder spacing increased the rotation in the first span; however, for the other spans, the percentage of difference was not significant because the wet concrete load and other loads balanced the system.

Span Ratio

In this parametric study, the effect of the span length of the interior span was evaluated. Two FEMs were compared, including the 260 ft Standard Bridge and a similar bridge with an increased interior span length. The standard bridge had an interior to exterior span ratio of 1.33. For this investigation, the second model was built with a ratio of 1.5. The exterior span length was the same as that of the Standard Bridge. Thus, the new span length of the interior span was assumed to be 117 ft 0 in. Another assumption in the second model that differs from the 260 ft Standard Bridge is the number of permanent diaphragms. In the Standard Bridge model, four continuous permanent diaphragms were present at 13 ft 4 in. from each of the interior spans spaced at 19 ft 4 in. within the interior span. For the second FEM, it was assumed that the continuous permanent diaphragms were located at 13 ft 4 in. from either of the interior spans and spaced equally at 18 ft 0 in. within the interior span. Thus, there were five continuous permanent diaphragms assumed in the interior span. The results of this investigation are presented in Figure 126 through Figure 133.

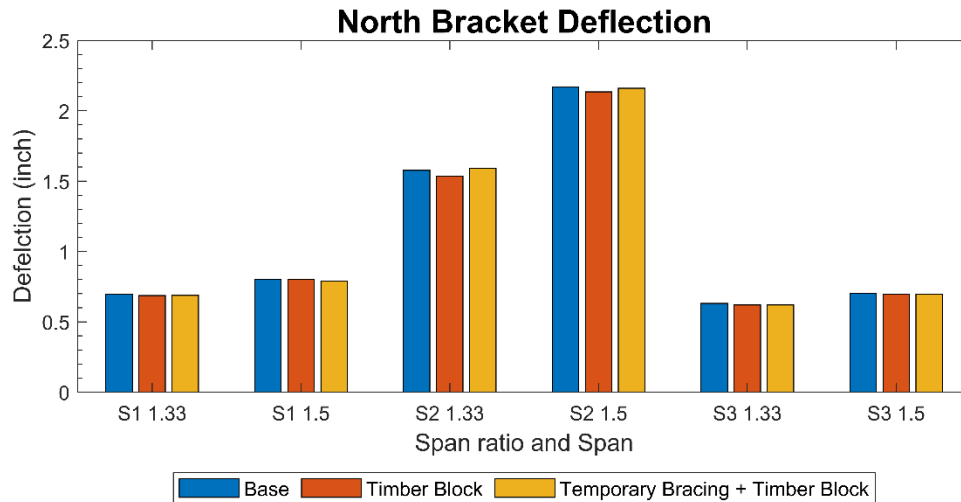


Figure 126. 260 ft Standard Bridge north bracket deflection (span ratio)

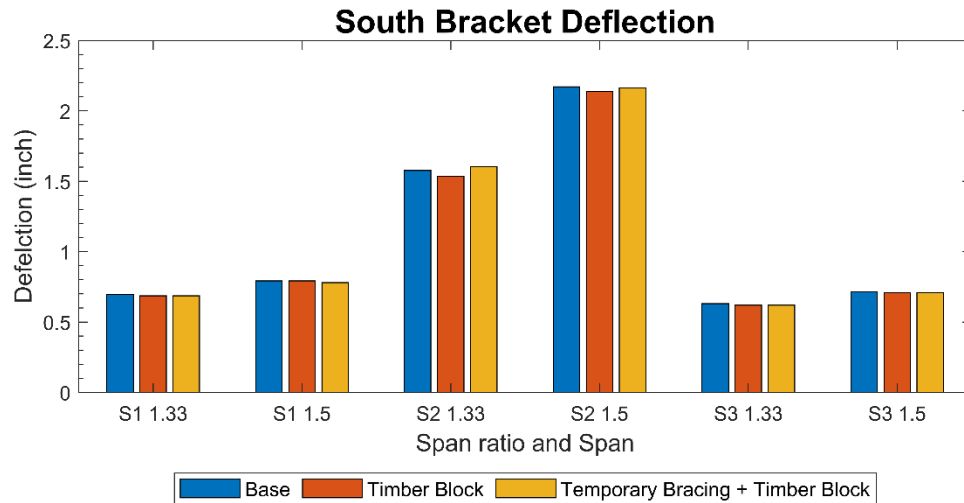


Figure 127. 260 ft Standard Bridge south bracket deflection (span ratio)

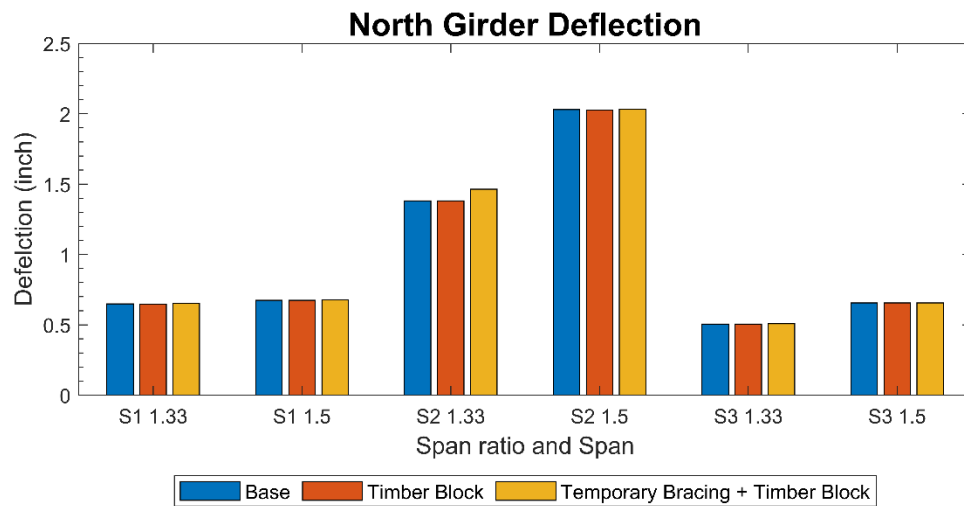


Figure 128. 260 ft Standard Bridge north girder deflection (span ratio)

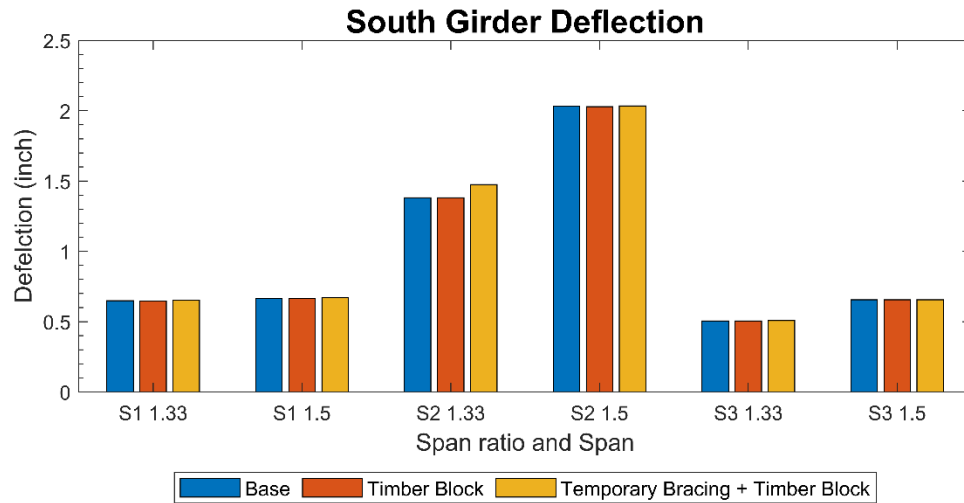


Figure 129. 260 ft Standard Bridge south girder deflection (span ratio)

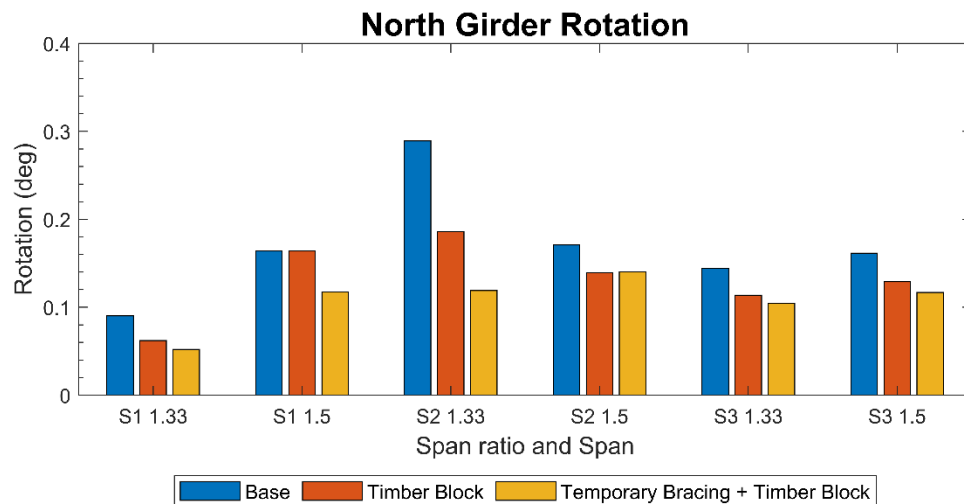


Figure 130. 260 ft Standard Bridge north girder rotation (span ratio)

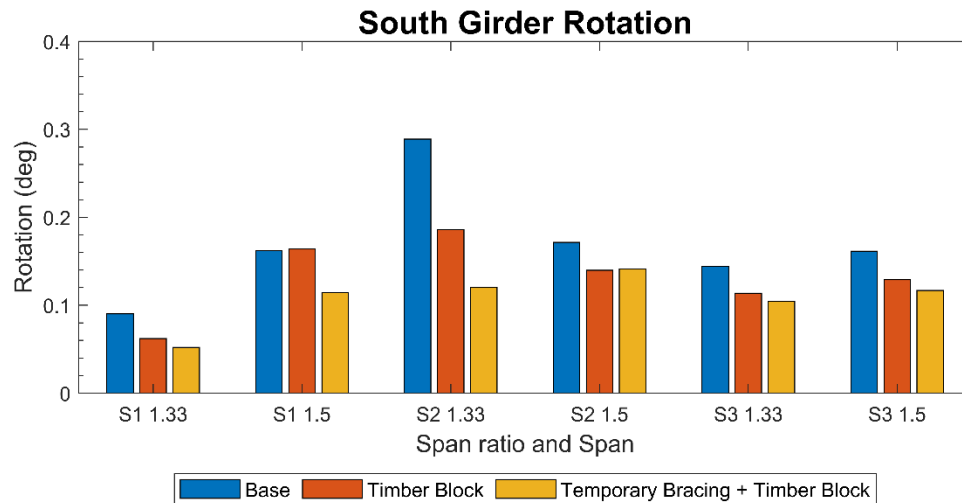


Figure 131. 260 ft Standard Bridge south girder rotation (span ratio)

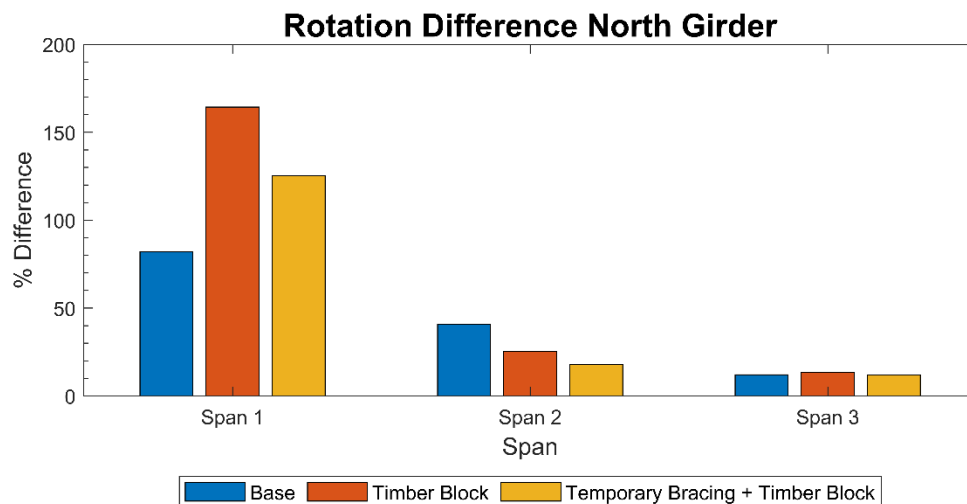


Figure 132. 260 ft Standard Bridge rotation difference for north girder (span ratio)

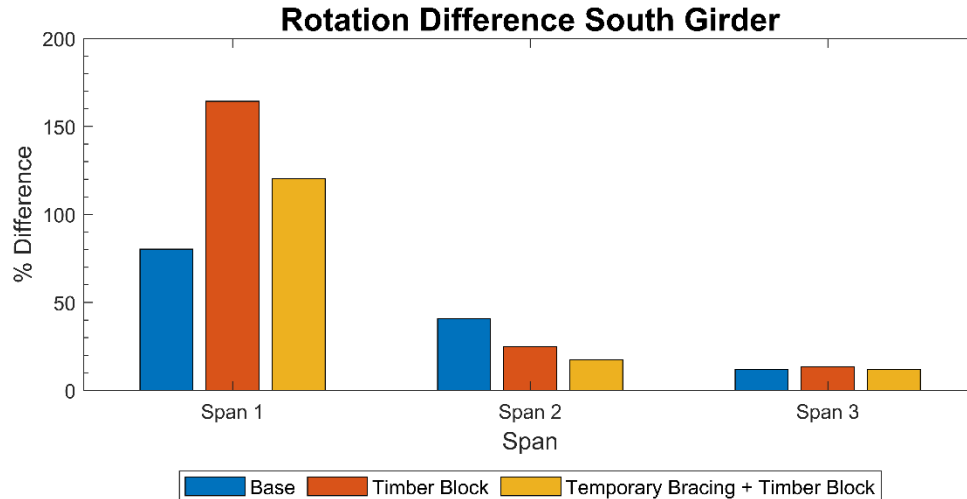


Figure 133. 260 ft Standard Bridge rotation difference for south girder (span ratio)

As expected, an increased interior to exterior span ratio increased the deflection of girders and brackets when compared with the 260 ft Standard Bridge. In the first span, rotation also increased. Because of the additional cross-frames with the increased span length, rotation of the exterior girders was limited in the second bridge model when compared with the 260 ft Standard Bridge. The use of timber blocking in the second model did not help reduce the rotation of Span 1 when the load was at mid-span. The temporary bracing in the interior span was ineffective although the rotation was significantly lower than that of the standard bridge.

Girder Flange Thickness

In this parametric study, thickness of the flange was varied. The 260 ft Standard Bridge was made up of six W40×199s and W40×167s at the spliced location. The thickness of the flange for the W40×199 is 1.07 in. In this study, for the second FEM, a flange thickness of 0.625 in. was assumed. However, this led to a self-weight reduction of 47 plf. Figure 134 through Figure 141 present the results for this parametric variation.

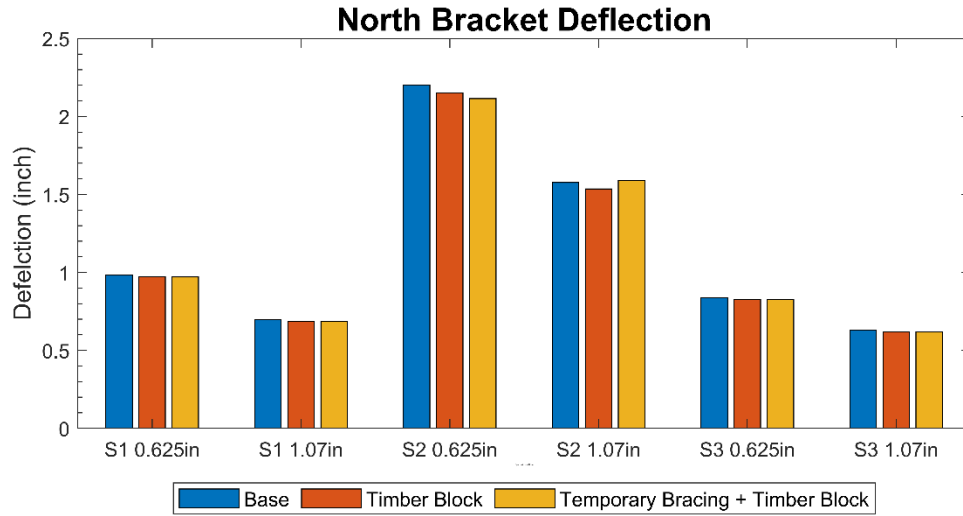


Figure 134. 260 ft Standard Bridge north bracket deflection (flange thickness)

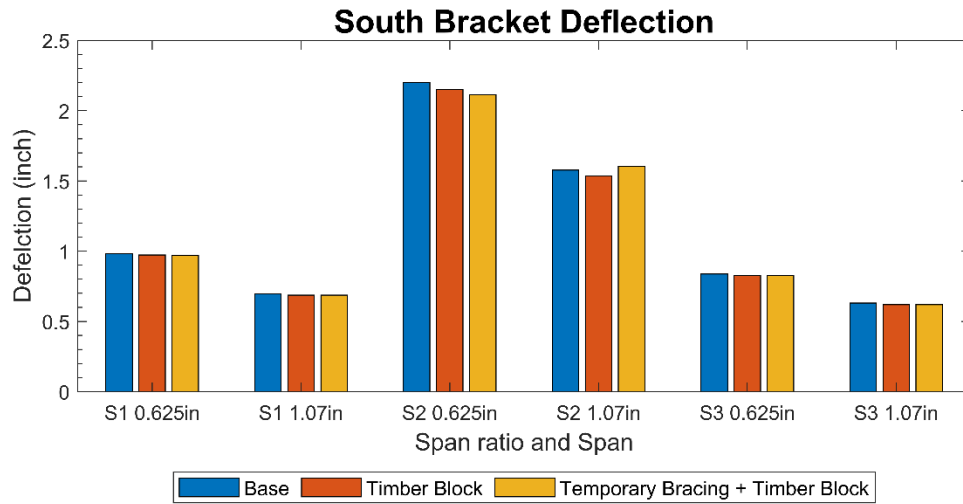


Figure 135. 260 ft Standard Bridge south bracket deflection (flange thickness)

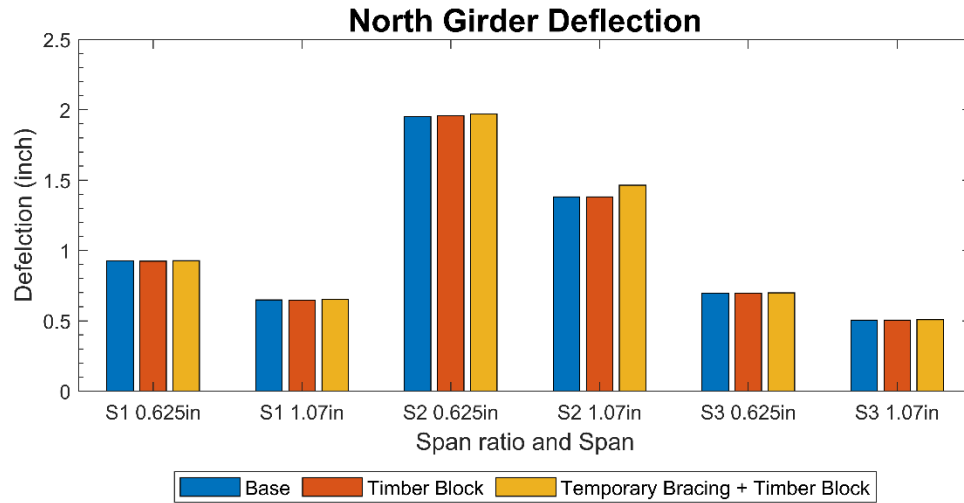


Figure 136. 260 ft Standard Bridge north girder deflection (flange thickness)

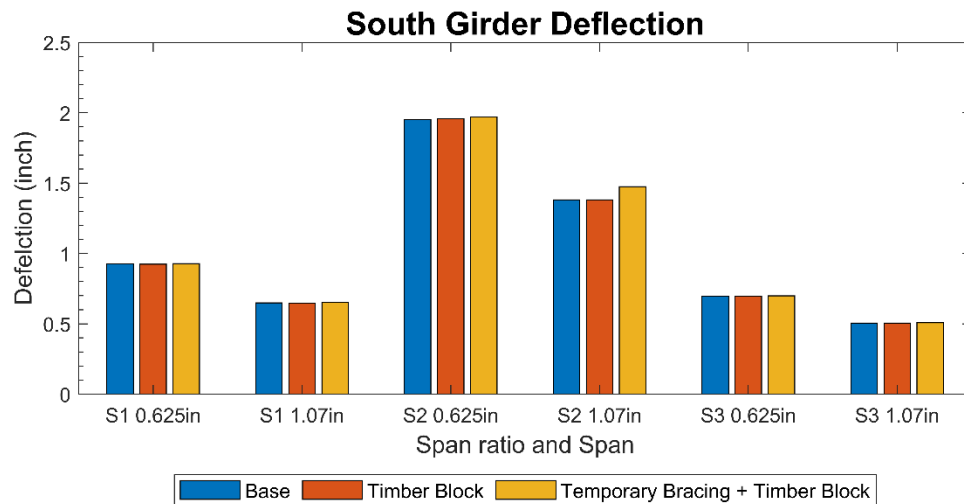


Figure 137. 260 ft Standard Bridge south girder deflection (flange thickness)

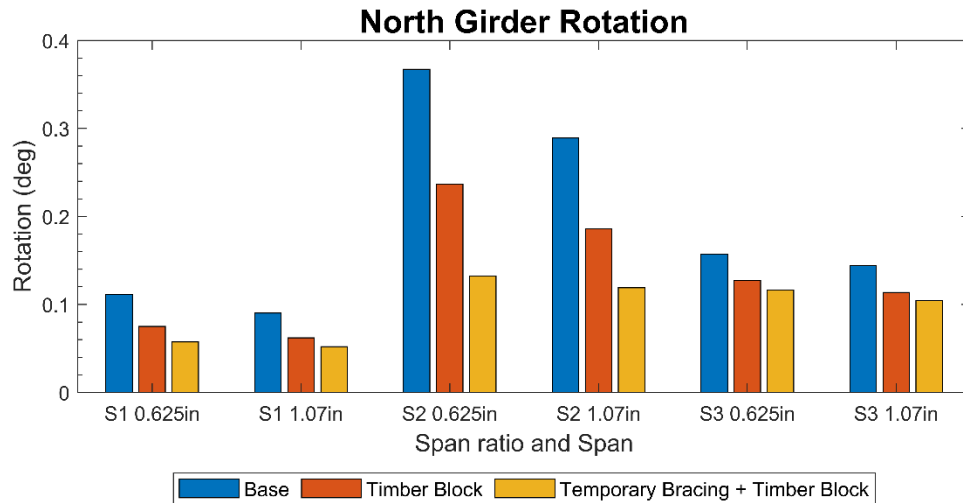


Figure 138. 260 ft Standard Bridge north girder rotation (flange thickness)

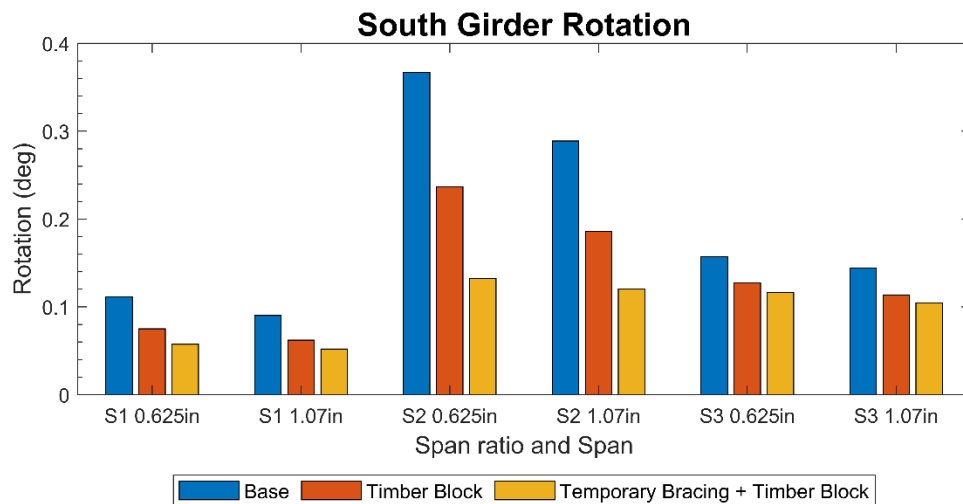


Figure 139. 260 ft Standard Bridge south girder rotation (flange thickness)

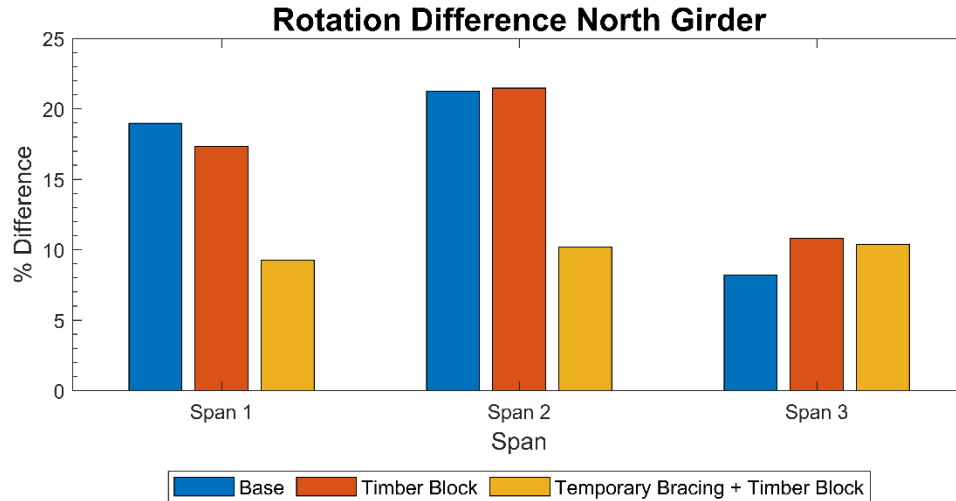


Figure 140. 260 ft Standard Bridge rotation difference for north girder (flange thickness)

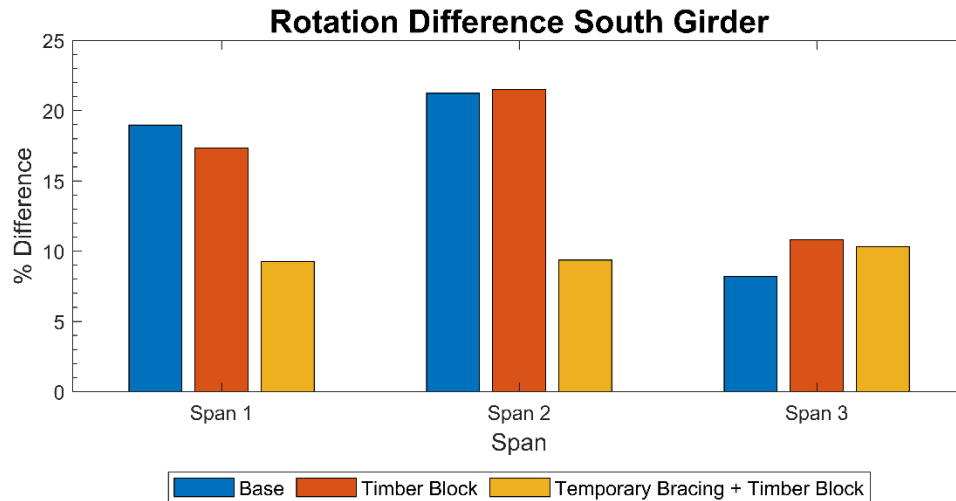


Figure 141. 260 ft Standard Bridge rotation difference for south girder (flange thickness)

The increased thickness of the flanges was found to directly help reduce deflection and rotation in the bridge models considered in this parametric investigation.

CHAPTER 6. FINDINGS AND CONCLUSIONS

The following findings are from the field review of construction practices:

- Concern for exterior girder rotation increased with an increase in skew. This is due to the unequal loading of the exterior girders when the screed is not oriented along the skew.
- While exterior girder rotation was evident for all instrumented deck placements, differential deflections were also present and seemed to have a greater effect on the deck thickness deficiencies that were observed at the Maple Bridge.
- The greatest exterior girder rotation observed for the three instrumented bridges was just over 1° , with a residual rotation of 0.75° . The greatest deflection observed during placement was approximately 2.5 in., with a residual deflection of just over 1 in.
- Temporary bracing of the exterior bays is not common practice based on conversations with contractors and field observations. Contractors mentioned that for other projects, if bracing was used by the contractor, but was not called for in the plans, timber blocking was most often used. While this is an effective means for reducing girder rotation, it does not protect against differential deflection. Alternate bracing methods to better reduce differential deflections would be advantageous. While not modeled in this research, the feasibility and performance of cross bracing is something to consider to combat differential deflections and would be beneficial to include in future research efforts.
- Of the three deck placements that were monitored in the field, deck thinning was only noticed at one site.

The following findings are from the analytical and parametric study:

- The models confirmed that both differential deflection and exterior girder rotation can lead to deck thickness deficiencies during deck placement, with the largest contribution coming from the differential deflection.
- Diagonal bracing in the exterior bays, combined with timber blocking in the adjacent bay, greatly reduced the exterior girder rotation for straight bridges. This bracing system also reduced the deflections, although to a limited extent.
- The skew angle influences the deflection and rotation of exterior girders, as deflection and rotation of the two exterior girders are not equal. Unsymmetrical load distribution due to skewness increases the deflection and rotation of exterior girders, depending on the skew angle. The temporary bracing system was highly effective in reducing rotation of the 0° bridge. However, for a skew angle 30° and greater, the temporary bracing was not found to be effective in reducing rotation.

Based on the modeling and field investigation efforts, it appears that the cause of any deck thinning (or the greatest movement in the girders) is a result of differential deflections, not from the rotation of exterior girders. While the bracing methods considered in this research were effective at restraining girder rotation for straight bridges or those with low skew, they were not as effective at reducing differential deflections caused by the concentrated screed load. Alternate bracing methods or construction techniques (such as reducing the moment arm of the screed load) should be utilized where possible. While reducing the moment arm of the screed load would be more effective at combating rotation rather than deflection, this reduction would still improve differential deflections to some extent, especially if diagonal cross bracing is used.

While differential deflections during deck placement are not surprising due to the screed loading location, the field data showed that, while the bridge does begin to return to its original location, there is permanent differential deflection of the bridge cross-section even after the screed load is off the bridge. Further work is needed to address concerns regarding differential deflections and their impact on the long-term behavior and performance of bridges.

In addition to differential deflection concerns, more work is also needed to address the effect of skew, as neither of these variables were the direct focus of this research. Of particular interest is determining what level of skew necessitates the positioning of the screed parallel to the skew, rather than perpendicular to the roadway, as is often the current practice. The field documentation portion of this research showed that the concrete is being placed right in front of the screed to keep up with placement, rather than placing the concrete unequally in front of the screed to combat the unequal loading of concrete caused by the skew.

REFERENCES

- AASHTO. 2017. *Load and Resistance Factor Design (LRFD) Bridge Design Specifications*. Eighth Edition. American Association of State Highway and Transportation Officials, Washington, DC.
- Ashiquzzaman, M., Hui, L., Schmeltz, J., Merino, C., Bozkurt, B., Ibrahim, A., Lindquist, W., and Hindi, R. 2016a. *Effectiveness of Exterior Beam Rotation Prevention Systems for Bridge Deck Construction*. Illinois Center for Transportation, University of Illinois at Urbana-Champaign, Rantoul, IL.
- Ashiquzzaman, M., L. Hui, A. Ibrahim, W. Lindquist, M. Thomson, and R. Hindi. 2016b. Effect of Inconsistent Diaphragms on Exterior Girder Rotation during Overhang Deck Construction. *Structures*. Vol. 8, Part 1, pp. 25–34.
- Clifton, S. P. and O. Bayrak. 2008. *Bridge Deck Overhang Construction*. University of Texas at Austin, TX.
- Computers and Structures, Inc.. 2016. *CSI Analysis Reference Manual*. Computers and Structures, Inc., Berkeley, CA.
- Fasl, J. 2008. The Influence of Overhang Construction on Girder Design. MS thesis. University of Texas at Austin, TX.
- GOMACO. 2016. Cylinder Finishers.
https://www.gomaco.com/resources/finishers_generalinfo.html.
- Halvorsen, G. T. 1992. Bridge Deck Paving and Finishing Machines. *Concrete Construction*.
https://www.concreteconstruction.net/how-to/site-prep/bridge-deck-paving-and-finishing-machines_o.
- Iowa DOT. 2016. *LRFD Bridge Design Manual*. Iowa Department of Transportation, Office of Bridges and Structures, Ames, IA.
- Iowa DOT. 2018. *RS40-14 Three Span Rolled Steel Beam Bridge Standards*. Iowa Department of Transportation, Highway Division, Ames, IA.
<https://iowadot.gov/bridge/standards/english/RS40-14.pdf>.
- Ohio DOT. 2007. *ODOT Bridge Design Manual*. Office of Structural Engineering, Ohio Department of Transportation, Columbus, OH.
- Roddis, W. M. K., M. Kriesten, and Z. Liu. 1999. *Torsional Analysis for Exterior Girders*. University of Kansas, Lawrence, KS.
- Roddis W. M. K., E. L. Winters, and S. Baghernejad. 2008. *Cross-Frame Diaphragm Bracing of Steel Bridge Girders*. Kansas University Transportation Center, University of Kansas, Lawrence, KS.
- Shergalis, M. and B. Law. 2016. Preliminary Steel Bridge Selection and Design. INDOT Structures Conference, February 16.
<https://www.in.gov/dot/div/contracts/standards/bridges/Steel%20Bridge%20Selection%20and%20Design%20Design%20-%20Part%202.pdf>.
- Suprenant, B. A. 1994. Setting Screed Rails for Bridge Deck Paving. *Concrete Construction*.
https://www.concreteconstruction.net/how-to/site-prep/setting-screed-rails-for-bridge-deck-paving_o.
- TEREX Corporation. 2019. Concrete. Bridge and Flatwork Paver.
<https://www.terex.com/concrete/en/products/terex-bid-well-roller-pavers/bridge-pavers>.

- Yang, S., T. Helwig, R. Klingner, M. Engelhardt, and J. Fasl. 2010. *Impact of Overhang Construction on Girder Design*. Center for Transportation Research, University of Texas at Austin, TX.
- Yura, J., B. Phillips, S. Raju, and S. Webb. 1992. *Bracing of Steel Beams in Bridges*. Center for Transportation Research, University of Texas at Austin, TX.

**THE INSTITUTE FOR TRANSPORTATION IS THE FOCAL POINT FOR TRANSPORTATION
AT IOWA STATE UNIVERSITY.**

InTrans centers and programs perform transportation research and provide technology transfer services for government agencies and private companies;

InTrans contributes to ISU's educational programs for transportation students and provides K–12 outreach; and

InTrans conducts local, regional, and national transportation services and continuing education programs.



IOWA STATE
UNIVERSITY

Visit InTrans.iastate.edu for color pdfs of this and other research reports.